



2007

Methane potential of upper Fort Union formation sandstones, Campbell County, Wyoming

Michael J. Blackstone
University of North Dakota

Follow this and additional works at: <https://commons.und.edu/theses>

 Part of the [Geology Commons](#)

Recommended Citation

Blackstone, Michael J., "Methane potential of upper Fort Union formation sandstones, Campbell County, Wyoming" (2007). *Theses and Dissertations*. 26.

<https://commons.und.edu/theses/26>

This Thesis is brought to you for free and open access by the Theses, Dissertations, and Senior Projects at UND Scholarly Commons. It has been accepted for inclusion in Theses and Dissertations by an authorized administrator of UND Scholarly Commons. For more information, please contact zeinebyousif@library.und.edu.

METHANE POTENTIAL OF UPPER FORT UNION FORMATION SANDSTONES,
CAMPBELL COUNTY, WYOMING

by

Michael J. Blackstone
Bachelor of Science, University of Wyoming, 2003

A Thesis
Submitted to the Graduate Faculty

of the

University of North Dakota

in partial fulfillment of the requirements

for the degree of

Master of Science

Grand Forks, North Dakota

May
2007

This thesis, submitted by Michael Blackstone in partial fulfillment of the requirements for the Degree of Master of Science from the University of North Dakota, has been read by the Faculty Advisory Committee under whom the work has been done and is hereby approved.

Chairperson

This thesis meets the standards for appearance, conforms to the style and format requirements of the Graduate School of the University of North Dakota, and is hereby approved.

Dean of the Graduate School

Date

PERMISSION

Title Methane Potential of Upper Fort Union Formation Sandstones, Campbell
County, Wyoming

Department Geology

Degree Master of Science

In presenting this thesis in partial fulfillment of the requirements for a graduate degree from the University of North Dakota, I agree that the library of this University shall make it freely available for inspection. I further agree that permission for extensive copying for scholarly purposes may be granted by the professor who supervised my thesis work or, in his absence, by the chairperson of the department or the dean of the Graduate School. It is understood that any copying or publication or other use of this thesis or part thereof for financial gain shall not be allowed without my written permission. It is also understood that due recognition shall be given to me and to the University of North Dakota in any scholarly use which may be made of any material in my thesis.

Signature _____

Date _____

TABLE OF CONTENTS

LIST OF FIGURES	vi
LIST OF TABLES	ix
ACKNOWLEDGMENTS	x
ABSTRACT	xi
CHAPTER	
I. INTRODUCTION	1
Purpose	2
II. PREVIOUS WORK	4
Geologic History	4
Laramide Orogeny	5
Gas-producing Sandstones	8
Tongue River Member Depositional Environment	11
III. METHODS	20
IV. RESULTS	24
V. DISCUSSION	57
Laramide Orogeny	57
Tongue River Member Depositional Environment	59
Gas-producing Sandstones	69
VI. CONCLUSION	73

APPENDIX	74
REFERENCES	87

LIST OF FIGURES

Figure	Page
1. Location of the study area in the Powder River Basin and the surrounding uplifts (after WGATSC, 1965, fig. 1).	2
2. Composite stratigraphic column of the Fort Union Formation in the Powder River Basin (after Ayers, 2002 fig. 22).	3
3. Stratigraphic Column of the Upper Cretaceous and Paleogene in the Powder River Basin (after USGS, Central Region Energy Resources Team, 2007, fig. 3).	4
4. Isopach map of the Lance and Foxhills Formations in the Powder River Basin (after Curry, 1971, fig. 6).	6
5. Map of the study area	8
6. Oedekoven prospect structural cross section (after Oldham, 1997, fig. 9).	9
7. Well log from Wyatt 83-1 Oedekoven gas well (after Oldham, 1997, fig. 12).	10
8. Fluvially dominated depositional environment model (after Flores, 1993, fig. 15).	12
9. Lacustrine with fluvio-deltaic deposition model (after Ayers, 1986, fig. 12)	13
10. Okefenokee Swamp, Florida (after McClurg, 1988, fig. 8).	14
11. Extent of Goolsby and Finley study area and data (after Goolsby and Finley, 2000, fig. 2).	16
12. Example of "Z" patterns and thin coalbeds in the center of the sections (after Goolsby and Finley, 2000, fig. 12).	17
13. Location of "loop" cross section in Campbell County, Wyoming (after Goolsby and Finley, 2000, fig. 19).	18
14. "Loop" cross section (after Goolsby and Finley, 2000, fig. 21).	19

15.	Paleocene stratigraphic column with the Smith to Pawnee coalbeds (after USGS, Central Region Energy Resources Team, 2007, fig. 6)	22
16.	Map of southern part of study area with locations of cross-sections A-A' through E-E'	25
17.	Cross-section A-A' (T. 42 N., R. 75 W. – R. 73 W.)	26
18.	Cross-section B-B' (T. 43 N., R. 75 W. – R. 73 W.)	26
19.	Cross-section C-C' (T. 44 N., R. 76 W. – R. 73 W.)	27
20.	Cross-section D-D' (T. 45 N., R. 75 W. – R. 72 W.)	27
21.	Cross-section E-E' (T. 46 N., R. 75 W. – R. 72 W.)	28
22.	Central part of study area with locations of cross-sections F-F' through L-L' . . .	29
23.	Cross-section F-F' (T. 47 N., R. 75 W. – R. 72 W.)	30
24.	Cross-section G-G' (T. 48 N., R. 75 W. – R. 72 W.)	31
25.	Cross-section H-H' (T. 49 N., R. 76 W. – R. 72 W.)	32
26.	Cross-section I-I' (T. 50 N., R. 76 W. – R. 72 W.)	33
27.	Cross-section J-J' (T. 50 N., R. 76 W. – R. 73 W.)	34
28.	Cross-section K-K' (T. 51 N., R. 76 W. – R. 73 W.)	35
29.	Cross-section L-L' (T. 52 N., R. 75 W. – R. 73 W.)	36
30.	Northern part of study area with location of cross-sections M-M' through S-S' .	37
31.	Cross-section M-M' (T. 53 N., R. 75 W. – R. 73 W.)	38
32.	Cross-section N-N' (T. 53 N., R. 74 W. – R. 73 W.)	39
33.	Cross-section O-O' (T. 54 N., R. 76 W. – R. 73 W.)	40
34.	Cross-section P-P' (T. 55 N., R. 75 W. – R. 73 W.)	41
35.	Cross-section Q-Q' (T. 55 N., R. 75 W. – R. 73 W.)	41
36.	Cross-section R-R' (T. 56 N., R. 75 W. – R. 73 W.)	42

37.	Cross-section S-S' (T. 57 N., R. 75 W. – R. 74 W.)	42
38.	Study area with the location of cross-sections T-T', U-U', and V-V'	44
39.	Cross-section T-T' (T. 57 N. – T. 42 N., R. 75 W.)	45
40.	Cross-section U-U' (T. 57 N. – T. 42 N., R. 74 W.)	47
41.	Cross-section V-V' (T. 56 N. – T. 42 N., R. 73 W.)	48
42.	Total study interval thickness (in feet)	50
43.	Total sandstone thickness for the study interval (in feet)	51
44.	Sandstone to total interval ratio isopach map	52
45.	Thickness of the abbreviated interval in the north (in feet)	54
46.	Sandstone thickness of the abbreviated interval in the north (in feet)	55
47.	Sandstone to total thickness ratio isopach map of the abbreviated interval. The Oedekoven gas field is located on the updip meander of the fluvial system	56
48.	Maximum coal thickness map (after Ayers, 2002, fig. 27)	60
49.	Sandstone percentage isopach map with sandstones greater than 40 ft thick (after Ayers 1986, fig. 12)	62
50.	Target location in the north part of the study area. The location chosen lies on the updip meander of the fluvial system according to the northern abbreviated interval data	71
51.	Target locations in the study area. The locations chosen lie on the updip meanders of the fluvial system according to the study interval data	72

LIST OF TABLES

Table	Page
1. Study area well data	74

ACKNOWLEDGMENTS

I would like to thank my committee members, Dr. Richard LeFever (chairman), Dr. Richard Josephs, and Dr. Joseph Hartman, for their advice and critical reviews of this thesis. I would especially like to thank Dr. LeFever for his encouragement and support.

I would also like to thank Mr. Jim Goolsby and Mr. Andrew Finley for providing me with the initial internship project that became this thesis, as well as their support. I would also like to extend my thanks to Mrs. Julie LeFever of the North Dakota Geological Survey for the use of the facilities at the Wilson M. Laird Core and Sample Library at the University of North Dakota campus, Grand Forks, North Dakota. I am also grateful for the support of my family, especially my wife, Nicole Blackstone.

ABSTRACT

Coalbed methane has been produced from the coalbeds of the Upper Fort Union Formation in the Powder River Basin for many years. The sandstones associated with these coals have also proven to be gas-charged, but industry has done little with the sandstones thus far. The purpose of this study is to determine the paleoenvironment responsible for the deposition of the coal and sandstone bodies in an attempt to locate gas-charged sandstone bodies in the Tongue River Member of the Fort Union Formation.

The 30-mile by 90-mile study area was chosen because of the presence of a decrease in thick coalbed accumulations in the western half of Campbell County, Wyoming. Gamma-ray wireline logs were used to construct 22 cross sections within the study area using IHS PETRA. These cross sections were used to correlate the study interval and the coalbeds, and to pick the 5 ft thick or greater sandstones within the interval. Thickness values of the total study interval and sandstones were used to construct total thickness, total sandstone thickness, and sandstone ratio isopach maps of the study area. In the northern section of the study area, the upper part of the study interval crops out; therefore, a second set of maps were constructed for the northern area. The resulting maps depict an increase in sandstone thicknesses and percentages that coincides with the decrease in thick coalbeds, as well as an overall 1 to 2° dip to the west. This increase in sandstone forms a north-south trending swell with several east-west limbs attached to the main trunk.

The isopach maps were compared to previous depositional models for the Upper Fort Union Formation in the Powder River Basin. These models include a lacustrine model with westward-prograding deltas, a fluvially dominated model with raised bogs limiting lateral migration of the fluvial system, and a low-lying swamp model. The lacustrine model consists only of sandstones greater than 40 ft thick and does not display the north-south trending main trunk. The current evidence does not support the lacustrine model. The north-south trending main trunk in the current data supports the model for fluvially dominated deposition. The east-west trending limbs represent tributary systems. This model suggests a raised bog scenario for peat accumulation considering the basin's coalbeds are anomalously thick and low in sulfur and ash content. This scenario is supported by the current data, but it is not consistent throughout the study area. The swamp model hypothesized deposition to be from a low-lying swamp environment similar to that of the Okefenokee Swamp of Florida. Coalbed thickness may reach great thicknesses as peat accumulation keeps pace with basin subsidence. The current data support the swamp model for peat accumulation.

The resulting model for deposition of this study consists of a low-lying swamp environment with a fluvial system running through the study area from south to north. First order meandering of the system is present in the isopach maps. Raised bogs may be present, but are restricted to the southern section of the study area.

The Oedekoven gas field is producing gas from a sandstone body within the study area and selected interval. This 1 mi² field is located on the updip meander of the north-south trending main sandstone swell. Other locations with similar location characteristics have been selected for further study.

CHAPTER 1

INTRODUCTION

The study area incorporates a 30 mile east-west and 90 mile north-south section of Campbell County, Wyoming (Figure 1). This area was selected due to the presence of characteristically thick coalbeds of the Tongue River Member, as well as an anomalous lack of thick coalbeds at the center of the area. The study area also contains the Odekoven gas field that produces from a particular sandstone bed.

The Fort Union Formation of the Powder River Basin consists of three members: the lower Tullock, the Lebo Shale, and the upper Tongue River Members (Figure 2). The Tongue River Member contains multiple thick, low-grade coal beds. These coal beds have accounted for 170 Billion Cubic Feet (BCF) of the coalbed methane production in Campbell County, Wyoming between the years 2000 and 2006 (Wyoming Oil and Gas Conservation Commission, 2007). The Tongue River Member also contains fine-grained sandstone, siltstone, and shale beds interbedded with the coal beds.

Purpose

This thesis has three primary objectives. First, it attempts to determine the paleoenvironment responsible for the deposition of the coalbeds and sandstone bodies by analyzing geophysical well logs within the Powder River Basin. Second, the paper focuses on a part of the Tongue River Member where thick coalbeds abruptly thin, split,

and in some cases, are completely absent in an effort to determine the environmental cause for these anomalies. Finally, this work discusses the potential locations of other gas-bearing sandstone bodies within the study area.

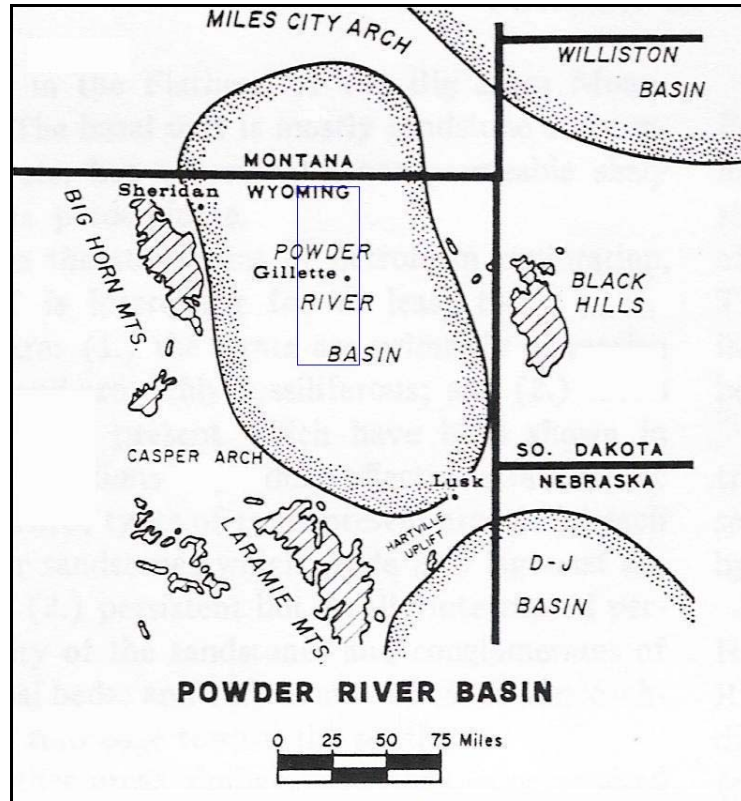


Figure 1. Location of the study area in the Powder River Basin and the surrounding uplifts (after WGATSC, 1965, fig. 1).

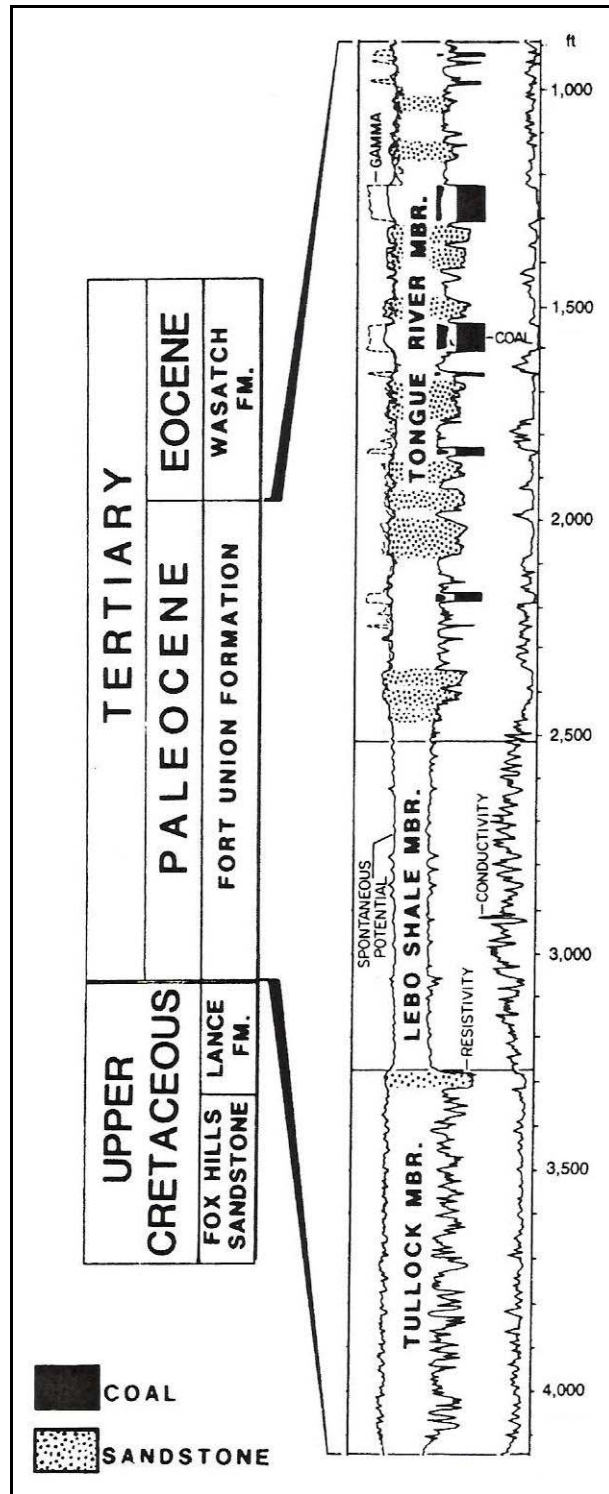


Figure 2. Composite stratigraphic column of the Fort Union Formation in the Powder River Basin (after Ayers, 2002 fig. 22)

CHAPTER 2
PREVIOUS WORK
Geologic History

The Powder River Basin is located in northeast Wyoming and southwest Montana (Figure 1). The geological section of the basin is divided into eight units separated by major unconformities (Weichman, 1964). Each unit represents a major transgressive-regressive cycle (WGATSC, 1965). For the purposes of this study, only units VII and VIII of Cretaceous and Paleogene age will be discussed (Figure 3).

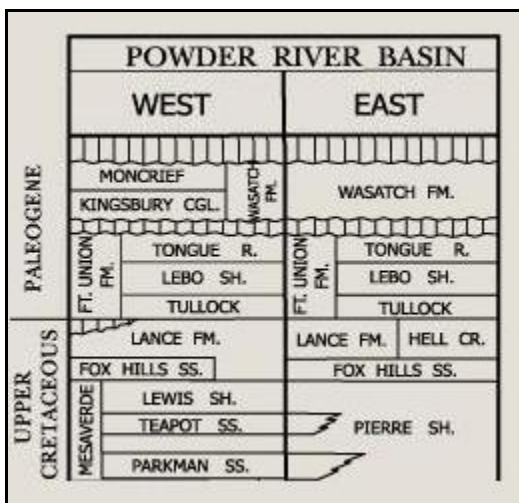


Figure 3. Stratigraphic column of the Upper Cretaceous and Paleogene in the Powder River Basin (after USGS, Central Region Energy Resources Team, 2007, fig. 3).

Rock Unit VII strata begin with early marine beds deposited in a Cretaceous sea that transgressed from both the north and south, merging in the central Rockies and Great Plains regions. This rock unit can be subdivided into five regressive cycles (WGATSC,

1965). During these regressive cycles, sandstone beds were deposited that separate the shales of the major transgressions.

The fourth and fifth regressive cycles are known as the Mesaverde cycle and the Lance cycle, respectively. These two cycles represent phases of uplift and an influx of coarser sediments into the basin. The Wyoming Geological Association Technical Studies Committee (1965) considers the Late Cretaceous uplift as the first episode of the Laramide Orogeny in the region of the Powder River Basin. Rapid subsidence also occurred within the basin during the Late Cretaceous, resulting in the thick deposits of the Lance Formation (WGATSC, 1965). The Lance Formation is comprised of 1000 to 1500 ft of sediment deposited in an environment of floodplains, meandering channel systems, and coastal plains.

Rock Unit VIII consists of the Paleocene Fort Union Formation and the Eocene Wasatch Formation. The rock unit encompasses the Paleogene within the Powder River Basin (WGATSC, 1965). Laramide deformation ceased prior to deposition of the Oligocene White River volcanic rocks, which buried the exposed Precambrian cores of the uplifted Black Hills, Laramie, and Big Horn mountain ranges (Curry, 1971).

Laramide Orogeny

Though rapid subsidence appears to have occurred during the late Maastrichtian deposition of the Lance Formation, Curry's (1971) isopach map (Figure 4) of the formation depicts greater subsidence towards the south. Curry notes that the Fox Hills Formation was included in his cross sections and isopach map of the Lance Formation due to the lack of recognizable differences between the two formations in the log curves.

Though this may raise some concerns with his interpretation, Curry (1971) states that there is no convincing evidence for the Laramide Orogeny during the late Maastrichtian Lance deposition. Curry's theory that the Laramide Orogeny began after the Cretaceous is similar to several other hypotheses concerning the timing of the Laramide Orogeny.

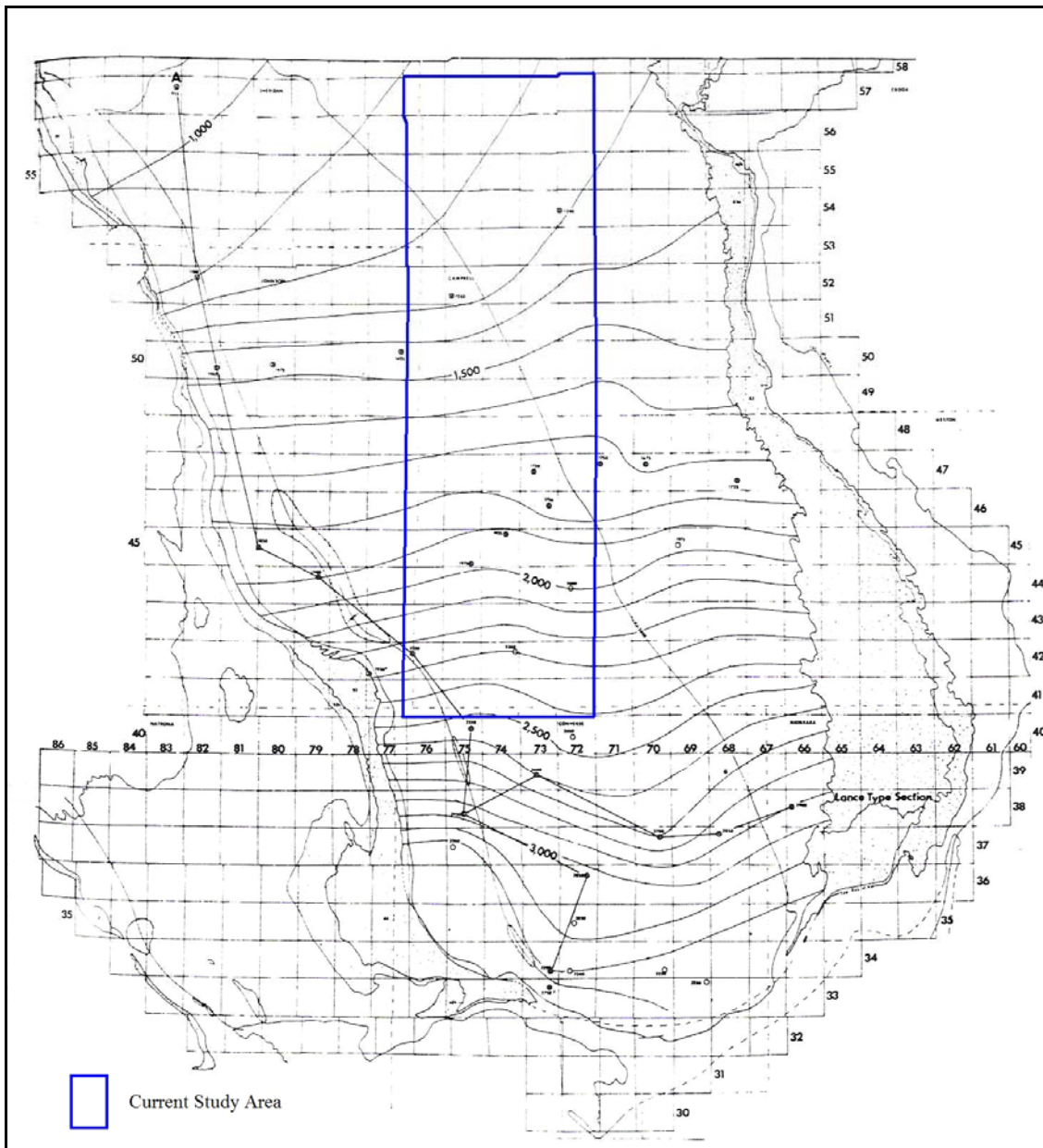


Figure 4. Isopach map of the Lance and Foxhills Formations in the Powder River Basin (after Curry, 1971, fig. 6).

Using paleocurrent data, Seeland (1988) was able to determine that flow direction was generally eastward during the Late Cretaceous. This suggests that the Black Hills had not yet undergone uplift. A continuation of the eastward trend, evidenced by the paleocurrent data during the deposition of the Lower Paleocene Tullock Member, suggests no uplift in the Black Hills.

Lisenbee's (1988) study of the sedimentation patterns in the Powder River Basin and Black Hills region during the latest Cretaceous through Oligocene indicate the timing of the Black Hills uplift. Upper Cretaceous fluvio-deltaic deposits of the Lance Formation provide evidence that the eastern Powder River Basin and Black Hills area were at sea level. Initial Laramide uplift to the west may have acted as a source for the progradation of a large delta extending eastward into the area.

Increases in sandstone percentages and a change to a westerly flow direction in the Tullock Member of the Fort Union Formation suggest uplift of the Black Hills during the lower Paleocene in the eastern part of the Powder River Basin (Lisenbee, 1988). Rare channel sandstone beds of the Lebo Shale Member of the Fort Union Formation indicate a shift in the direction of paleocurrent flow to the NNE. The flow direction of the Tongue River Member in the southern parts of the basin shifts to a direction subparallel to the basin axis on a NNW flow pattern. Furthermore, arkosic sandstones and fragments of metamorphic rock in the Tongue River Member, as well as igneous clasts in the conglomeratic sandstones of the Upper Fort Union, suggest that uplift and erosion in the Black Hills, Bighorn Mountains, and Laramie Mountains had exposed Precambrian rocks by this time (Seeland, 1988).

Gas-producing Sandstones

The Oedekoven Gas Field is located in the northeastern part of the study area in Section 19 of Township 55 N, Range 73 W (Figure 5). In 1986, Wyatt Petroleum Corporation began a shallow gas accumulation program in this section because the area possessed several encouraging characteristics.

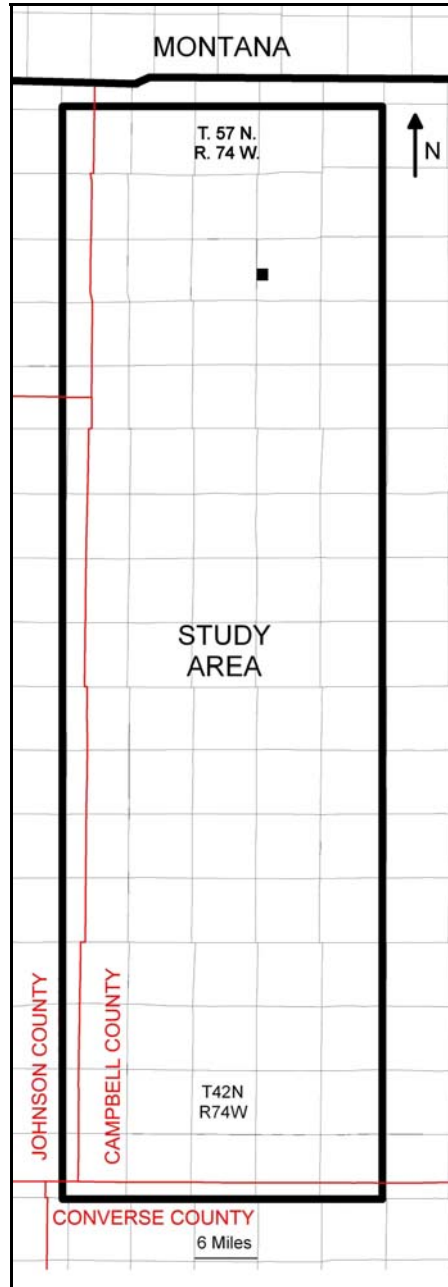


Figure 5. Map of the study area. The Oedekoven gas field is highlighted in T.55N. R.73W.

The Canyon coal bed forms a north-south trending anticline with over 140 ft of structural relief at the top of the coal (Oldham, 1997). The interval between the base of the Canyon coalbed and the top of the underlying Cook coalbed reflects a north-south trending maximum thickness that coincides with the anticline found in the Canyon coalbed (Oldham, 1997). The anticline and maximum thickness also coincide with a relatively high-resistivity sandstone body that transitions to a mudstone in the east and west (Figure 6). Finally, a blowout and subsequent rig fire occurred during the drilling of the Anschutz 2-B Oedekoven deep test well in 1969 (Oldham, 1997).

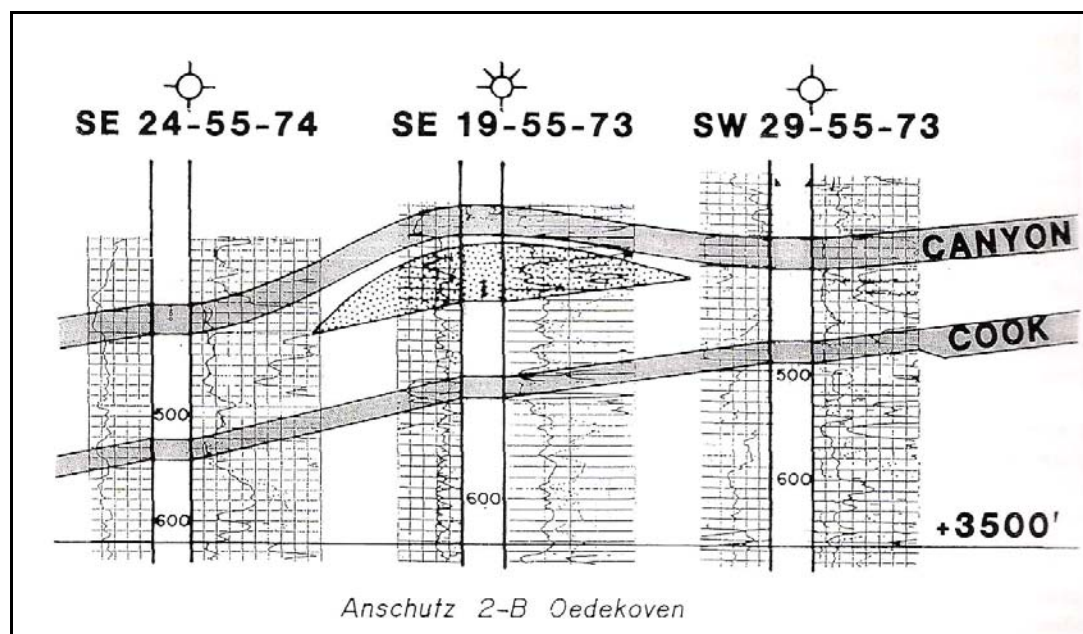


Figure 6. Oedekoven prospect structural cross section (after Oldham, 1997, fig. 9).

In 1986, Wyatt Petroleum drilled the 83-1 Oedekoven well to a total depth of 520 ft. using conventional methods. The well was cased and perforated across the interval 342 – 362 ft and completed as a gas well (Oldham, 1997). The well produced from the sandstone bed located below the Canyon coalbed (Figure 7).

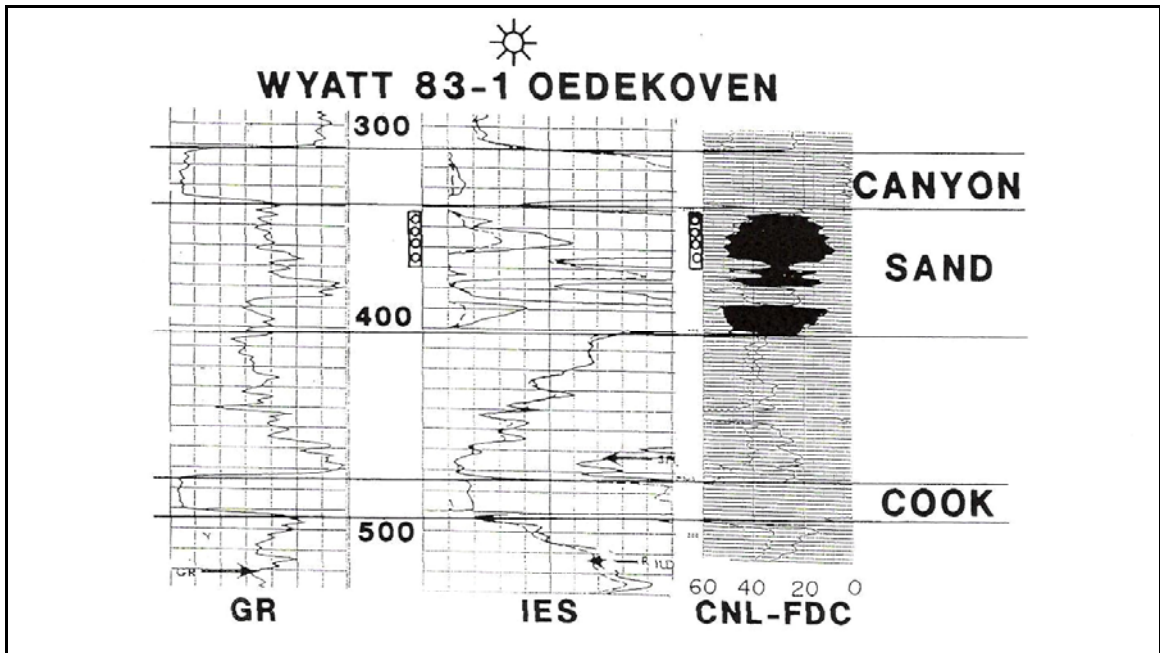


Figure 7. Well log from Wyatt 83-1 Oedekoven gas well (after Oldham, 1997, fig. 12).

The well was offset by the Wyatt 83-2 Oedekoven. The two wells resulted in a cumulative production of 302,573 MCFG and 545,877 MCFG through June, 1994. Though these two wells are the field's two best producing wells, a total of 14 wells were completed with a cumulative production of 1,826,631 MCFG through June, 1994 (Oldham, 1997).

Oldham also notes that the economic factors for this particular gas field are favorable due to the pay's shallow depth and rapid rate of recovery. Unlike other methane-producing wells completed in the coals, the Oedekoven field has produced no water. The lack of water produced from the field is another positive economical and environmental factor because no treatment, removal, or sequestering measures are needed during the field's production. Though methane-producing sandstones like that of the Oedekoven field are present in the Powder River Basin, little research has been done to determine why these sandstone beds are present or where other such fields may exist.

Tongue River Member Depositional Environment

The paleoenvironment of the Tongue River Member deposition has long been debated. In order to best locate potential coalbed methane-producing sandstones in the Powder River Basin, the paleoenvironment responsible for the deposition of these beds must be determined.

One model for the depositional paleoenvironment is described by Flores (1993) as a meandering to anastomosing, fluvially dominated setting with raised or domed peat bogs adjacent to the fluvial system. Flores recognizes the presence of crevasse splay and lacustrine deposits in the region. In the fluvial model, the depositional environment (Figure 8) undergoes a transition from a low, flat swamp-like environment, with a meandering fluvial system, to a matured, raised bog environment (Flores, 1993). The original meandering system bifurcates along crevasse splays into the flood basin to promote early anastomosis (Flores, 1993). The low-lying peatlands between the channel pathways mature into the raised bogs. The raised bogs then act to confine the fluvial channels and promote vertical aggradation of the channel deposits, as well as the peatlands (Flores, 1993).

Flores (1993) discusses the different peatland ecosystems, ranging from the raised bogs to fens, swamps, and marshes. He compares these with modern analogues, such as the tropical bogs along the Baram River of Sarawak, Malasia (Flores, 1993). The bogs found there are up to 90 ft thick, span 32 mi², and are domed up to 48.5 ft above the adjacent drainage (Flores, 1993). Flores states that the low ash and sulfur contents of the Tongue River Member coalbeds also support the “raised bog” model.

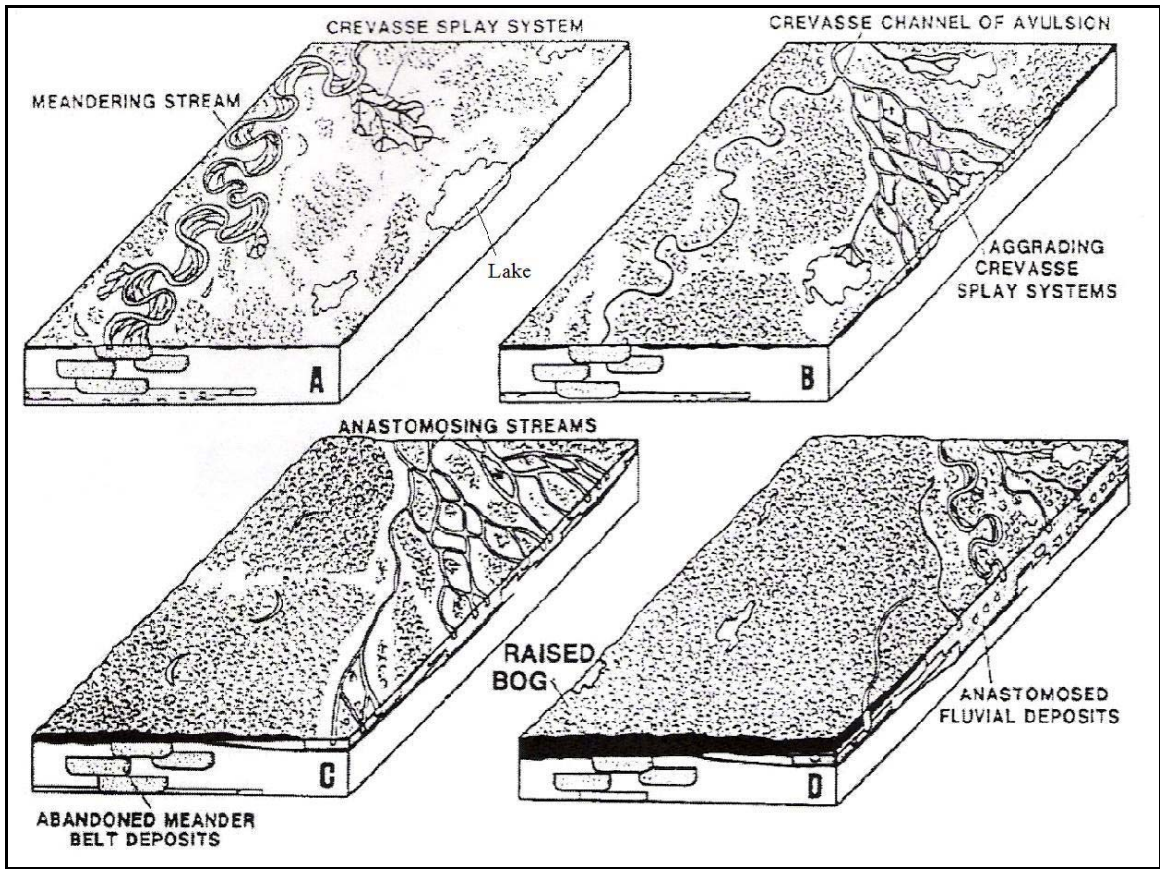


Figure 8. Fluvially dominated depositional environment model (after Flores, 1993, fig. 15).

The peat accumulation in this model is rain-fed and disconnected from the ground and surface water. Peat deposits from low-lying fens, swamps, and marshes form thin peat deposits. Interaction with the surface and ground water in other peatland models results in higher ash and sulfur-bearing coals. Flores (1993) concludes that only the raised bog model is capable of creating the thick coalbeds and sandstone packages found in the Powder River Basin.

Another model proposed by Ayers (1986) considers the depositional environment of the Middle to Late Paleocene to be lacustrine. Ayers used structural cross sections and isopach and lithofacies maps to construct the model. The model is characterized by the presence of a large lake along the basin axis (Figure 9). “Lake Lebo” was filled

peripherally by basinward-prograding deltas, as evidenced by a decrease in sandstone percentages towards the basin axis (Ayers, 1986). Ayers (1986) concludes that Laramide-induced subsidence formed Lake Lebo, which covered more than 10,000 mi². Streams from the Laramide highlands formed the prograding deltas that filled the lake. The thick coalbeds found in the basin are the result of extensive peat deposits that developed on broad, interdeltic plains (Ayers, 2002).

Comparing the conditions that existed during the Late Paleocene in the basin with a list of conditions responsible for different coal depositional environments, McClurg (1988) concludes that both the Ayers and Flores models for the depositional environment have fundamental flaws. This combination of factors may not act to produce the anomalously thick and laterally extensive coals found in the Tongue River Member of the basin (McClurg, 1988).

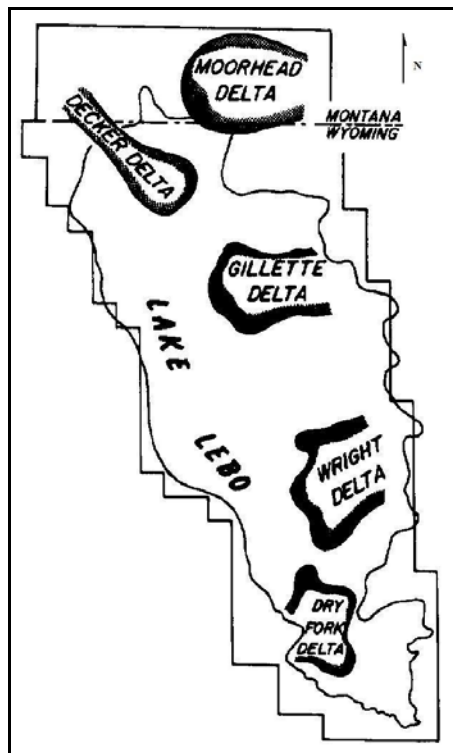


Figure 9. Lacustrine with fluvio-deltaic deposition model (after Ayers, 1986, fig. 12).

Using his depositional guidelines and basin parameters, McClurg (1988) relates the Tongue River depositional environment to several modern analogues. He states that the depositional environment is most similar to the Okefenokee Swamp in Florida. The Okefenokee Swamp is essentially a shallow lake with trees, which originates in the middle of the swamp (Figure 10). It is fed by several streams along the periphery and drained by the Suwannee River. The river flows through the swamp without forming natural levees to protect the peat deposition. The depth of the stagnant water within the swamp can reach 6 to 7 ft before rooted vegetation can no longer persist and peat accumulation ceases (McClurg, 1988).

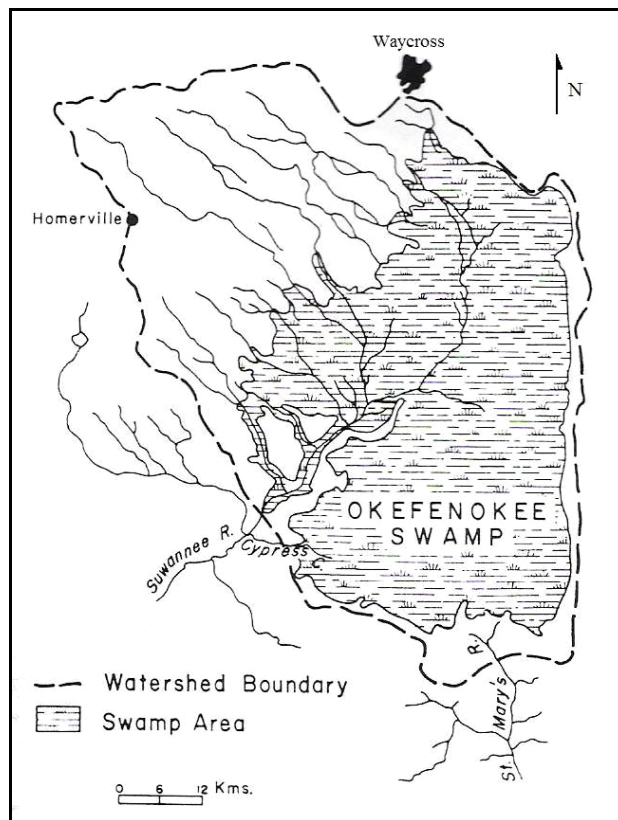


Figure 10. Okefenokee Swamp, Florida (after McClurg, 1988, fig. 8).

To illustrate how such a swamp may evolve through time, as must have occurred in the Powder River Basin, McClurg (1988) states that differential subsidence within the basin may cause the swamp to migrate. Areas that become inundated with deeper waters will cease to accumulate peat and that part of the swamp will become a shallow lake. Thereafter, lacustrine sedimentation begins. As the area fills, the fall in water level allows vegetation to once again proliferate, and the swamp returns to the area (McClurg, 1988). The resulting section will have two peats separated by lacustrine sediment.

Goolsby and Finley (2000) constructed an extensive database consisting of cross sections and structural and isopach maps of their study area (Figure 11). The data were collected to correlate the coalbeds and determine the stratigraphic relationships between the individual coalbeds of the Upper Tongue River Member found in the basin.

The east-west oriented cross-sections depict the coals as laterally persistent features that often display “Z” patterns in their splitting behavior (Figure 12). Goolsby and Finley (2000) conclude that these patterns are the result of a migrating area of peat deposition. The noticeably persistent thinning of the coals in the center of the sections is hypothesized to be caused by a south-to-north flowing fluvial system (Goolsby and Finley, 2000).

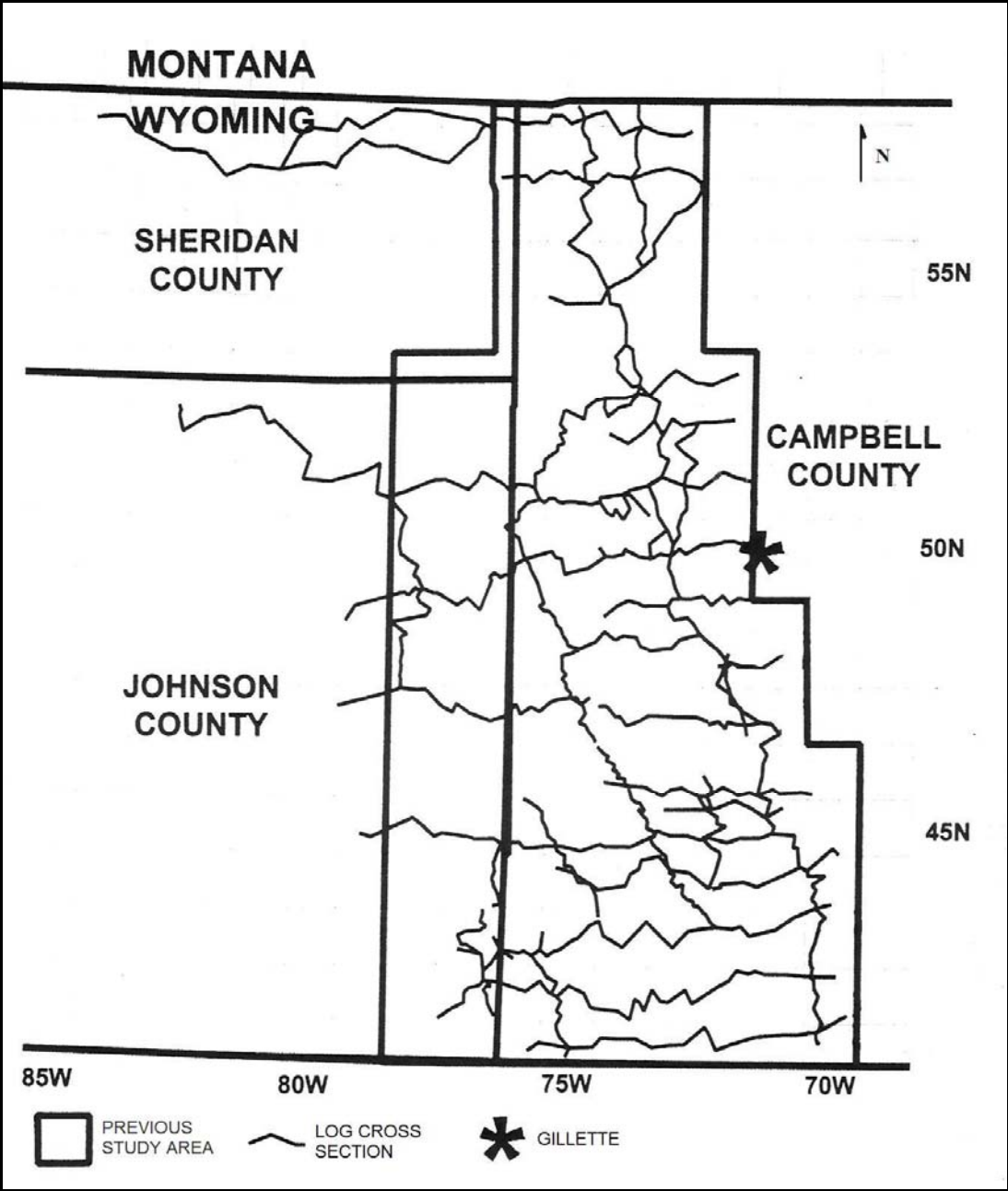


Figure 11. Extent of Goolsby and Finley study area and data (after Goolsby and Finley, 2000, fig. 2).

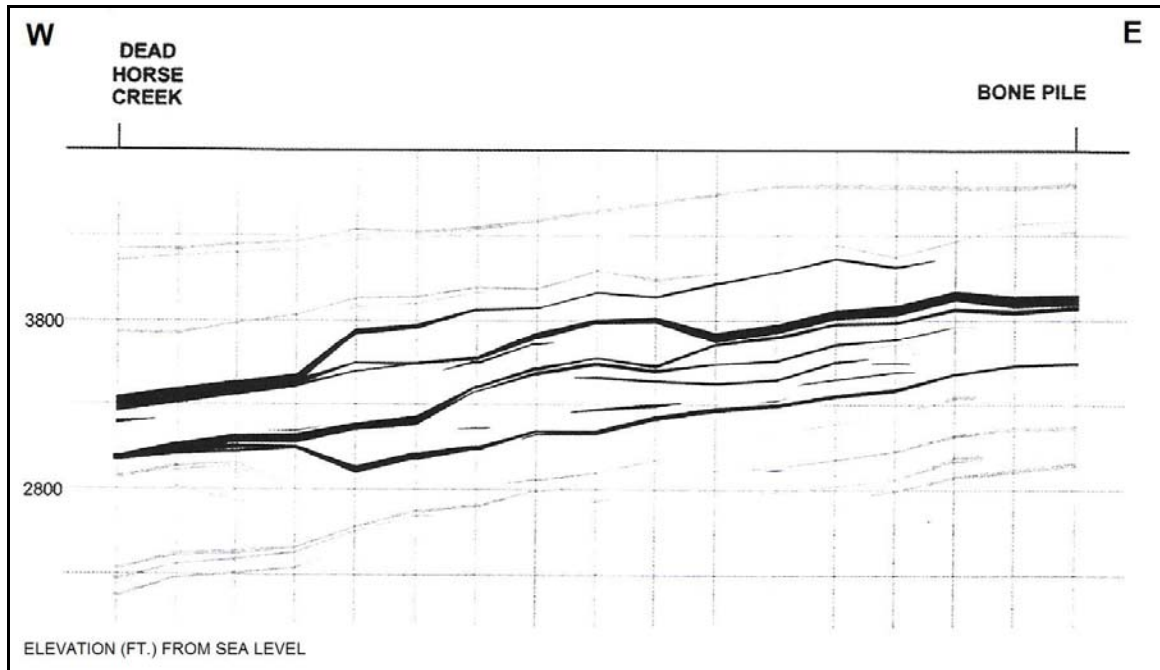


Figure 12. Example of "Z" patterns and thin coalbeds in the center of the sections (after Goolsby and Finley, 2000, fig. 12).

Recognition of the migrating area of deposition from a two-dimensional cross-section led Goolsby and Finley (2000) to create a "loop" cross-section to illustrate the relationship of the individual coals and three-dimensional migration of the area of deposition (Figure 13). Using the Wyodak coal as their marker bed, the "loop" illustrates the presence of this particular coal and the resulting splits that the Wyodak undergoes (Figure 14). The authors conclude that the Wyodak coalbed actually overlies itself (Goolsby and Finley, 2000). The accumulation and deposition of peat was part of a single lithologic unit that was deposited continuously in a migrating depocenter around the study area (Goolsby and Finley, 2000). The migration of this peat-forming environment is considered to be the result of tectonic activity within the basin and along the basin margins (Goolsby and Finley, 2000).

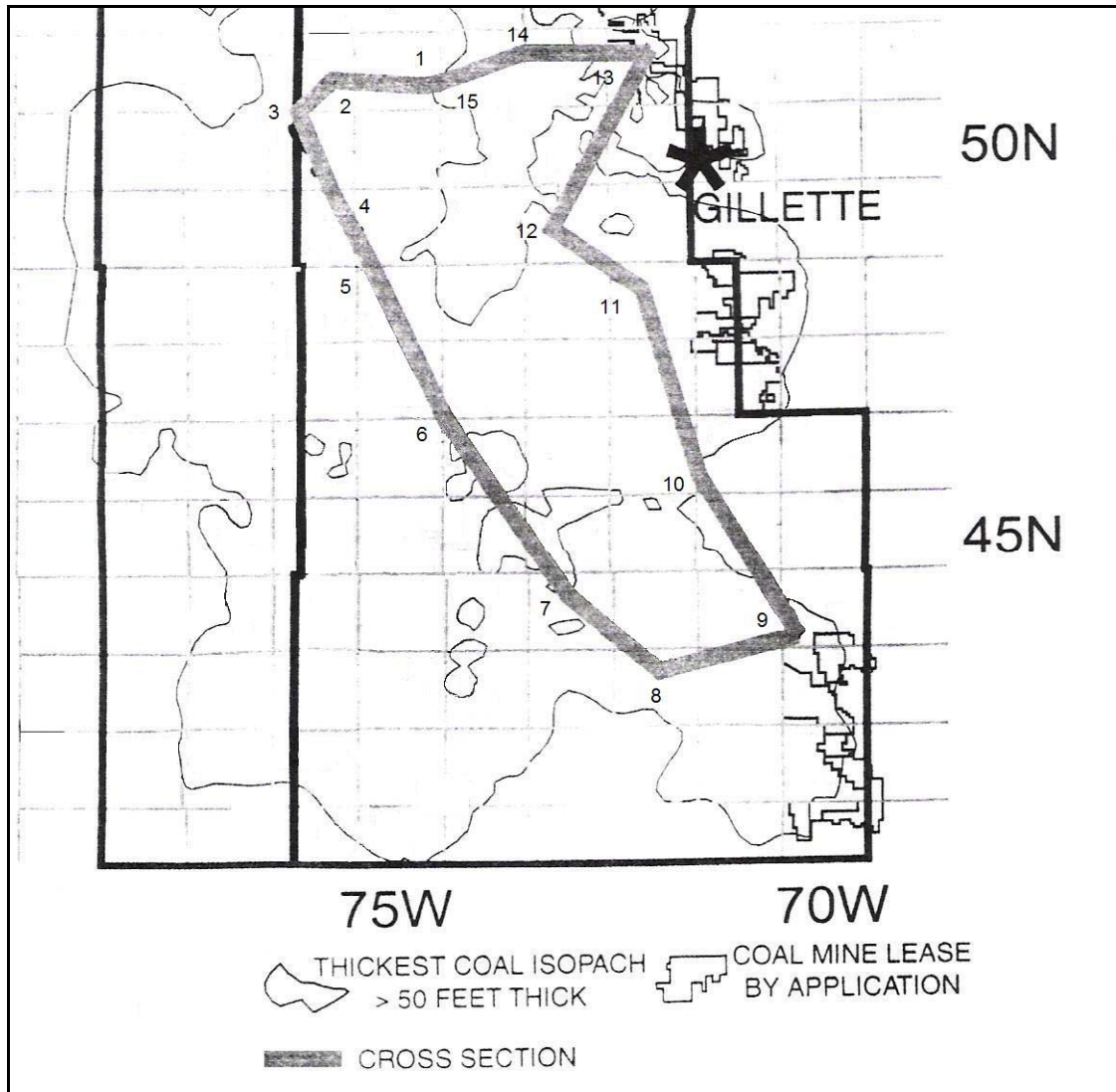


Figure 13. Location of "loop" cross section in Campbell County, Wyoming.
 (after Goolsby and Finley, 2000, fig. 19).

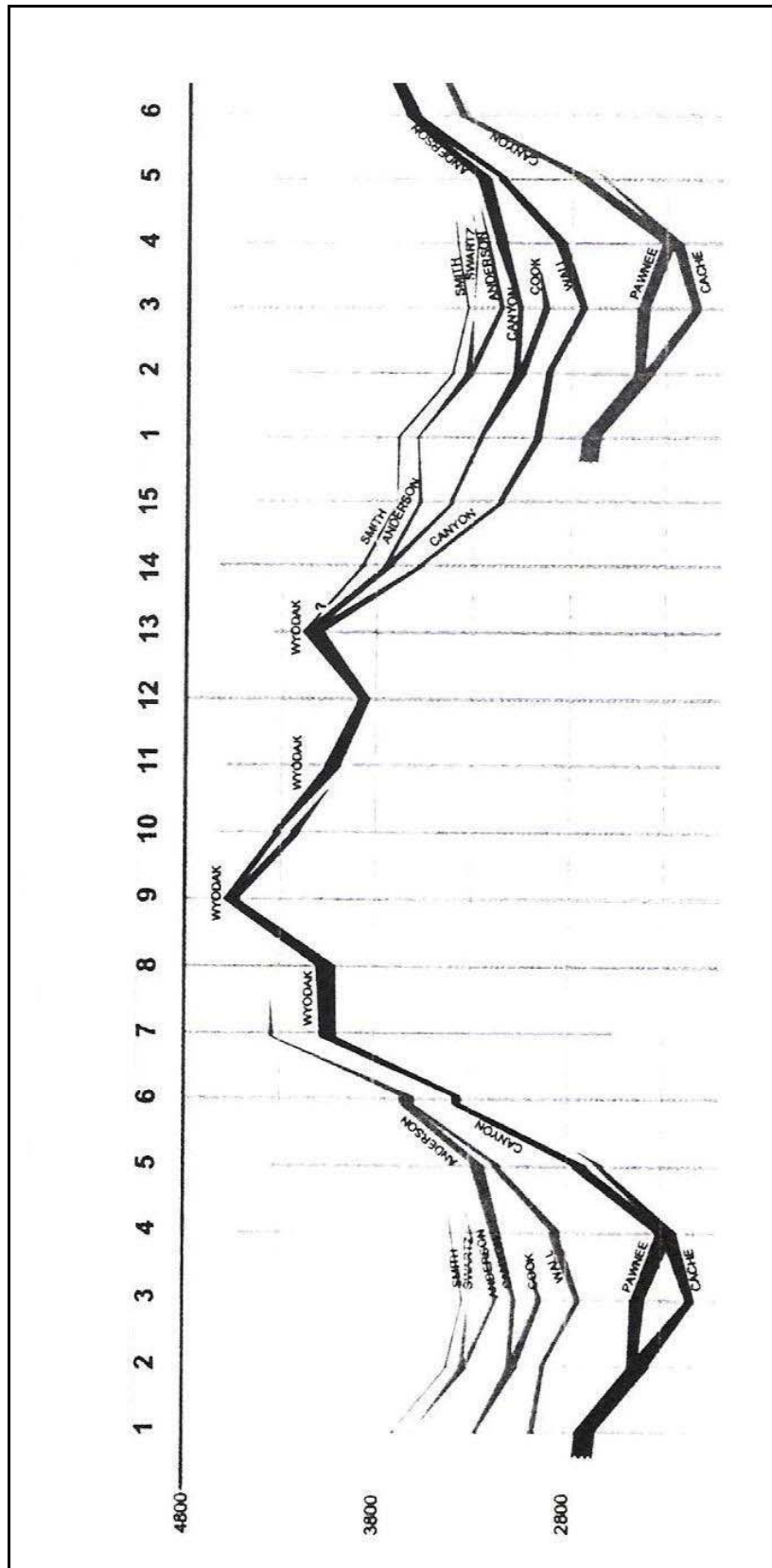


Figure 14. "Loop" cross section (after Goolsby and Finley, 2000, fig. 21).

CHAPTER 3

METHODS

The data collected for this study were derived from geophysical well logs of 597 wells in the area. The specific wells were chosen by location to create cross sections of the study area. Wells incorporating a complete log spanning the Smith coalbed to the Pawnee coal interval within the Tongue River Member are selected. The Smith coalbed crops out in the northern part of the study area. For this reason, wells that contained the Anderson to Pawnee coalbeds were selected.

Well logs consist of gamma ray, resistivity, and neutron-density logs of coalbed methane, oil/conventional gas, and water wells drilled in the area. All logs were downloaded from the Wyoming Oil and Gas Conservation Commission website. Due to the shallow depth of the study interval, the majority of the logs are gamma ray logs due to their low cost. Other logs, such as resistivity and neutron-density logs, were used when available.

The common scale on the gamma ray logs ranges from 0 to 120 API. Low gamma ray readings of 30 or below were picked using the program PETRA and designated as a coalbed for each log. A “shale line” on the gamma ray scale was picked at an API of 70 for each log. Any value between 30 API and the shale line was considered to be sandstone. Any value greater than 70 API is considered shale.

The top of the Smith coalbed is the study interval top for each log. Similarly, the bottom of the Pawnee coalbed, where present, serves as the study interval bottom. In some cases, the Pawnee coalbed is not present in the log. If the Pawnee coalbed is not present, the bottom of the interval is taken as the base of the Wall coalbed. As stated previously, in the northern part of the study area, the upper part of the Tongue River Member study interval crops out and the Anderson coalbed is considered to be the top of the study interval. The sandstone beds picked for each log in the northern part of the study area are designated with a different pick value and color using PETRA.

The logs were used to create 22 structural cross sections of the study area. One cross section was constructed for each township row within the study area. This produced 19 east-west oriented cross sections labeled A-A' for the southern-most cross section through S-S' for the northern-most cross section. Three additional north-south trending cross sections were constructed for range columns R. 75 W., R. 74 W. and R. 73 W. and labeled T-T', U-U' and V-V', respectively. Each cross section includes one well for each township section for better control. In some cases, lack of wells in a section, or lack of logs spanning the stratigraphic interval of interest, made some cross sections less complete.

The resulting cross sections were used to correlate the coalbeds from the uppermost Smith coalbed to the lowermost Pawnee coalbed within the Tongue River Member of the Fort Union Formation. This interval may contain multiple coalbeds commonly named the Smith, Anderson, Canyon, Cook, Wall and Pawnee in descending order in the stratigraphic column (Figure 15). Names applied to these coalbeds vary in industry because each company working in the area has adopted a different nomenclature

based on their own datasets. Though an interval must be determined for the purpose of isopach mapping, correlating these coalbeds may prove problematic, as Goolsby and Finley (2000) demonstrated with their “loop” cross-section (Figure 14).

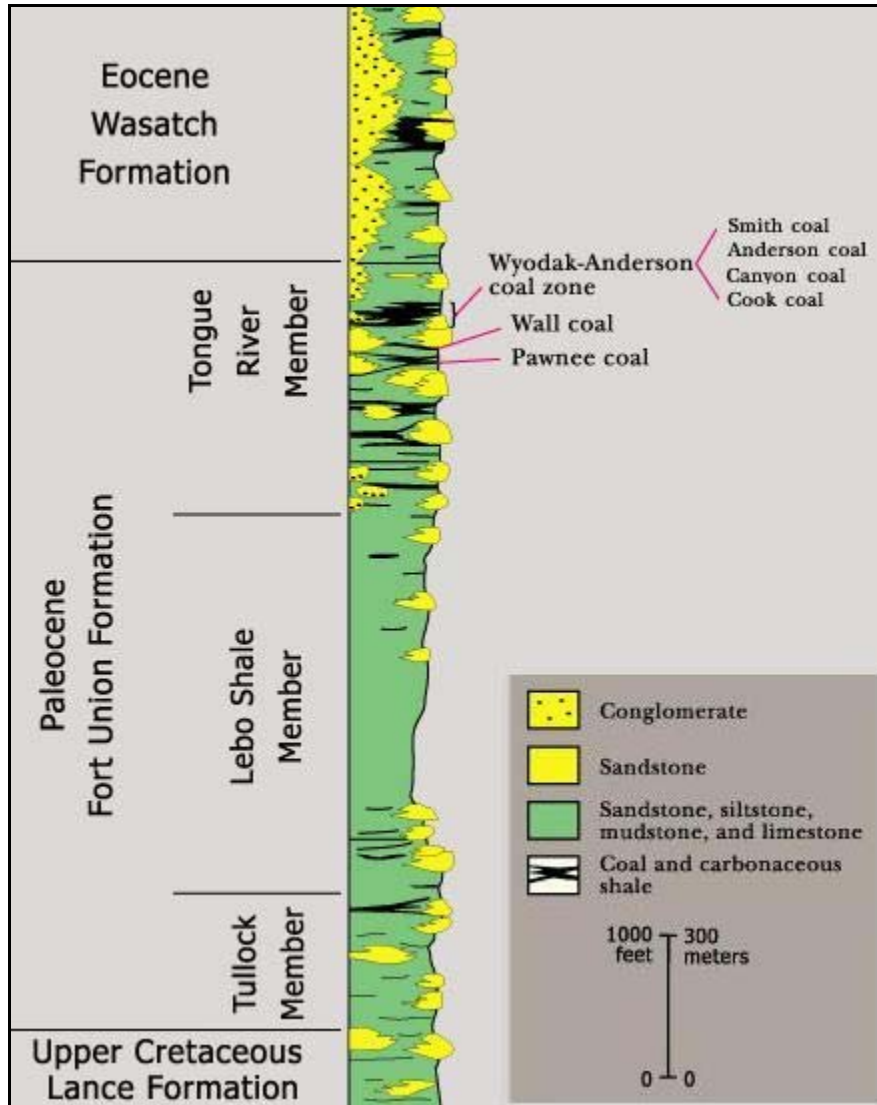


Figure 15. Paleocene stratigraphic column with the Smith to Pawnee coalbeds (after USGS, Central Region Energy Resources Team, 2007, fig. 6).

Wells were designated by the American Petroleum Institute (API) number in the cross sections. The standard API number for the state of Wyoming is 049-XXX-XXXXX, where the 049 designates the state, the second set of digits is assigned to each county, and the third set of digits is assigned once the application to drill is approved.

Wells located in Campbell County, Wyoming, are designated by 049-005-XXXXX. To fit the API numbers for each well in the cross sections, the state number, the first digit of the county number, and the hyphen after the county number were omitted. The resulting number for each well is an abbreviated seven-digit form of the original API number. For example, a well designated with an API number of 049-005-12345 is abbreviated to 0512345.

The picks from each well are used to create isopach maps of the study area. The set includes a total thickness isopach, a sandstone thickness isopach, and a sandstone to total thickness ratio isopach. Due to the outcropping of the Smith coal in the northern part of the study area, a second set of isopach maps was constructed for the north. The total thickness value was calculated with PETRA using the difference in depth between the interval top and bottom for each well log. The sandstone thickness isopach is produced by adding the sandstones picked within the study interval on each well log. Finally, the ratio of sandstone thickness to total thickness is calculated using the respective values for each well log.

CHAPTER 4

RESULTS

The computer program PETRA was used to produce cross sections for correlation purposes and maps for analysis of the sandstone present in the study interval. To enhance control of the coalbed correlation, one cross section was constructed for each township row across the study area. An additional cross section was constructed for range columns R. 73 W., R. 74 W., and R. 75 W. The resulting cross sections consist of evenly spaced logs with coal correlations and sandstone bodies displayed. Due to their size, the cross sections were modified to consist of depth “stick” place holders with wireline logs added only in the center and on the ends of each cross section.

The east-west cross sections located in the southern portion of the study area display a relatively simple study interval. The average interval of 600 ft consists largely of two laterally persistent coal seams. The upper, thin coal is identified as the Smith coalbed. The lower coalbed is the target for the coalbed methane industry due to its thickness. This lower coalbed has a variety of different names applied by various companies according to each company’s dataset and nomenclature. For the purposes of this thesis, the lower coal is considered the Wall coalbed.

As the cross section locations move northward in the study area, between two and four coalbeds are present. The lower coalbed often splits in the eastern portion of the cross sections, while remaining a single, thick coalbed in the west. The location of the

initial split in the lower coalbed migrates to the west in each progressive cross section towards the north in the study area. Figure 16 displays the locations for the southern east-west cross sections.

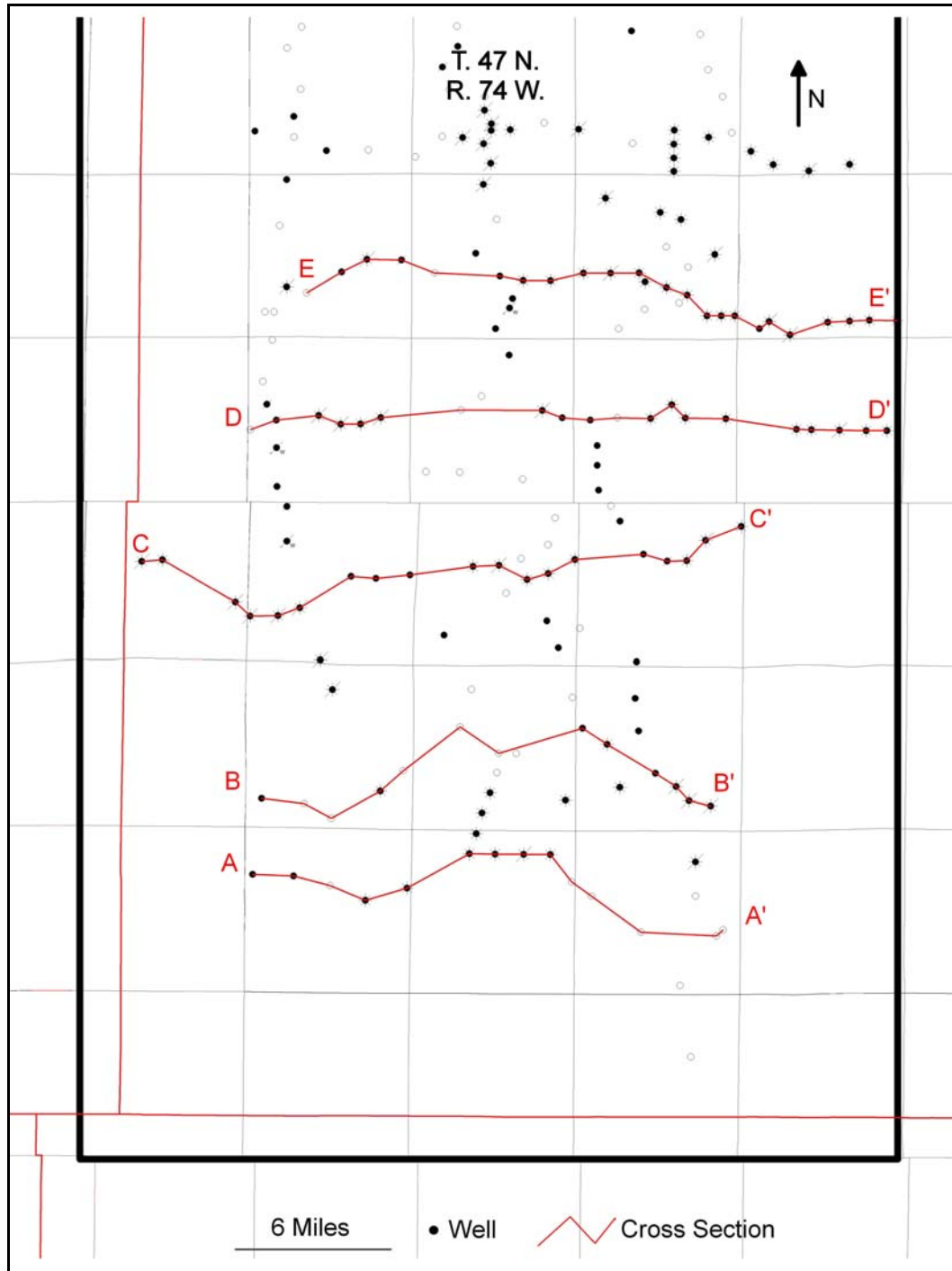


Figure 16. Map of southern part of study area with locations of cross-sections A-A' through E-E'.

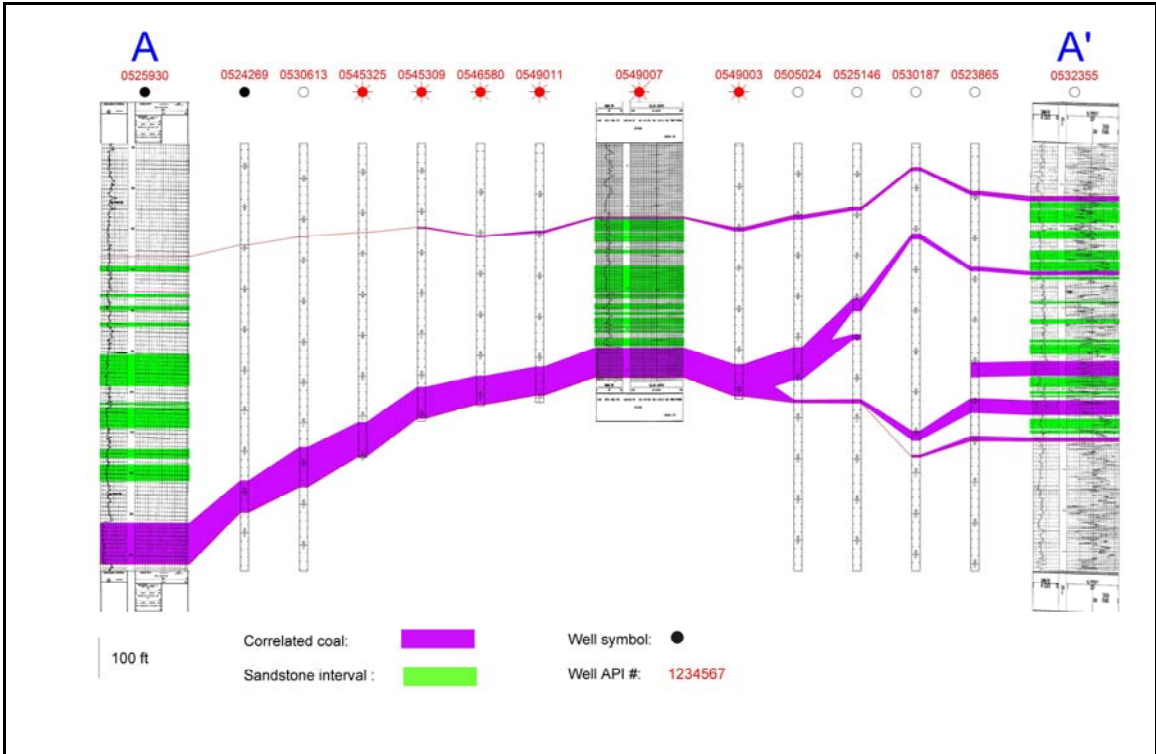


Figure 17. Cross-section A-A' (T. 42 N., R. 75 W. – R. 73 W.).

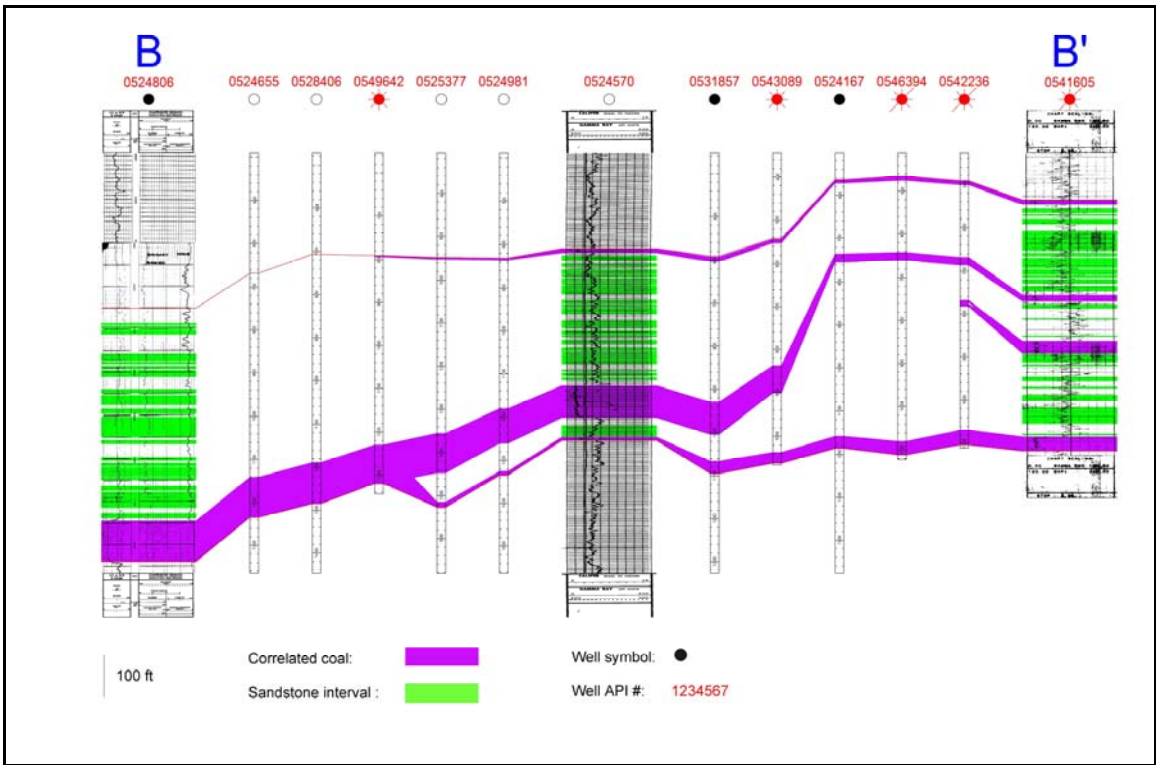


Figure 18. Cross-section B-B' (T. 43 N., R. 75 W. – R. 73 W.).

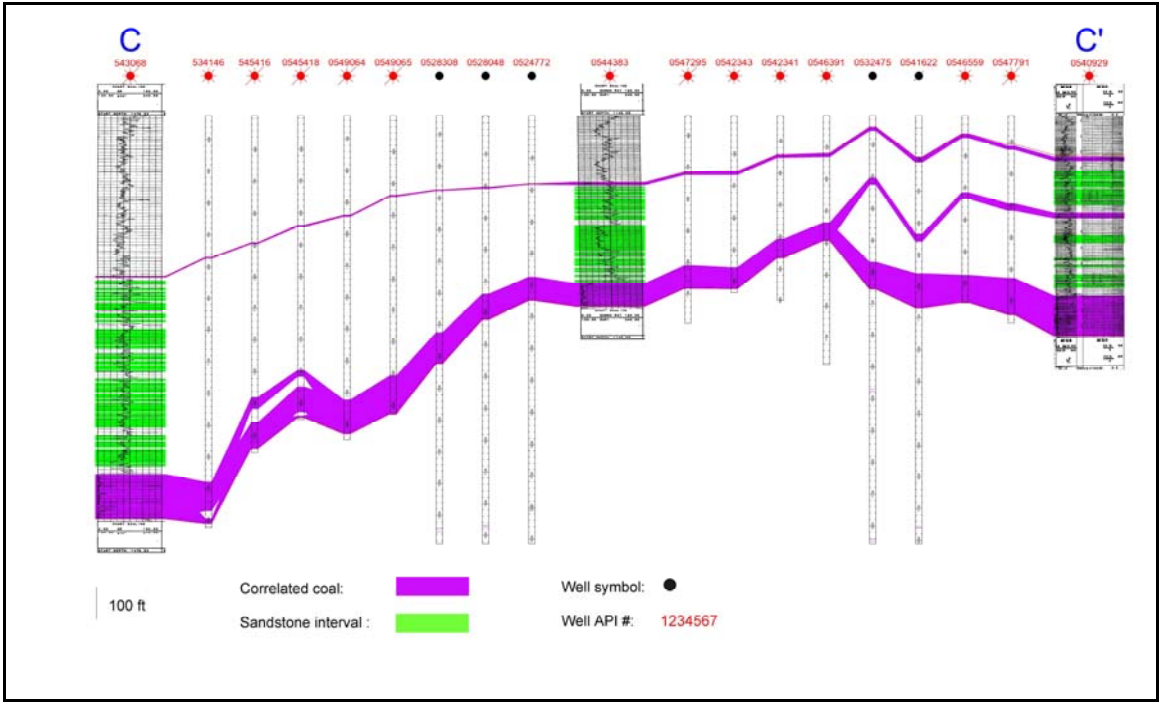


Figure 19. Cross-section C-C' (T. 44 N., R. 76 W. – R. 73 W.).

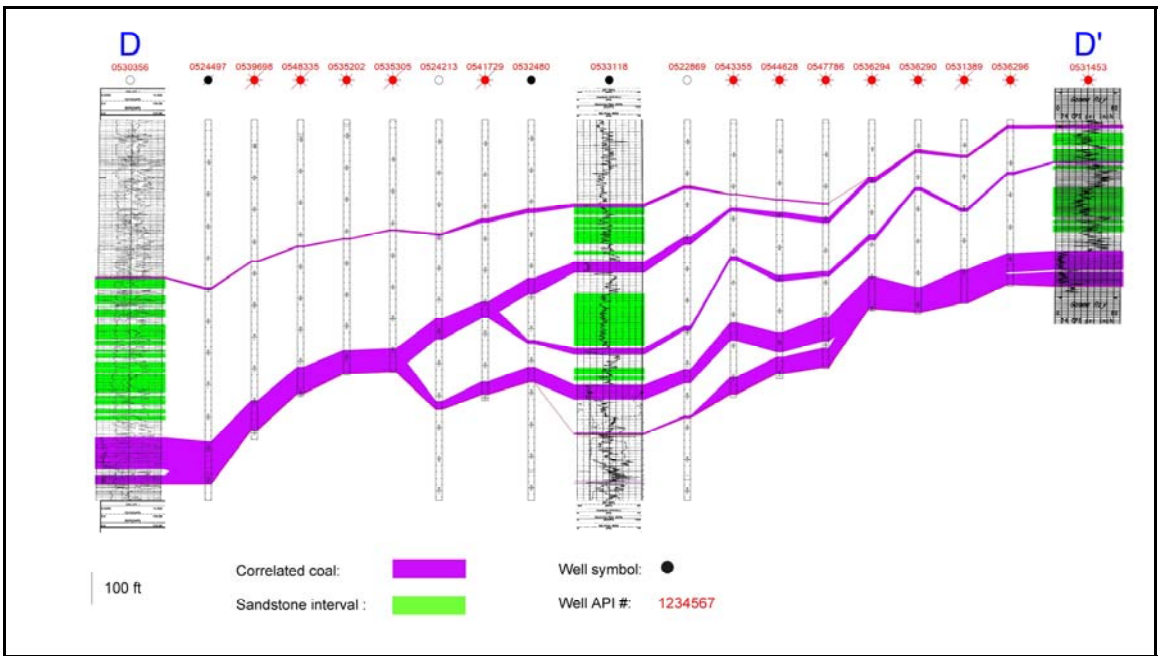


Figure 20. Cross-section D-D' (T. 45 N., R. 75 W. – R. 72 W.).

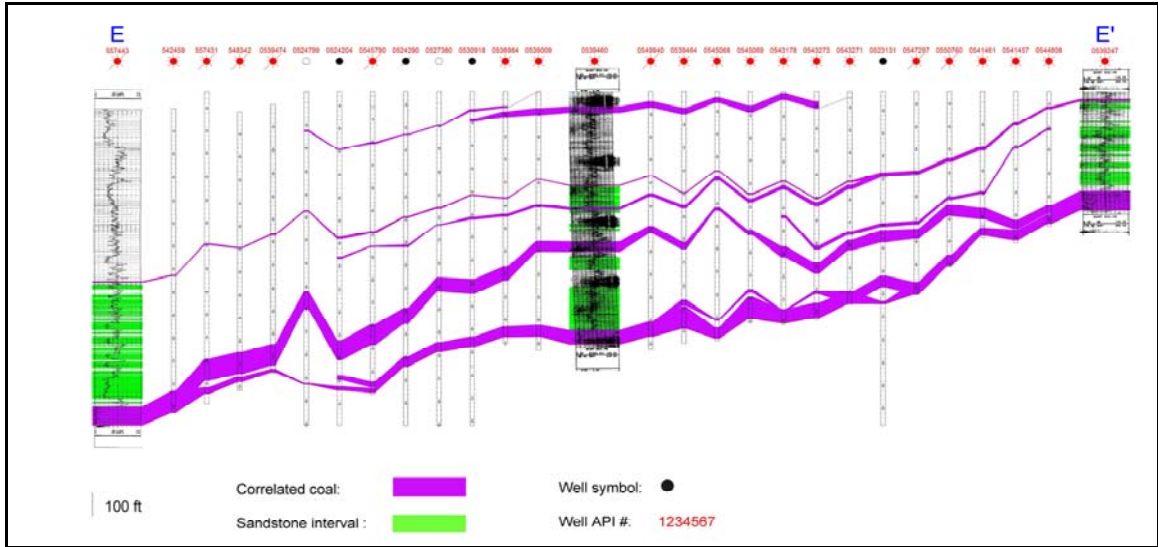


Figure 21. Cross-section E-E' (T. 46 N., R. 75 W. – R. 72 W.).

The east-west cross sections located in the central part of the study area are more complex. Here, the location of the initial split of the lower coalbed, noted previously, has migrates beyond the western border of the study area. Complete correlation of the coal seams cannot be preformed due to the uncertainty of the thin coalbeds' independency or lateral core coalbed counterpart. Figure 22 shows the location of the east-west cross sections in the central part of the study area.

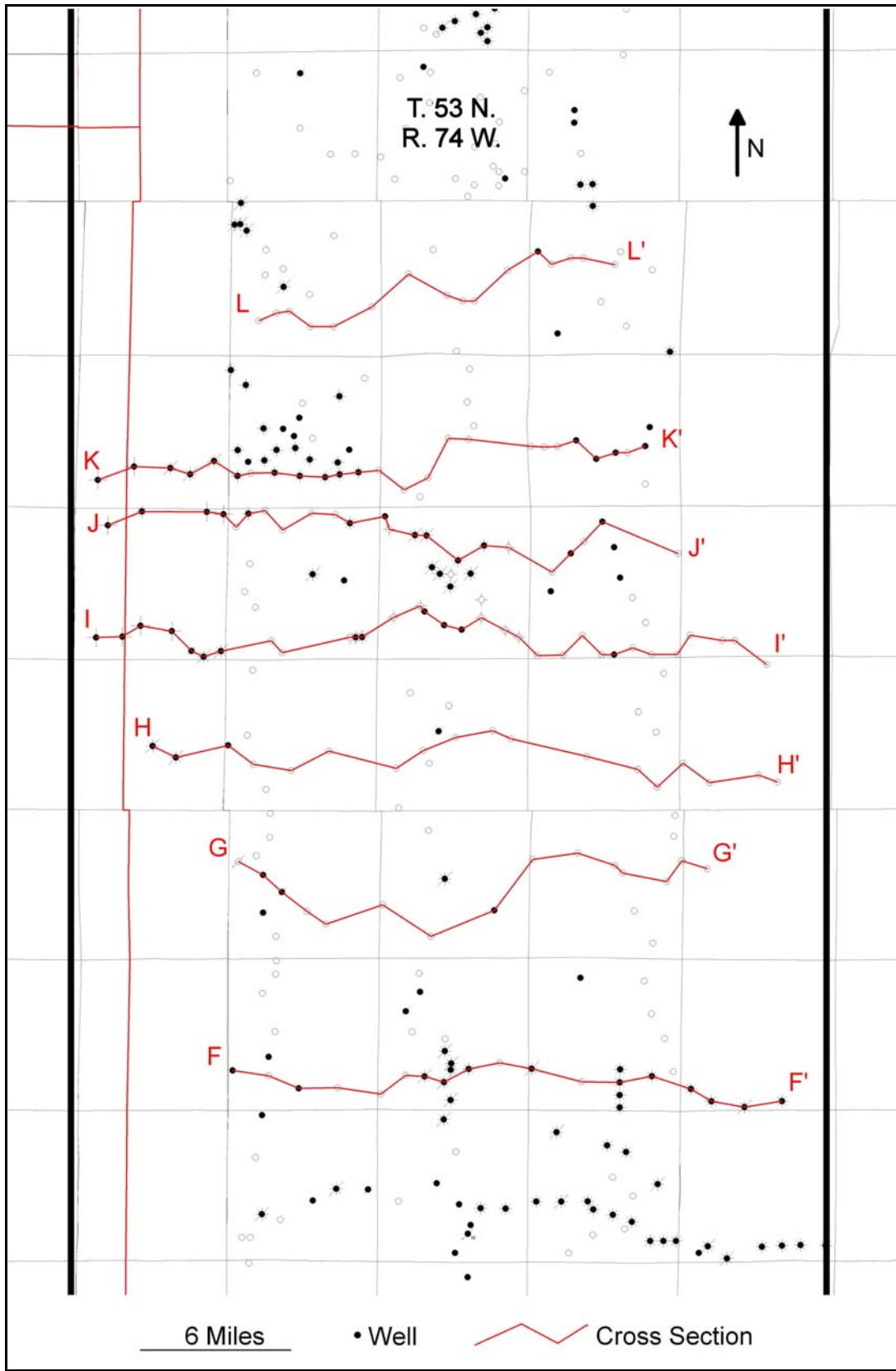


Figure 22. Central part of study area with locations of cross-sections F-F' through L-L'.

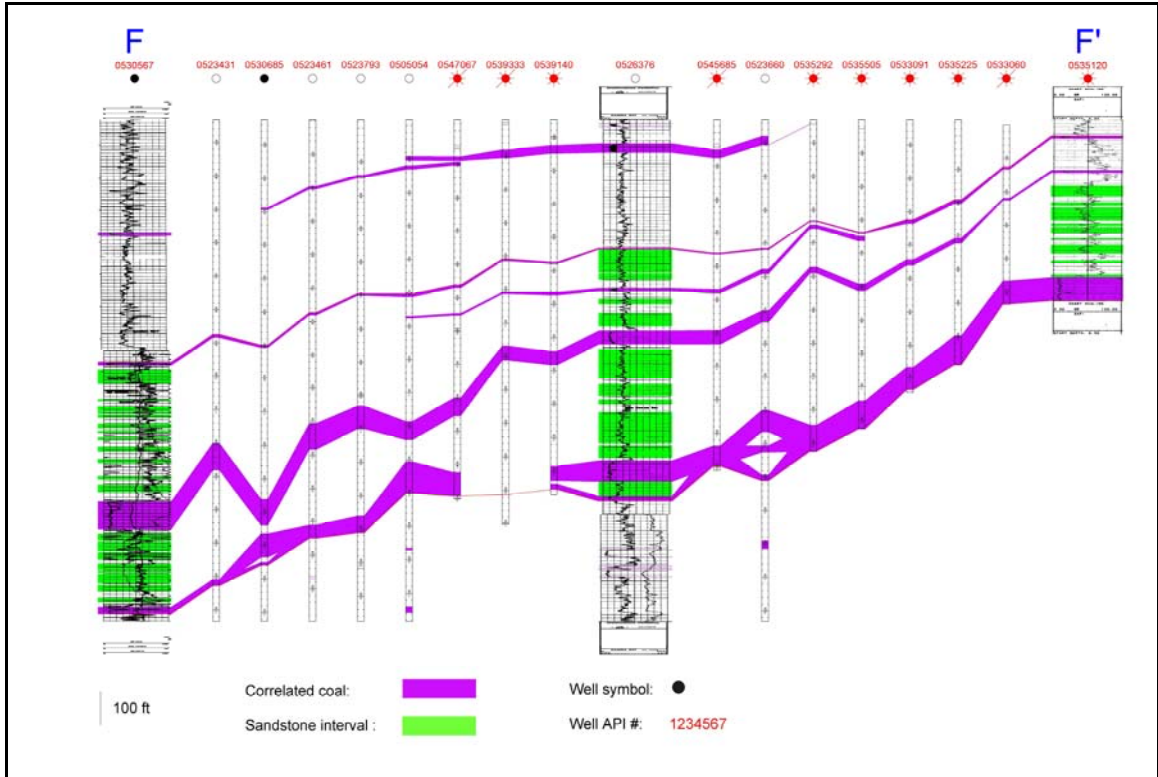


Figure 23. Cross-section F-F' (T. 47 N., R. 75 W. – R. 72 W.).

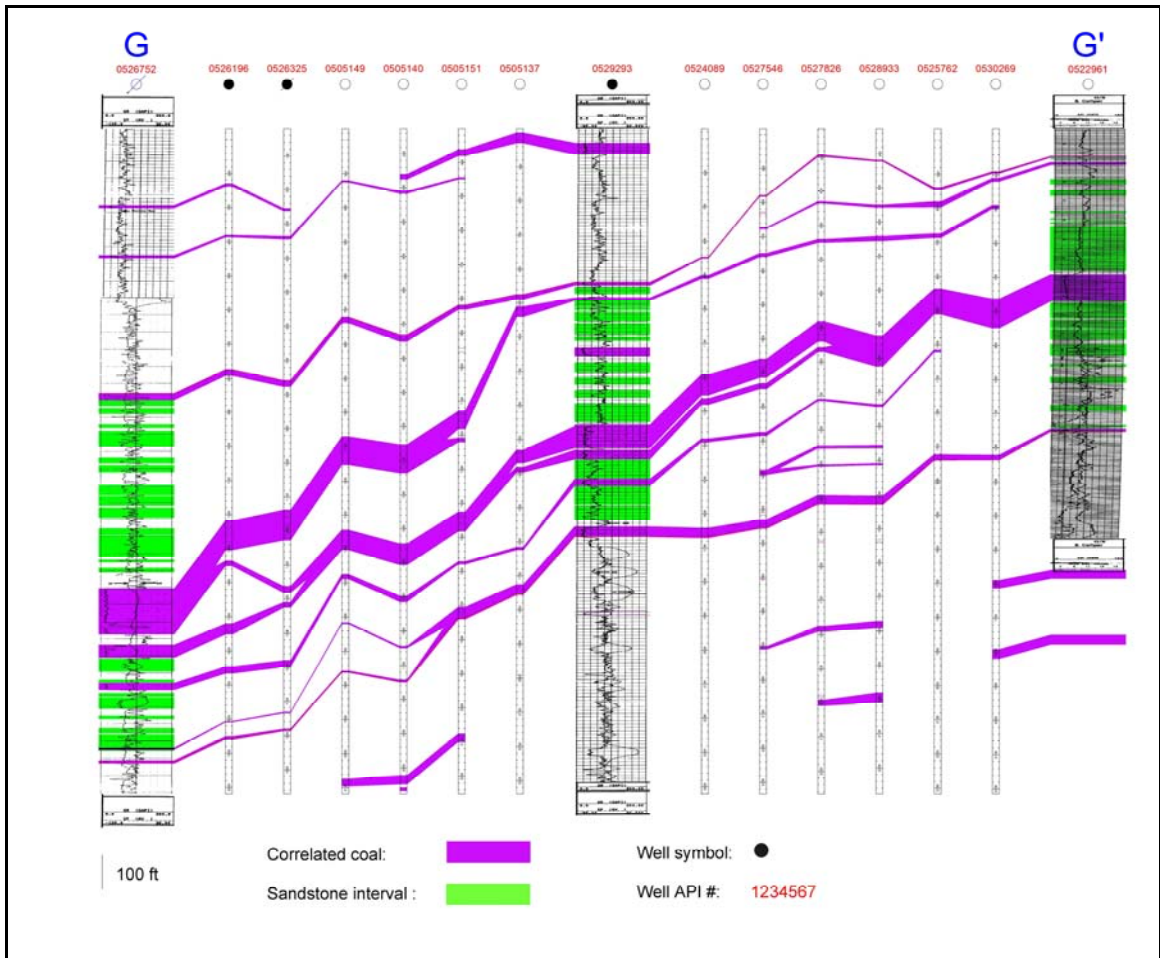


Figure 24. Cross-section G-G' (T. 48 N., R. 75 W., - R. 72 W.).

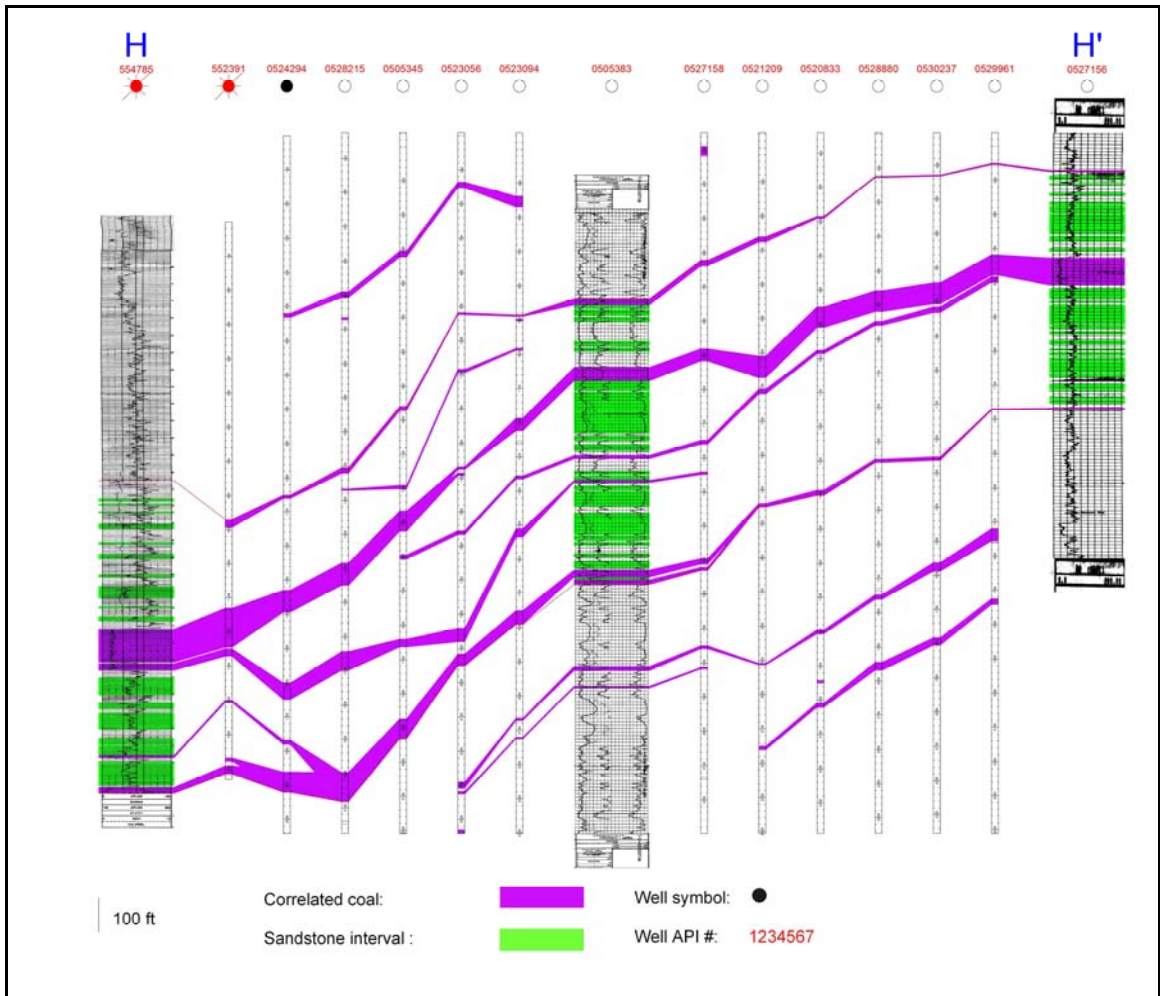


Figure 25. Cross-section H-H' (T. 49 N., R. 76 W. – R. 72 W.).

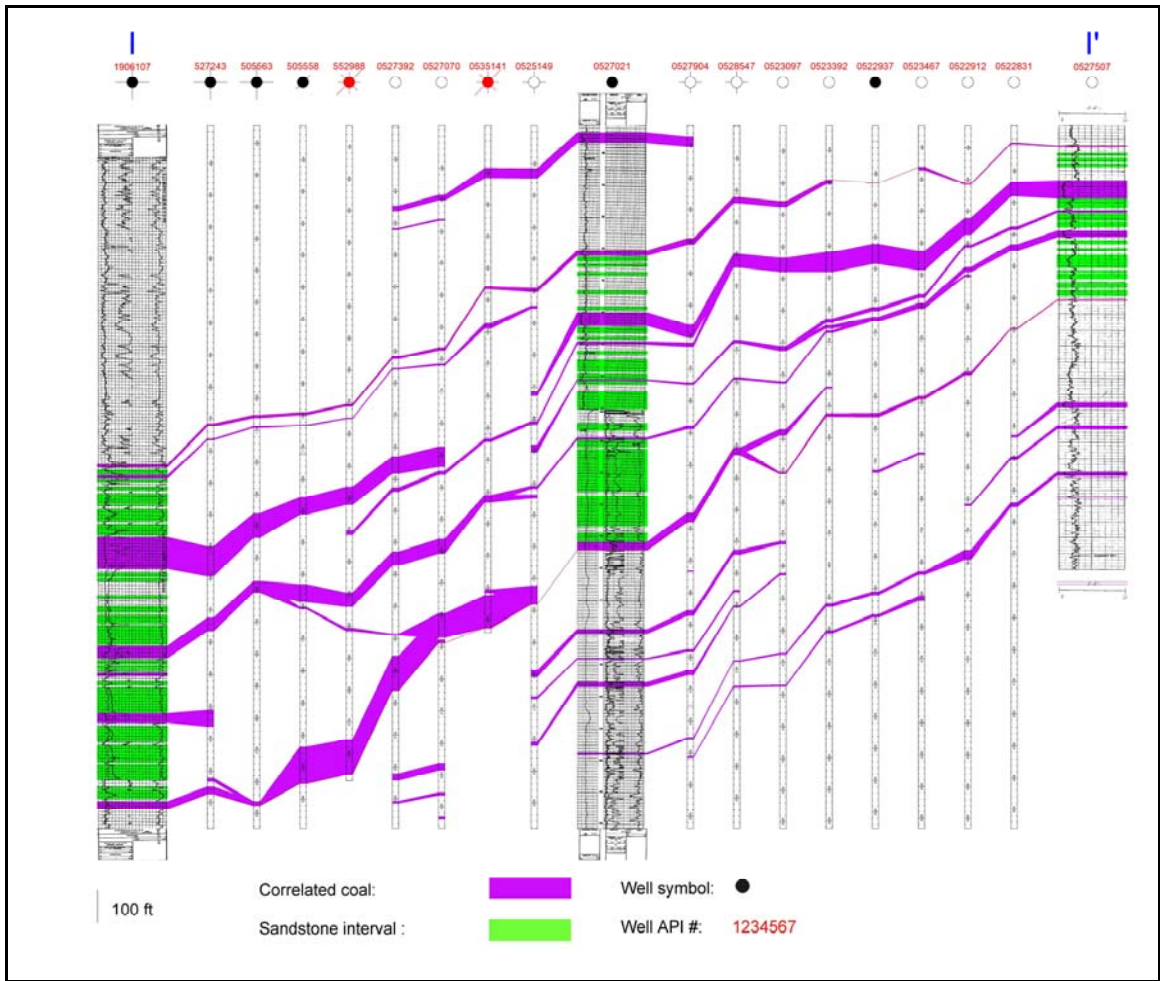


Figure 26. Cross-section I-I' (T. 50 N., R. 76 W. – R. 72 W.).

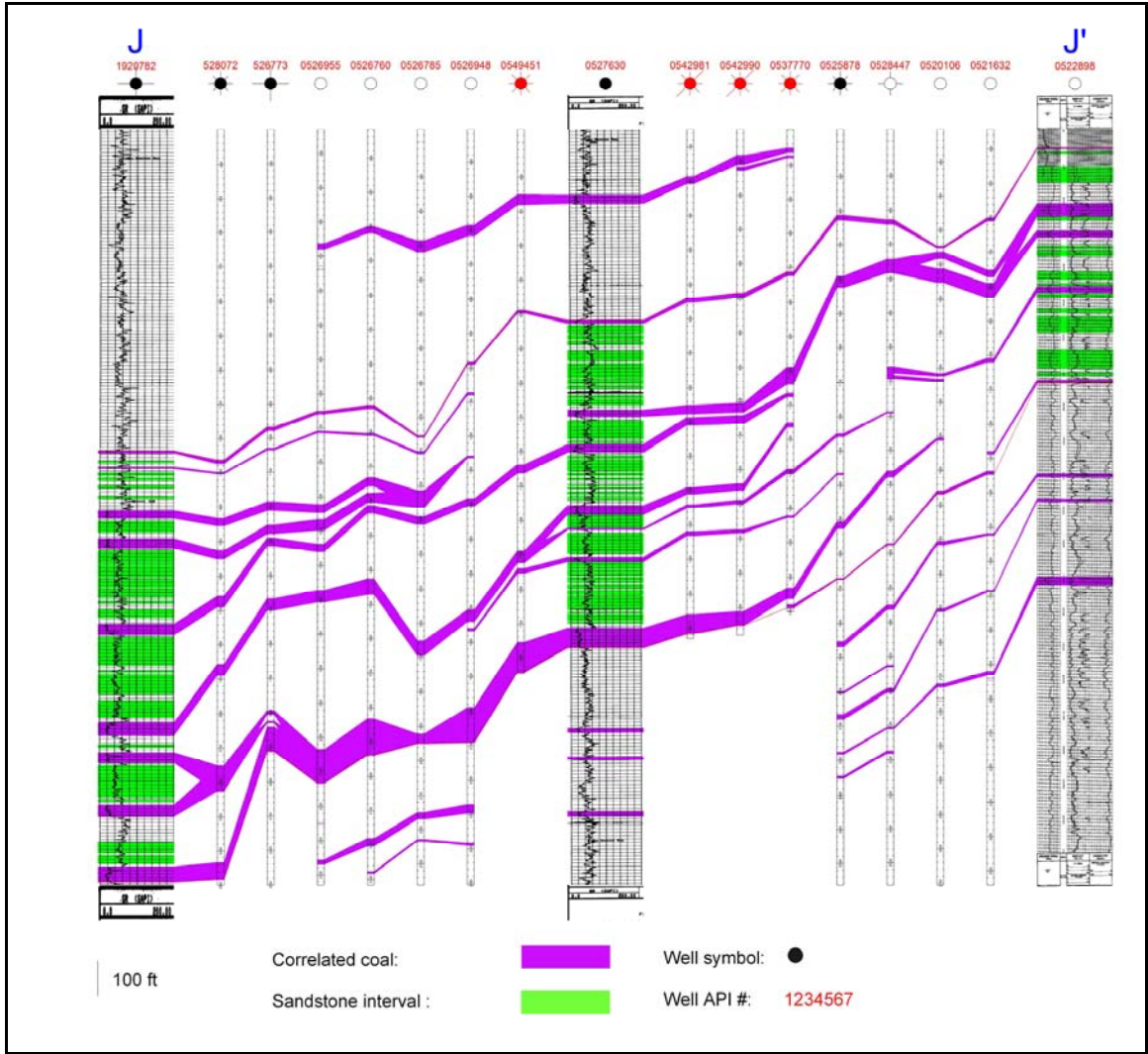


Figure 27. Cross-section J-J' (T. 50 N., R. 76 W. – R. 73 W.).

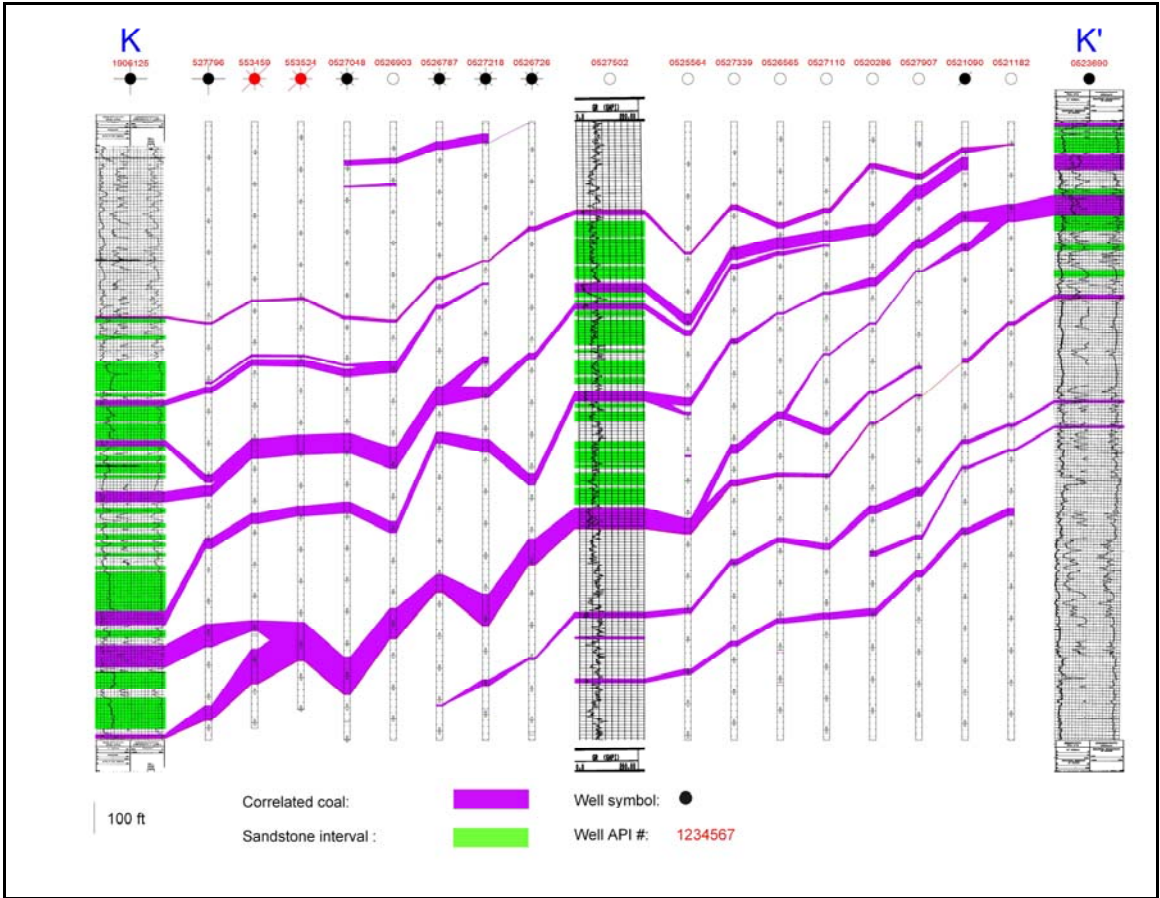


Figure 28. Cross-section K-K' (T. 51 N., R. 76 W. – R. 73 W.).

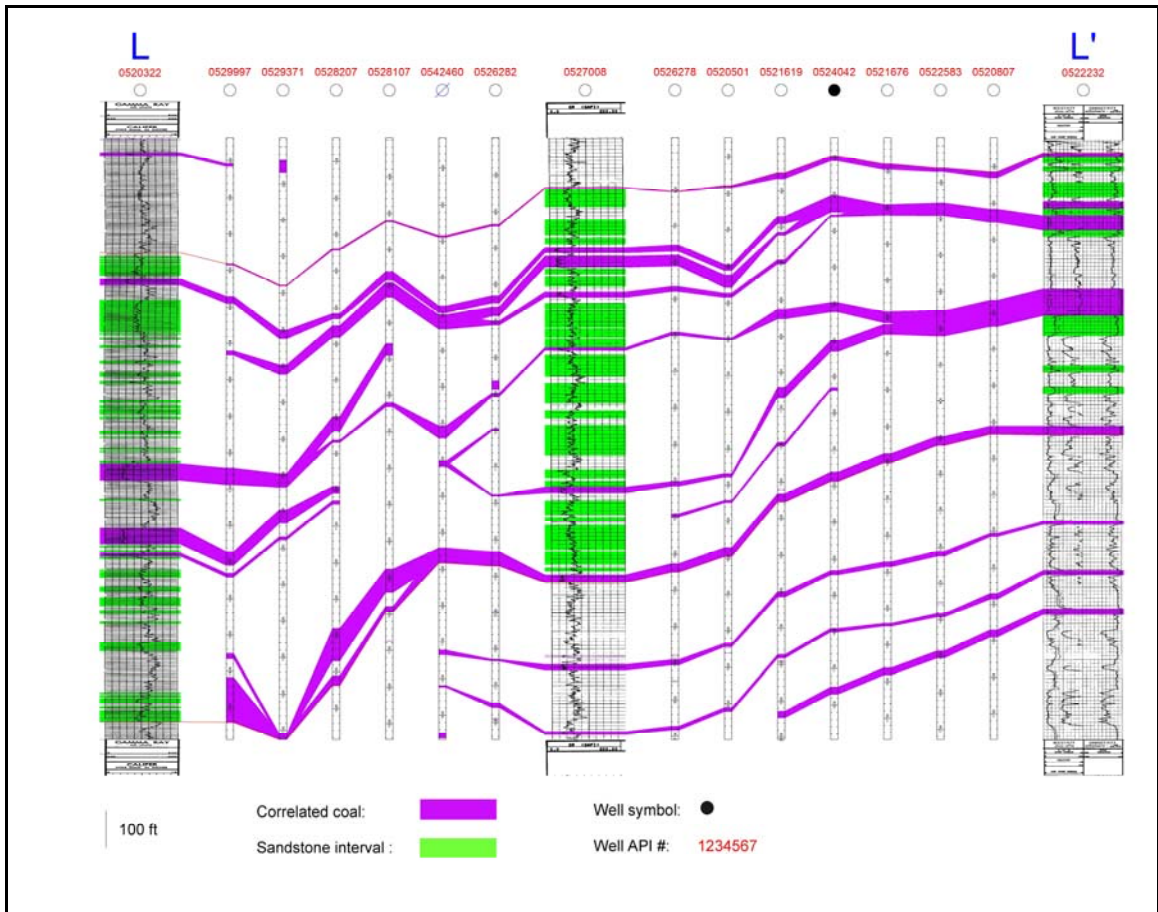


Figure 29. Cross-section L-L' (T. 52 N., R. 75 W. – R. 73 W.).

The east-west cross sections located in the northern part of the study area display both the total study interval from the Smith to the Pawnee coal seams, when present, and the abbreviated Anderson to Pawnee coal seams in locations where the Smith either was not logged or was exposed and eroded. The entire interval is marked at the top and bottom with gray picks indicating the sandstone bodies. The abbreviated interval consists of light gray picks indicating the sandstone bodies. The coalbeds in the northern part of the study area are complex, but do not display the same variability in coal thickness or degree of splitting as evidenced in the central cross sections. Figure 30 shows the location of east-west cross sections in the northern part of the study area.

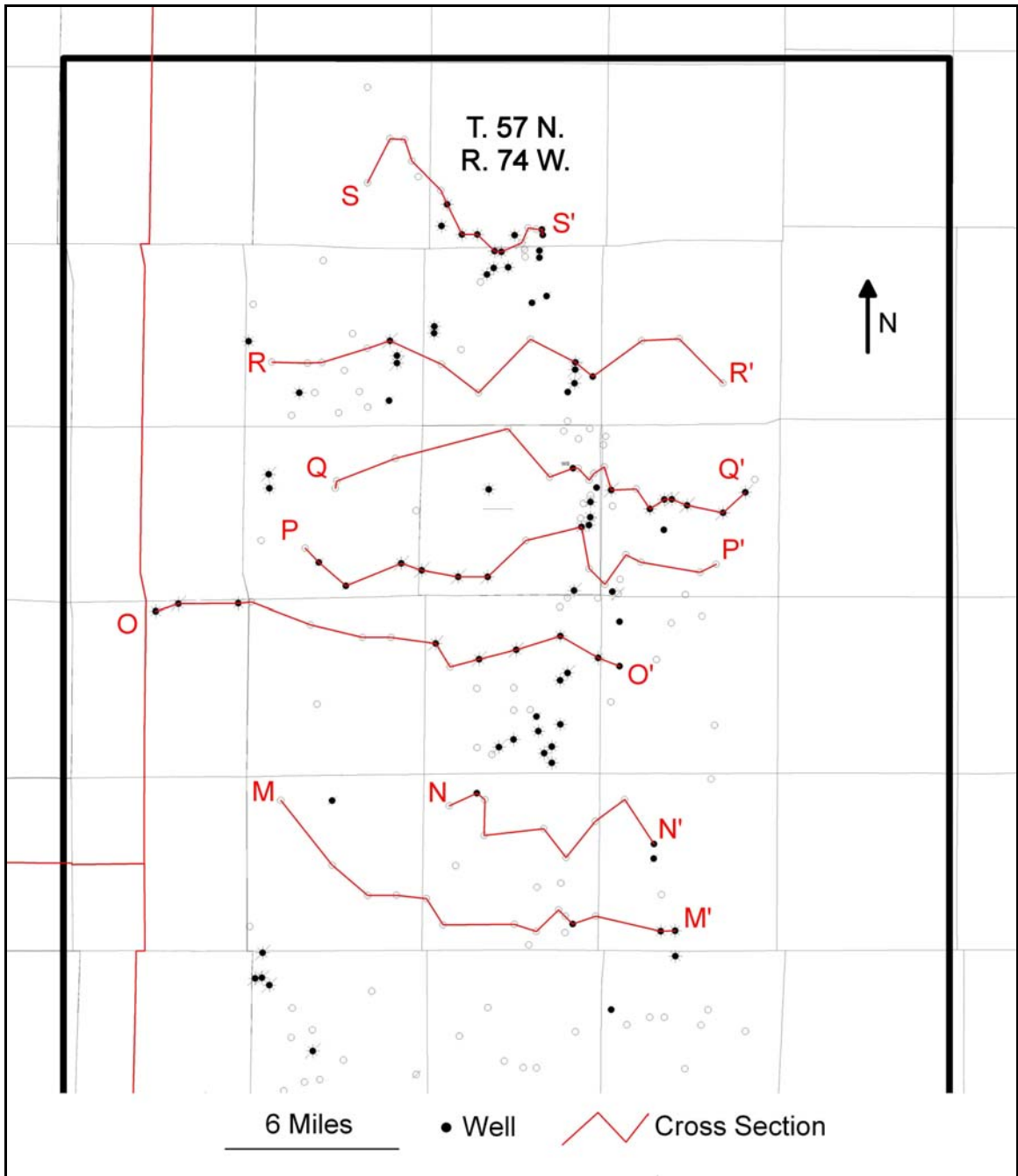


Figure 30. Northern part of study area with location of cross-sections M-M' through S-S'.

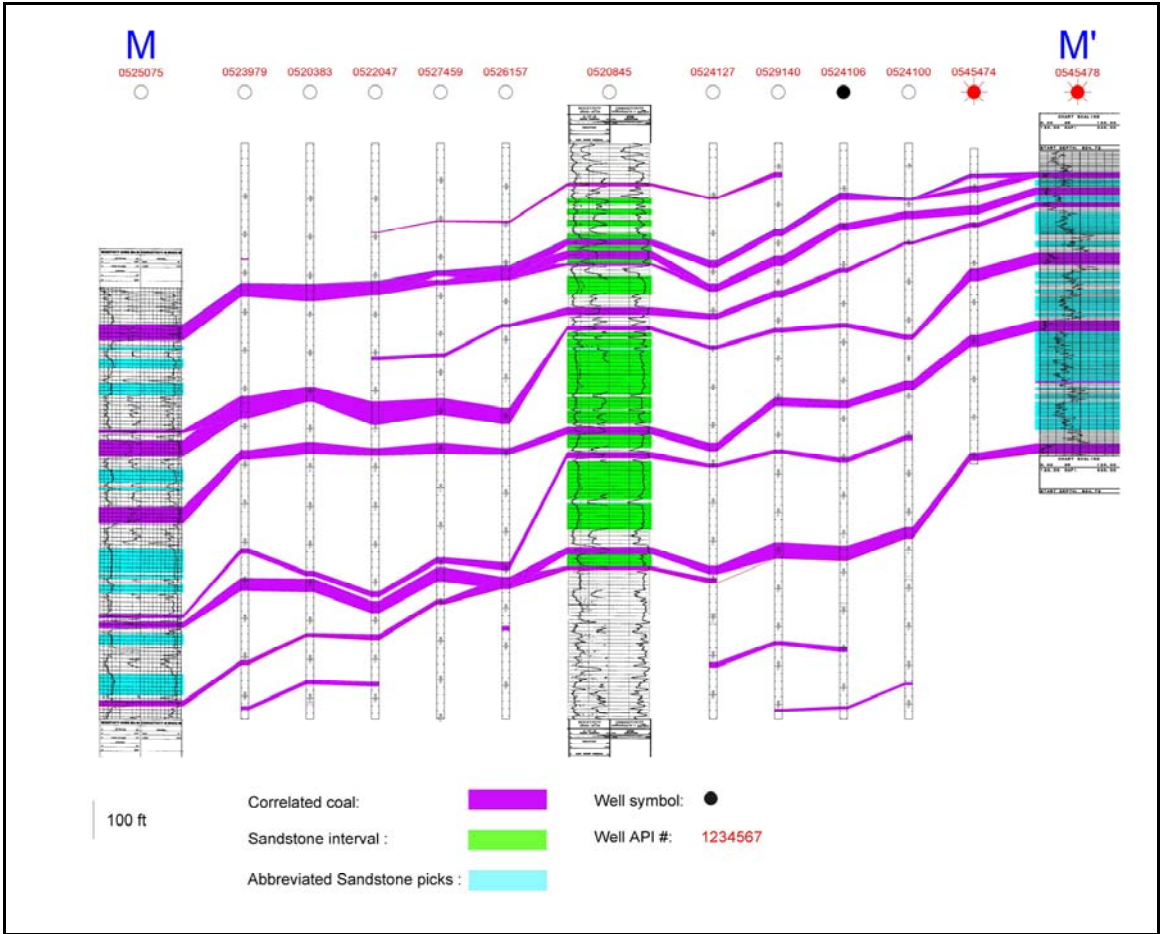


Figure 31. Cross-section M-M' (T. 53 N., R. 75 W. – R. 73 W.).

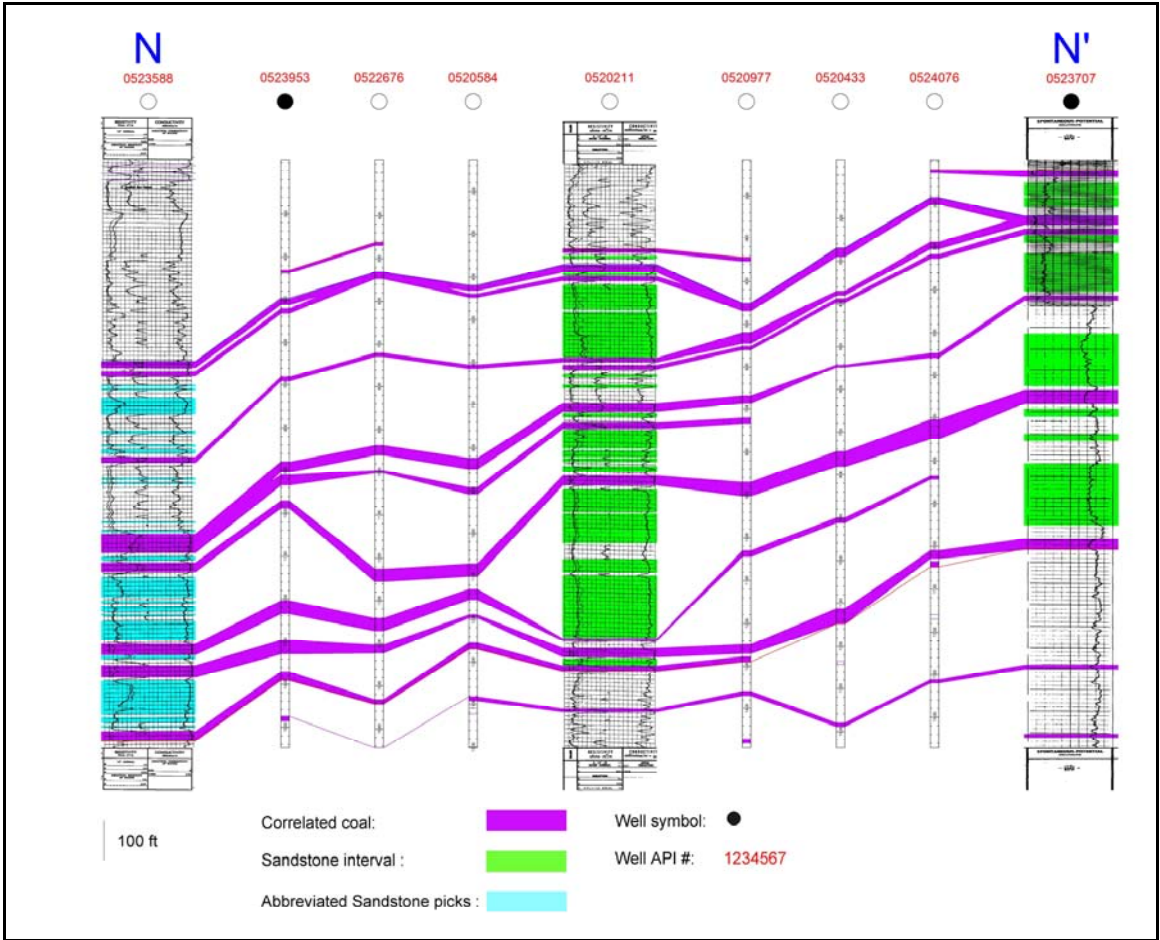


Figure 32. Cross-section N-N' (T. 53 N., R. 74 W. – R. 73 W.).

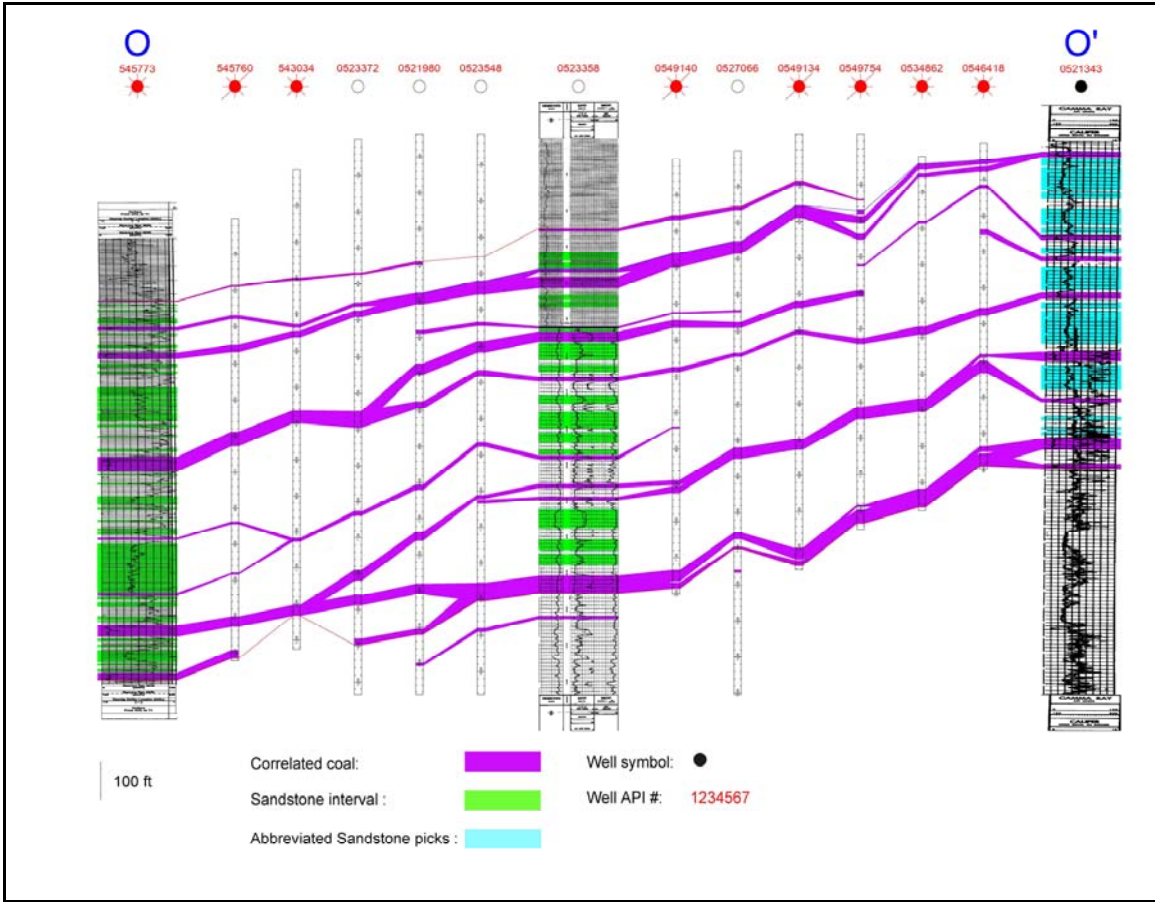


Figure 33. Cross-section O-O' (T. 54 N., R. 76 W. – R. 73 W.).

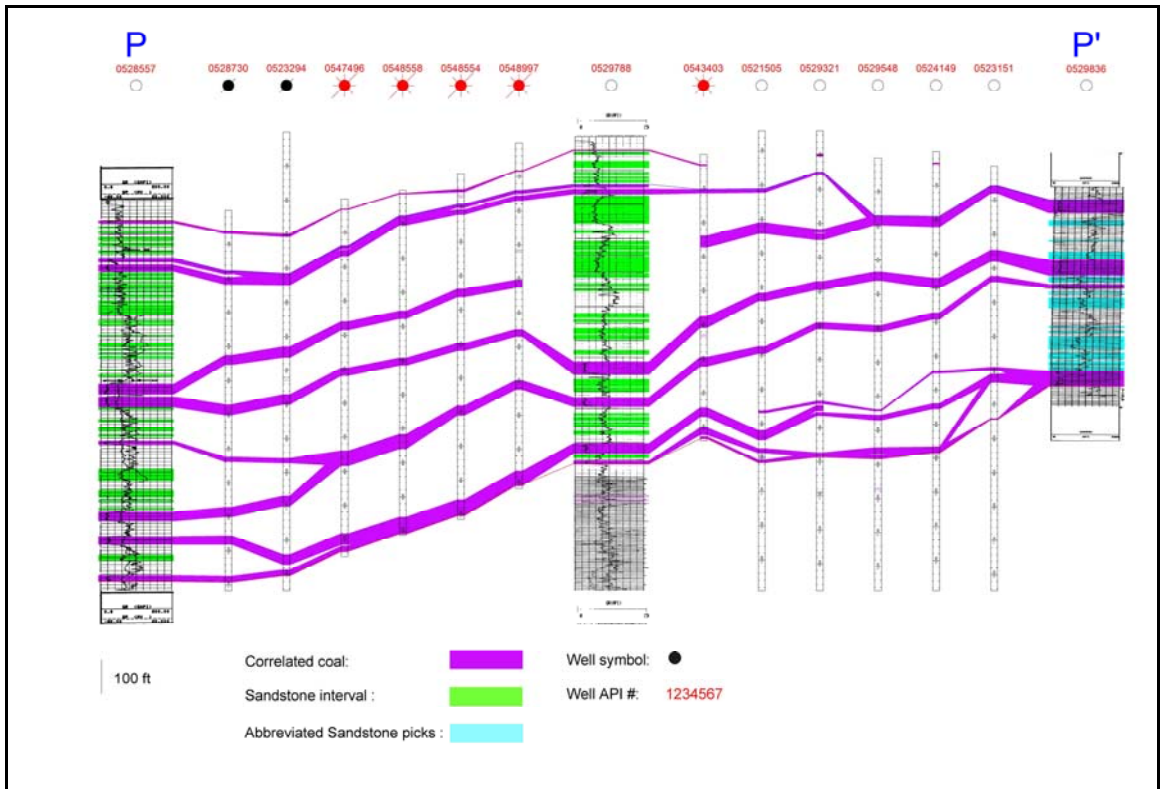


Figure 34. Cross-section P-P' (T. 55 N., R. 75 W. – R. 73 W.).

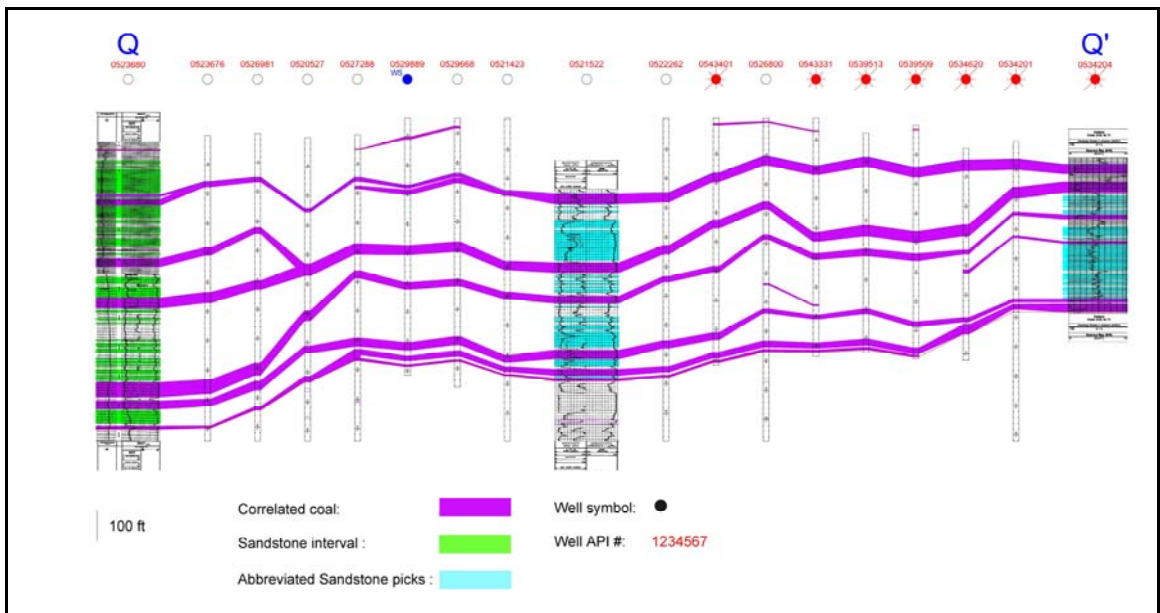


Figure 35. Cross-section Q-Q' (T. 55 N., R. 75 W. – R. 73 W.).

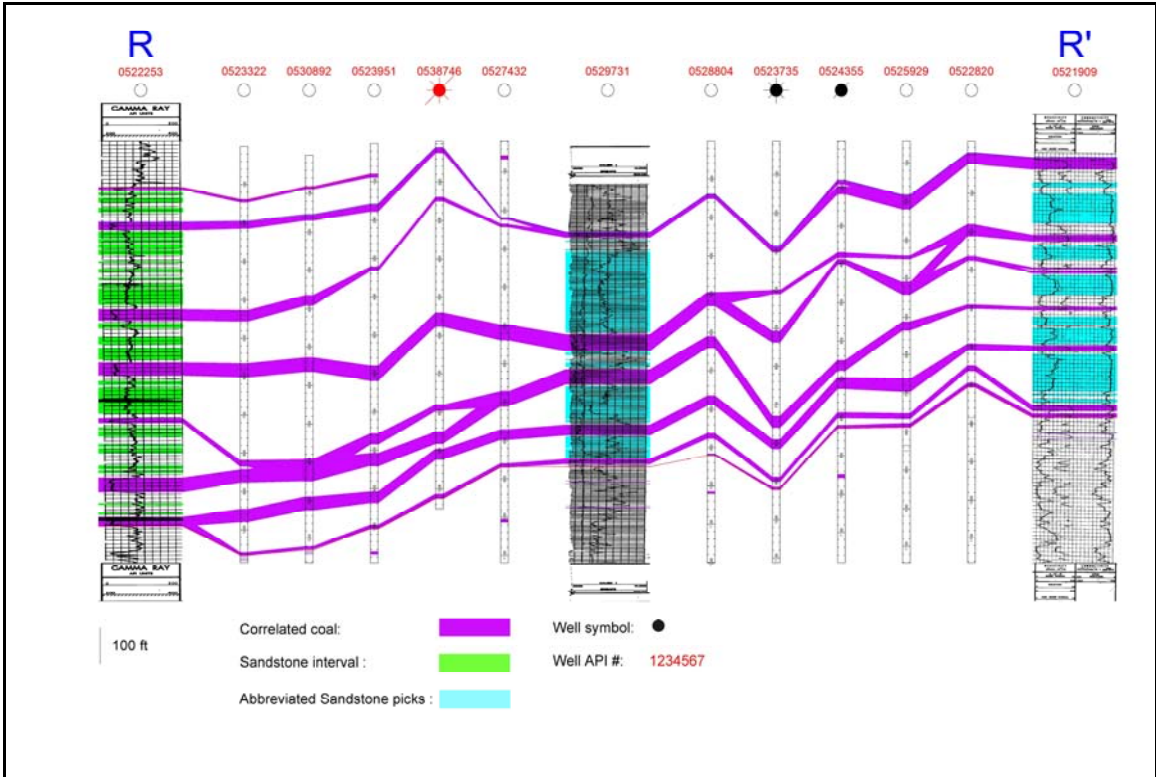


Figure 36. Cross-section R-R' (T. 56 N., R. 75 W. – R. 73 W.).

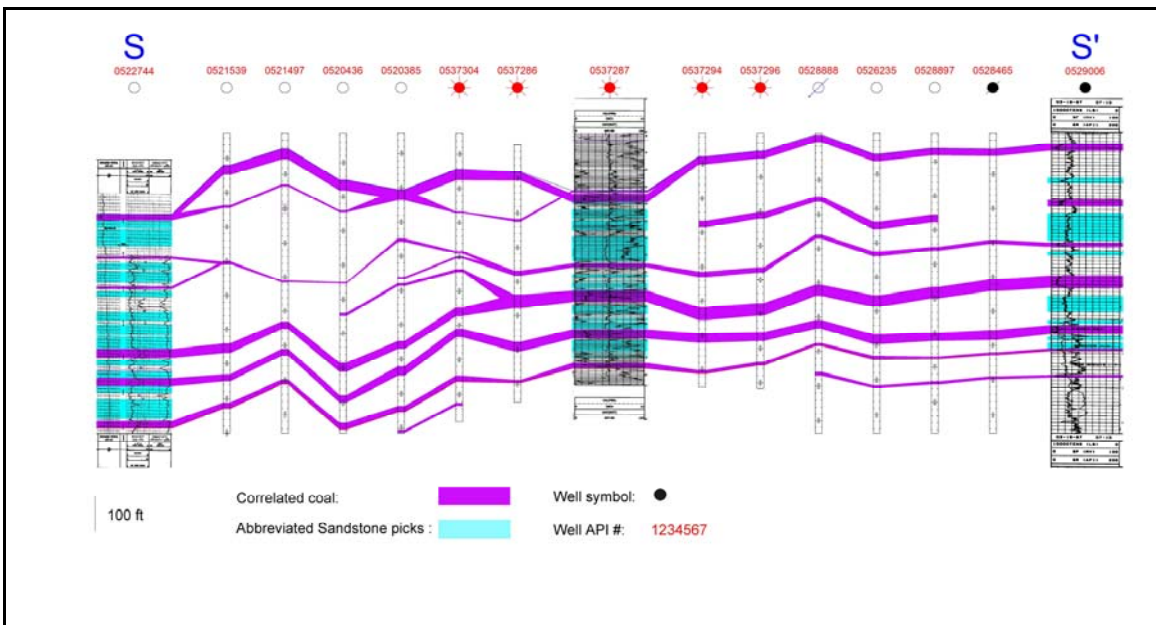


Figure 37. Cross-section S-S' (T. 57 N., R. 75 W. – R. 74 W.).

The north-south cross sections express change in the overall coal characteristics similar to the three sets of east-west cross sections. The coalbeds vary from a more uniform thickness and limited coal splitting in the north, to variable thickness and a high frequency of coalbeds splitting in the central region, to the simpler, two-coal interval in the south. Figure 38 displays the locations of the three north-south cross sections in the study area.

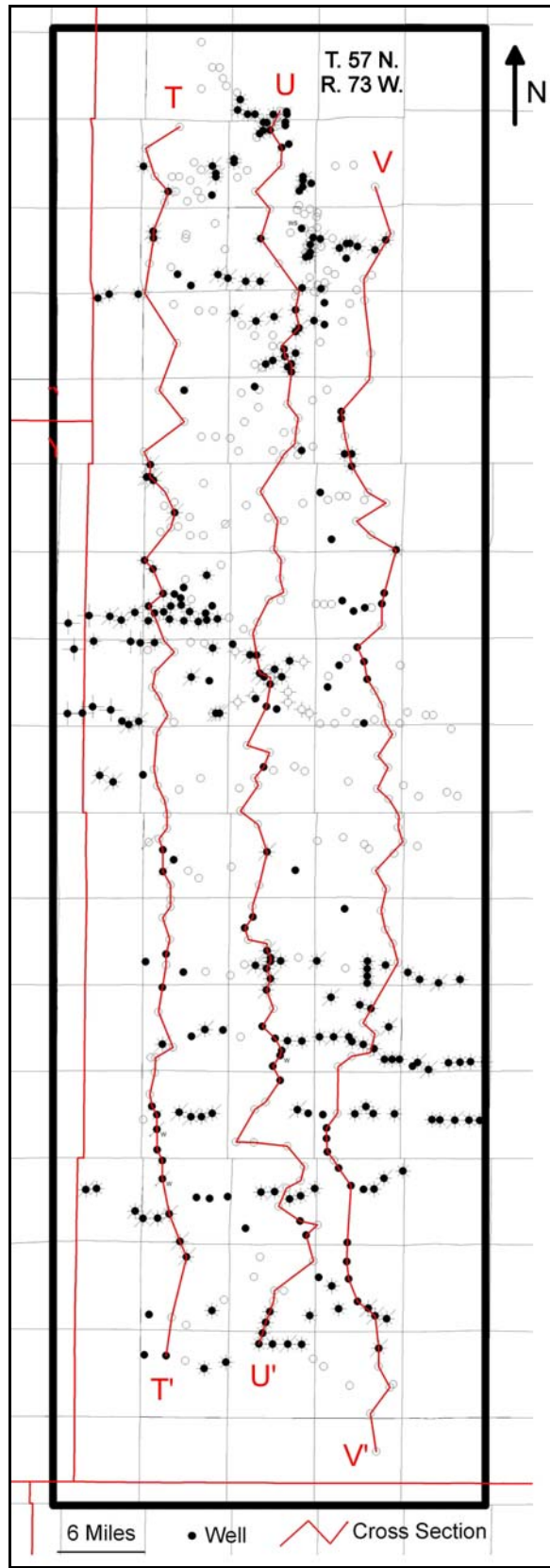


Figure 38. Study area with the location of cross-sections T-T', U-U', and V-V'.

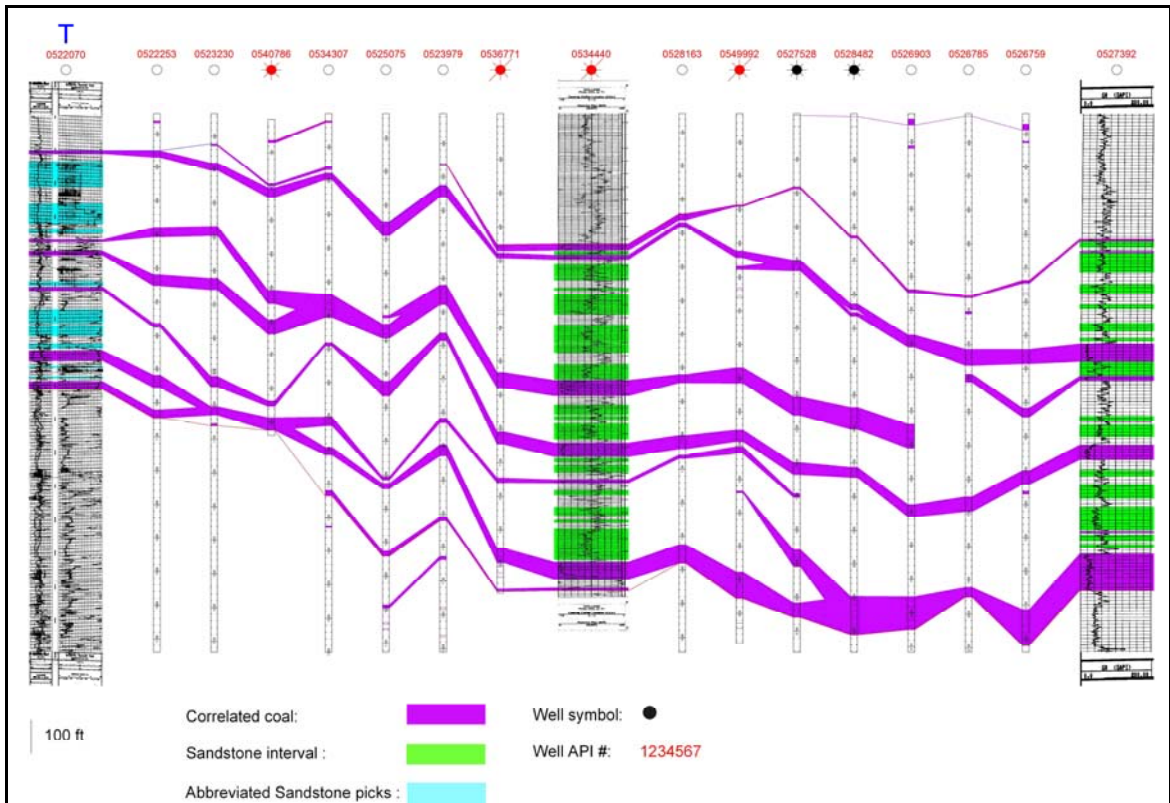


Figure 39a. Cross-section T-T' (T. 57 N. – T. 42 N., R. 75 W.).



Figure 39b. Cross-section T-T', continued.

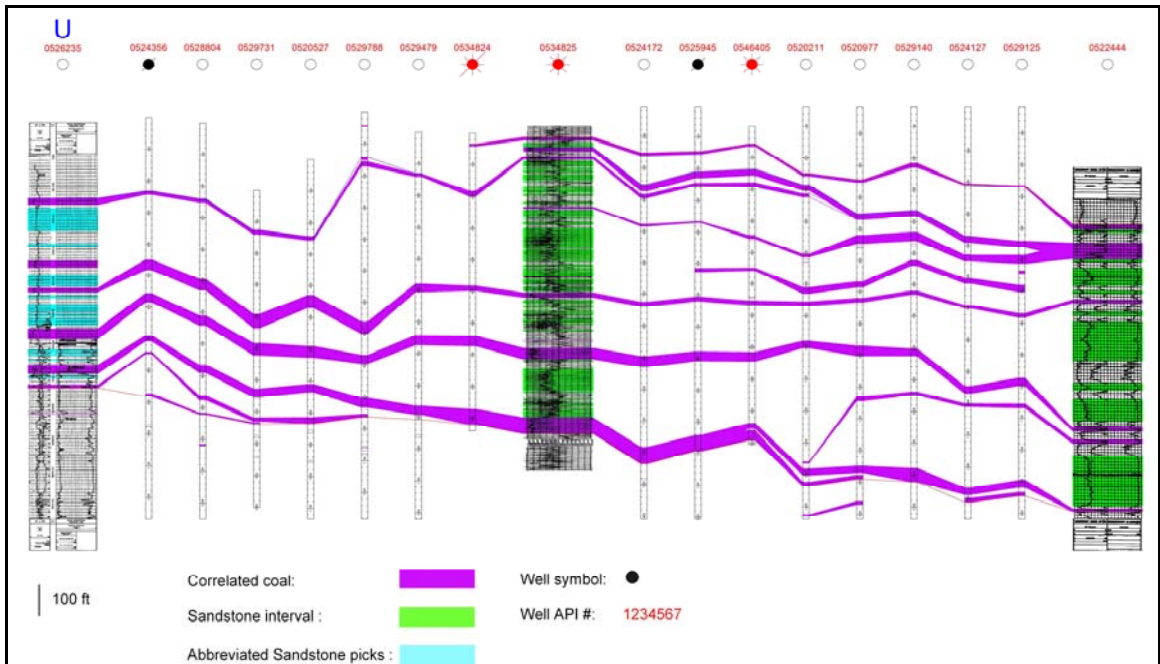


Figure 40a. Cross-section U-U' (T. 57 N. – T. 42 N., R. 74 W.).

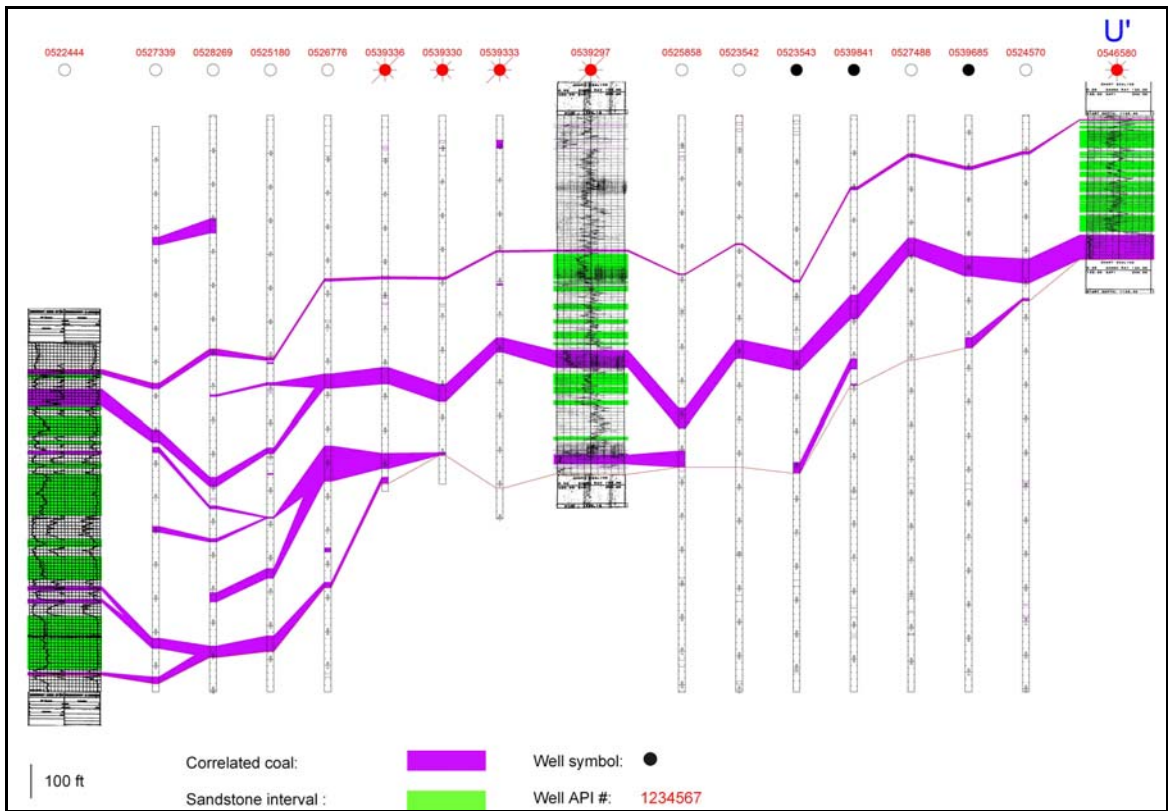


Figure 40b. Cross-section U-U', continued.

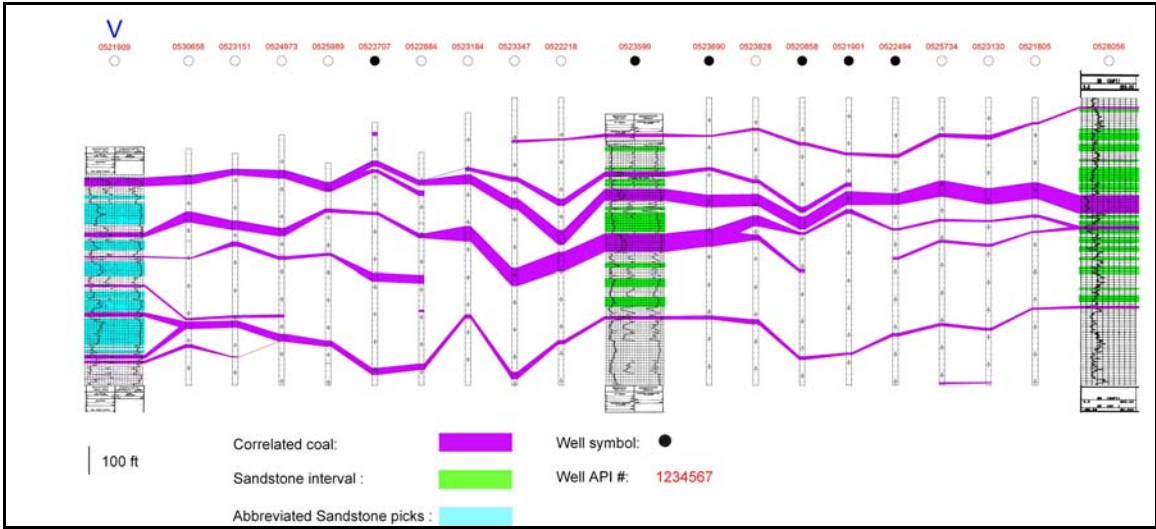


Figure 41a. Cross-section V-V' (T. 56 N. – T. 42 N., R. 73 W.).

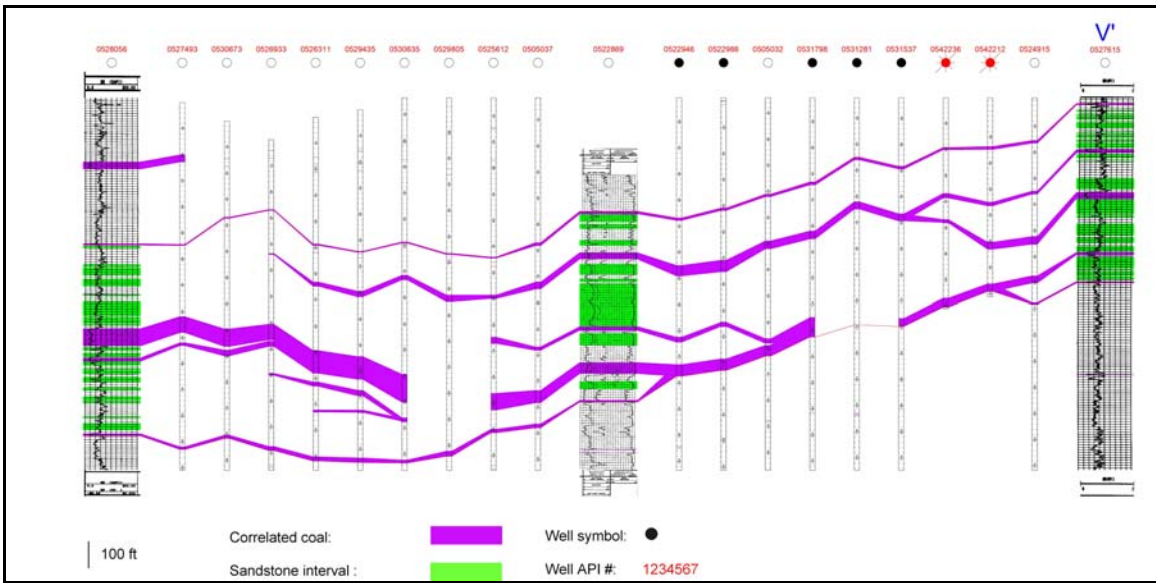


Figure 41b. Cross-section V-V', continued.

The resulting total coal and sandstone thickness data compiled from the wireline logs were used to create isopach maps using PETRA. These maps include a total interval thickness map, a total sandstone thickness map, and a sandstone ratio isopach map for the complete study interval as well as for the abbreviated interval in the northern part of the study area.

The total interval thickness isopach map (Figure 42) shows a general thickening of the study interval towards the basin axis, west of the study area. The greatest thicknesses are located in T. 51 N., R. 76 W. and T. 52 N., R. 76 W. The sandstone thickness isopach map of the entire interval (Figure 43) displays a thicker area in the central part of the map, typically within T. 48 N., R. 74 W. to T. 54 N., R. 74 W. The higher thicknesses also extend west into the same general location as the thickest part shown in Figure 42. The sandstone to total thickness ratio isopach map (Figure 44) expresses a similarly thick sandstone anomaly as seen in Figure 43.

The sandstone anomaly extends the entire length of the study area in the north-south direction. The data suggest that the sandstone anomaly is sinuous, with limbs connecting to the main trunk from the east at T. 46 N. and T. 49 N., R. 72 W. The greater thicknesses shown in Figures 42 and 43 suggest a similar limb may combine with the main trunk from the west at T. 51 N., R. 76 W. The general location of the anomalous swell in sandstone is similar to that of the lack of thick coals mapped in Goolsby and Finley's (2000) thickest coalbed isopach (Figure 13).

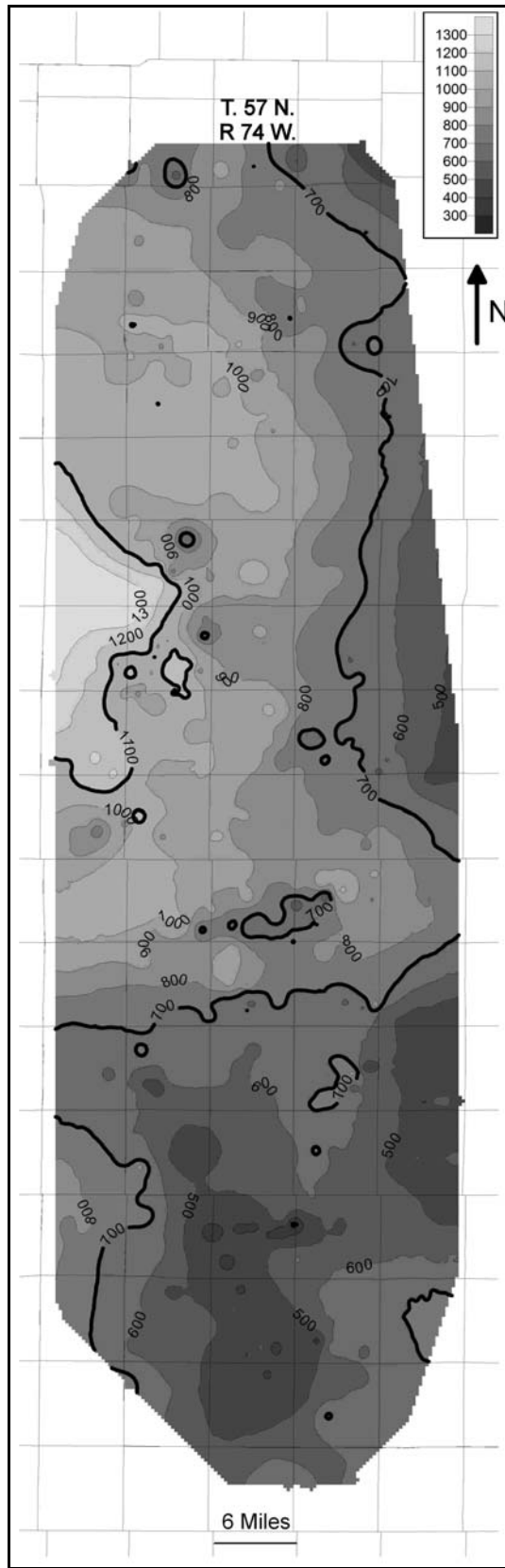


Figure 42. Total study interval thickness (in feet).

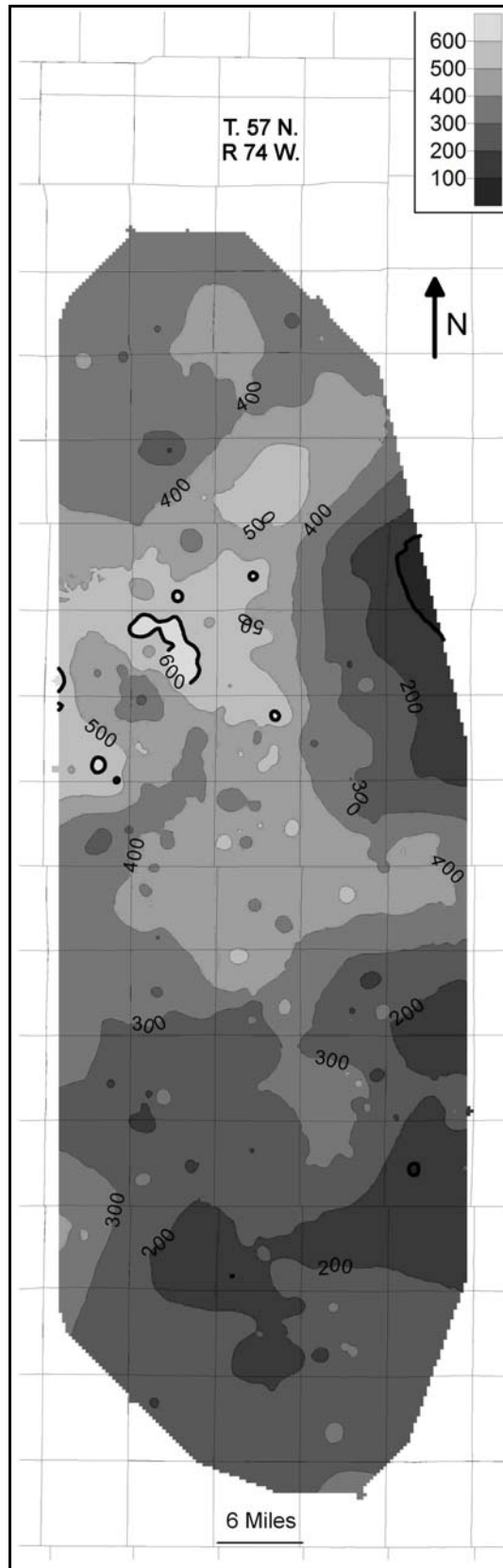


Figure 43. Total sandstone thickness for the study interval (in feet).

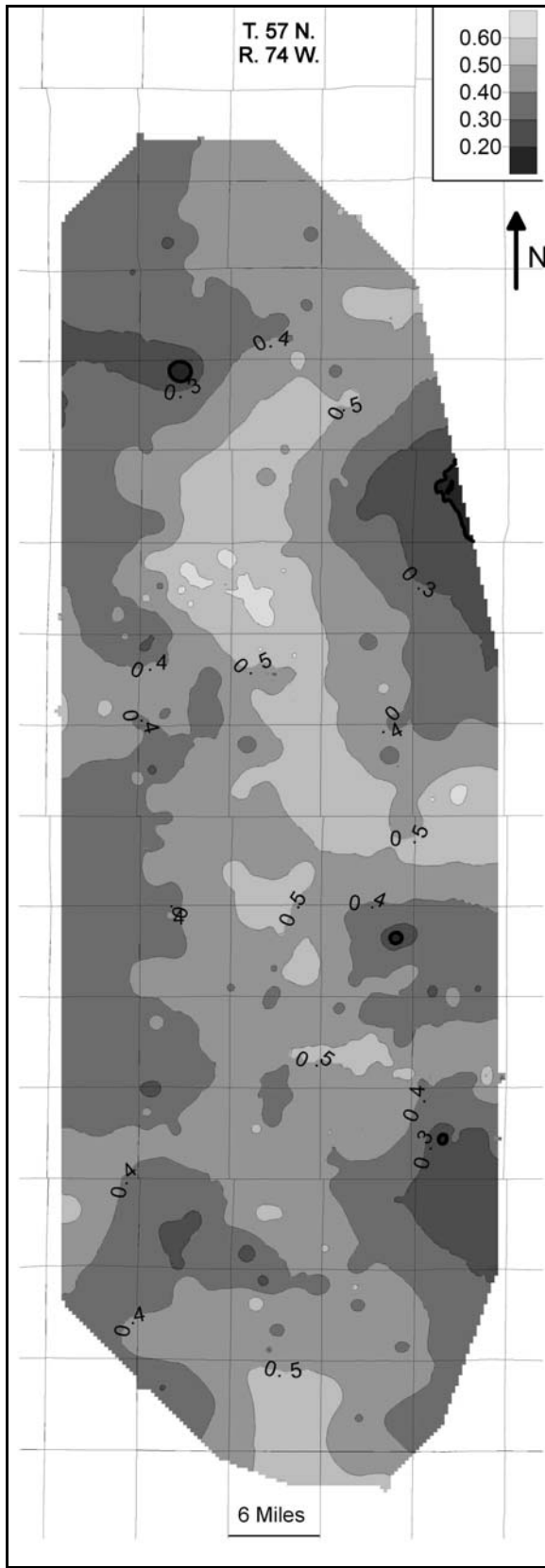


Figure 44. Sandstone to total interval ratio isopach map.

The second set of maps produced for the abbreviated interval in the north display similar trends in thicknesses and sandstone ratios as the first set of maps. The total thickness of the interval increases from east to west (Figure 45). Figures 46 and 47 indicate that the anomalous swell of sandstone extends north from T. 52 N., R. 74 W. to T. 57 N., R. 75 W.

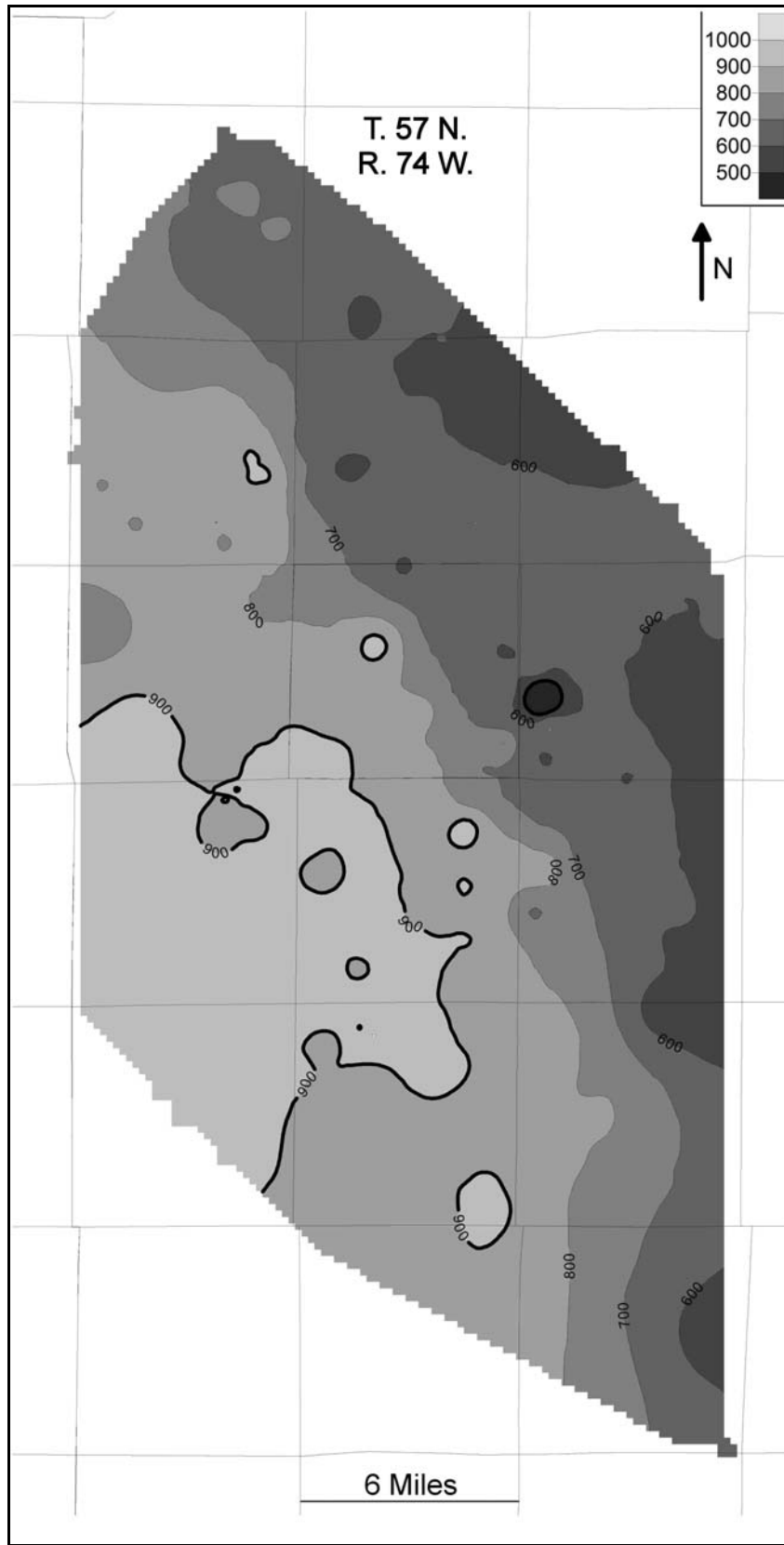


Figure 45. Thickness of the abbreviated interval in the north (in feet).

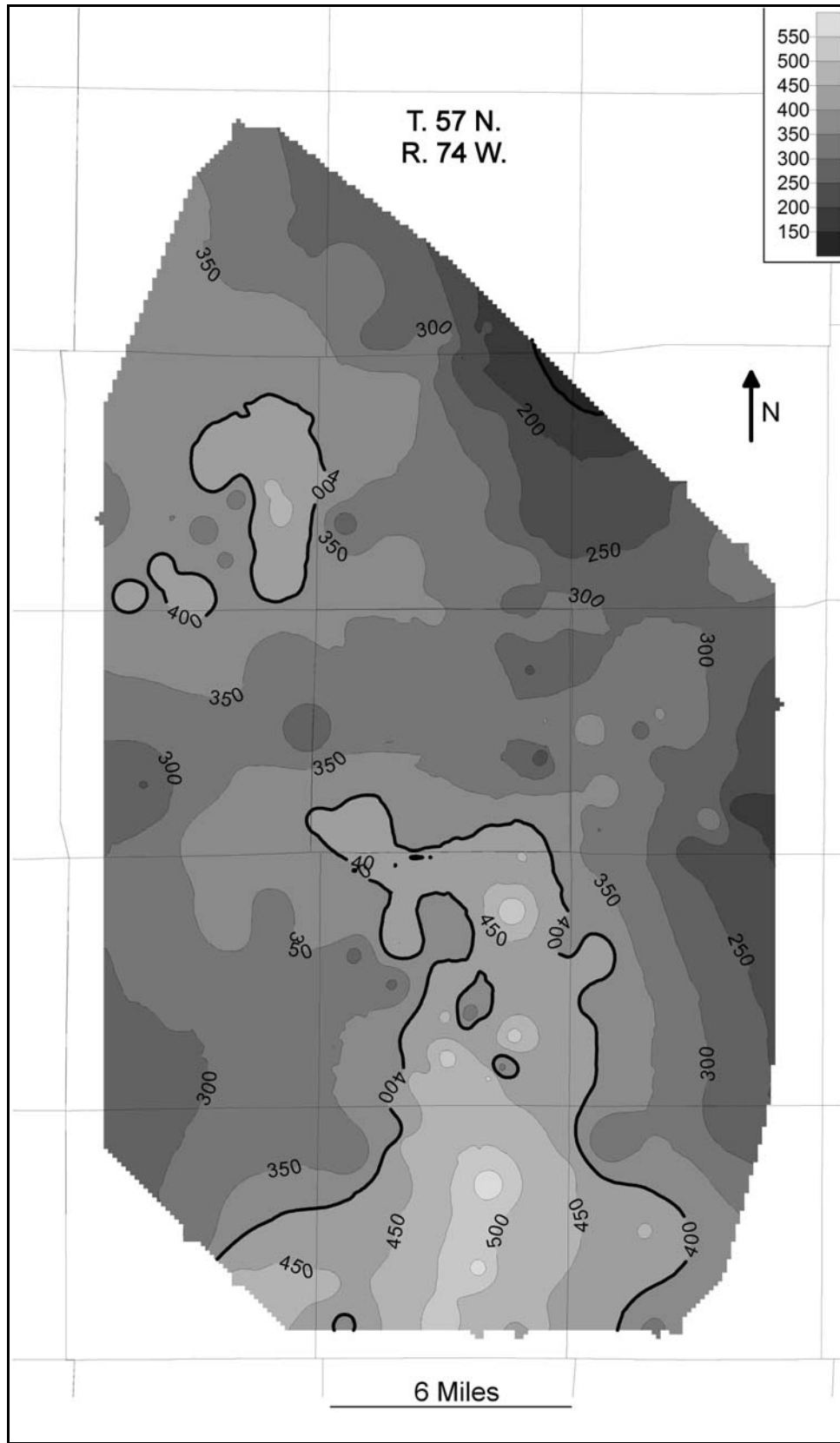


Figure 46. Sandstone thickness of the abbreviated interval in the north (in feet).

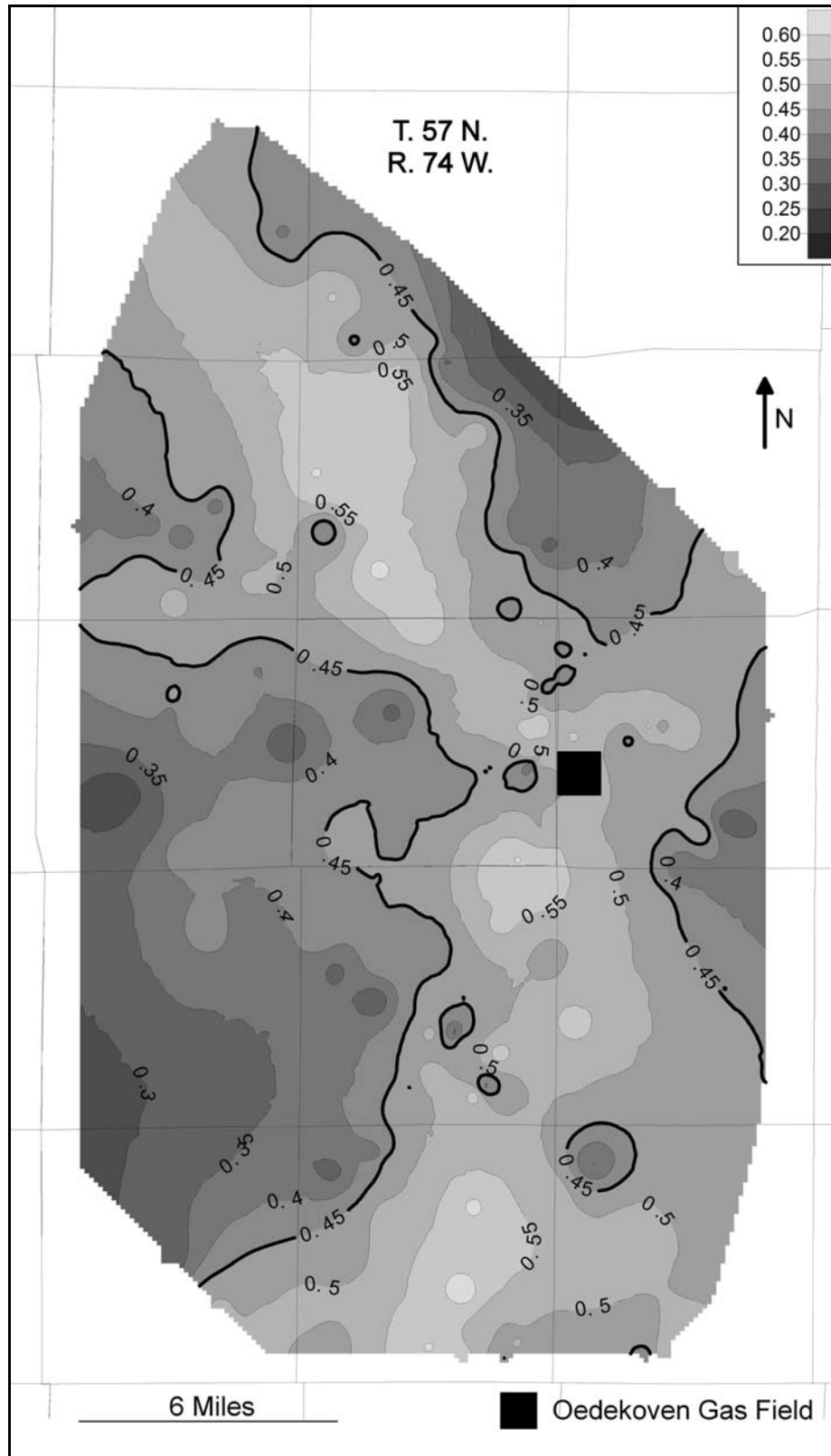


Figure 47. Sandstone to total thickness ratio isopach map of the abbreviated interval. The Oedekoven gas field is located on the updip meander of the fluvial system.

CHAPTER 5

DISCUSSION

The primary purpose of this thesis is to determine potential locations of migrated coalbed methane in the sandstone stratigraphic traps. Logs from previously drilled wells within the study area were analyzed according to lithology to determine the greatest amounts of sandstone within the study interval. The maps prepared from this information provide evidence of the paleoenvironment responsible for the deposition of the different lithologies. Given the described basin history during the Late Cretaceous through the Eocene, several models have been constructed to determine the depositional environment of the Tongue River Member in the Fort Union Formation.

Laramide Orogeny

The initial pulse of the Laramide Orogeny in the northeastern Wyoming region is widely believed to have occurred after the latest Cretaceous (Curry, 1971; Seeland, 1988; Lisenbee, 1988). Curry (1971) considers the Tullock Member's deposition to mark the first evidence of Laramide deformation due to moderate thickening in the southwest of the basin. He concludes that slight, initial subsidence may have begun in the southwest part of the basin during Tullock time and that the distribution of the percentage of sandstone in the Tullock Member does not show an increase toward the basin margins. The slight thickening in the southwest region and the sandstone percentage decrease

towards all the basin margins mark the Early Paleocene and the initiation of the formation of Powder River Basin.

The Curry (1971) model of basin formation based on Tullock Member isopach maps coincides with the Lisenbee (1988) paleoflow data and resulting model for basin formation during Tullock Member deposition. As stated in Chapter 2, the Lisenbee (1988) paleoflow data changes from an easterly flow direction during the Late Cretaceous to a westerly flow direction along with increased sandstone percentages during the period of Early Paleocene Tullock deposition. Lisenbee concludes that the initiation of the Black Hills Laramide uplift is responsible for the change in flow direction.

However, Seeland's (1988) model for the timing of the Black Hills uplift differs from that of Lisenbee (1988). Seeland's data suggest that the eastern flow direction, as evidenced in the Late Cretaceous deposits continues through the Lower Paleocene Tullock deposition. According to the study, a more westerly flow direction does not occur until the Middle Paleocene Lebo Shale deposition.

Curry (1971), Lisenbee (1988), and Seeland (1988) all report the presence of metamorphic fragments in the Tongue River Member sandstone beds. The authors conclude that the Big Horn, Black Hills, and likely the Laramie Mountains had exposed Precambrian rock by the Late Paleocene in order for the metamorphic fragments to be present in the sandstone beds. The basin configuration and Laramide orogenic pulses continued through the Eocene and ceased prior to Oligocene time (Curry, 1971; Lisenbee, 1988).

Tongue River Member Depositional Environment

The deposition of the Tongue River Member has long been debated. The various depositional models consist of a lacustrine depositional setting with westward-prograding deltas (Ayers, 1986), a fluvially-dominated drainage basin (Flores, 1993), and a fluvially dominated lacustrine/swamp model (McClurg, 1988; Goolsby and Finley, 2000). Each model leaves certain depositional characteristics of the Tongue River Member unexplained. The data collected in this study provide further evidence for the depositional environment of the Upper Fort Union Formation.

The sandstone to total thickness ratio isopach map (Figure 44) provides evidence of a north-south trending swell in the sandstone body that passes through the middle of the study area. This sandstone anomaly is located in the same area as the location that lacks a coal deposit over 50 ft thick according to the Goolsby and Finley (2000) data (Figure 13) and the coal thickness map (Figure 48) of Ayers (2002). Therefore, the depositional environment responsible for the increase in sandstone also apparently acts to limit the accumulation of peat.

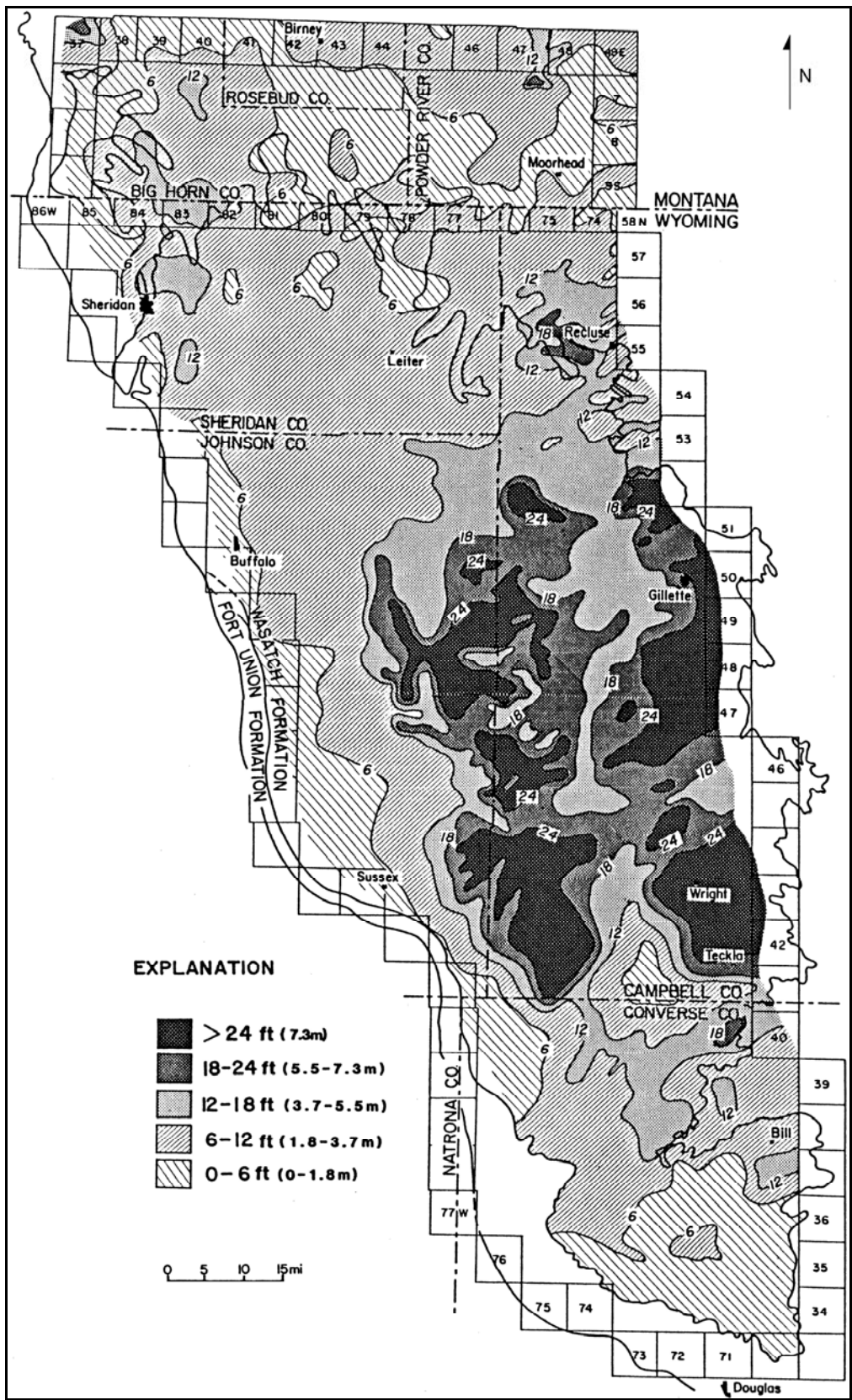


Figure 48. Maximum coal thickness map (after Ayers, 2002, fig. 27).

The Ayers (1986) model considers the upper parts of the Lebo Shale Member to be contemporaneous with the Tongue River Member. The Lebo Shale is the result of a vast lake in the Powder River Basin following the Tullock Member deposition. The lake was slowly filled from the margins by prograding deltas from the south, east, and northwest. The Lebo Shale and Tongue River Members form an interfingering clastic wedge that thins from the basin axis outward to the margins. Evidence for this model is illustrated in Ayers' sandstone percentage isopach map of the Tongue River Member (Figure 49). This isopach map consists only of sandstone bodies greater than 40 ft thick. Ayers also notes that the sandstone percentage decreases from the eastern basin margin towards the basin axis.

In comparison to the Ayers data, the present study included all sandstone bodies greater than 4 ft in thickness. The resulting data show a thickening of the entire interval towards the west and the basin axis (Figure 42). However, the total sandstone thickness also shows an increase to the west (Figure 43). Moreover, the sandstone to total interval ratio isopach map contradicts Ayers' (1986) statement that the sandstone percentage decreases towards the basin axis from the east. The north-south trending anomalous sandstone swell indicates a clear increase in the sandstone percentage from the east for the given interval. Furthermore, the sandstone swell present in Figure 44 appears to have east-west-trending limbs in the same general locations as Ayers' proposed prograding deltas. The limbs located in T. 49 N., R. 72 W. and T. 46 N., R. 72 W. compare well to the respective locations of the Gillette and Wright deltas. Ayers portrays these deltas as extending westward across the present study area. In Figure 40, the limbs do not cross the main swell in the north-south trending sandstone.

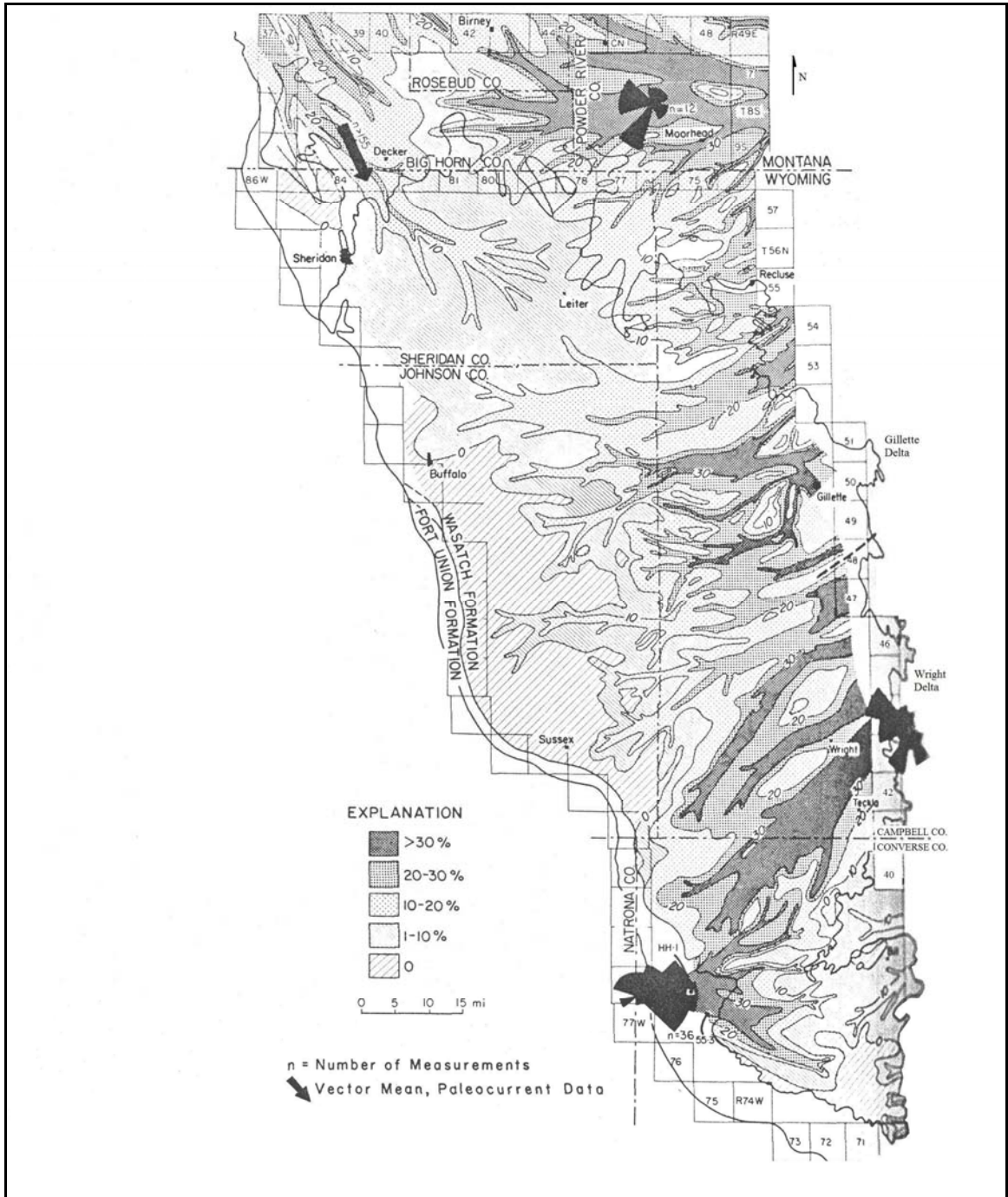


Figure 49. Sandstone percentage isopach map with sandstones greater than 40 ft thick (after Ayers 1986, fig. 12).

The Ayers (1986) data may suggest the presence of prograding deltas in the Upper Lebo Shale Member and Lower Tongue River Member. The interval of the Tongue River Member as plotted from this study does not display the presence of deltaic sandstones similar to the lacustrine model presented by Ayers (1986). The presence of shales in the study interval implies that the depositional environment may have been classified as being more lacustrine at times. However, the deposition of the anomalous sandstone swell that limited peat accumulation, noted by Ayers (1986) and Goolsby and Finley (2000) in the study area, more closely resembles the fluvially dominated model of Flores (1993).

The fluvial model presented by Flores (1993) considers the sandstone in the Tongue River Member to be the result of a meandering to anastomosing fluvial system that drained the part of the basin located in Wyoming in an overall northerly direction. The depositional environment undergoes a transition from a low, flat swamp-like environment with a meandering fluvial system to a matured, raised bog environment (Figure 8). The study performed by Flores suggests that the raised bog peatland is the most favorable scenario for peat deposition considering the large thickness and the low sulfur and ash contents of the coalbeds. These raised bogs, in turn, acted to limit lateral migration of the fluvial system within the study area (Flores, 1993).

The sandstone swell is more suited to a fluvial system due to the linear shape and meandering pattern portrayed by the sandstone percentage data. Furthermore, the north-south trend that it displays coincides with the model presented by Flores (1993). The limbs discussed previously are considered tributary systems draining the eastern part of

the Powder River Basin into the main trunk of the fluvial system. This explains the lack of higher sandstone percentages on the western side of the north-south main trunk.

The current data suggest that the Powder River Basin was fluvially dominated during Tongue River deposition. The lateral extent of the raised bogs is also supported by the present data. The Flores (1993) model considers the areas of peat accumulation to be raised or domed bogs due to the coalbeds' thicknesses, extent, and low sulfur and ash content. Flores considers the Baram River of Sarawak, Malaysia a modern analogue for the peat deposition in the Tongue River Member. In the Malaysian bogs, the peat accumulation reaches the potential thicknesses needed. Furthermore, the maximum lateral extent of these bogs is 32 mi². Though the current study area limits the east-west extent of the data, the north-south boundaries allow for the coalbeds' lateral extent.

The lateral extent of the thick coalbeds found in cross-section U-U' (Figure 40) supports the model for raised bogs in some, but not all, cases. The lowest coalbed in the interval, found in the southern part of the cross section, splits into two coalbeds near sec. 22, T. 43 N., R. 74 W. The lower of the two coalbeds then terminates in sec. 30, T. 44 N., R. 73 W. A coalbed of similar thickness and structural depth occurs in sec. 26, T. 44 N., R. 74 W., extends 16 mi northward, and terminates in sec. 16, T. 46 N., R. 74 W. The upper coalbed slowly thins and undergoes further splitting as the coalbed extends northward, nearly the entire length of cross-section U-U', and terminates in sec. 14, T. 54 N., R. 74 W. The coalbed can be correlated over a distance of 70 mi.

The raised bog acts to limit the lateral migration of the fluvial channels. Vertical aggradation of the bogs and fluvial channels produce thick peat. The result is very thick coals found directly next to thick accumulations of fluvial sandstone and siltstone without

any coal present. Such an occurrence is considered a “want.” If the raised bogs acted to limit migration of the fluvial system, the cross sections should commonly display such wants in the study area.

The abrupt breaks in the lower split coal that are apparent in cross-section U-U' are examples of a want. A want also occurs in the north-south cross-section V-V' (Figure 41). This particular want occurs in T.46N., R.73W., which coincides with the tributary system found in the sandstone ratio map. Wants are also present in cross-sections F-F' (Figure 23), L-L' (Figure 29), and P-P' (Figure 34). If the Flores (1993) model of an anastomosing fluvial system bound by raised bogs were correct, the frequency of wants would be much greater in the thick coalbeds plotted on the cross sections.

Another potential flaw in the raised bog scenario has to do with the thickness of the coalbeds present in the study interval. Numerous coalbeds reach or exceed the thickness of 90 ft, as suggested by the Flores (1993) modern analogy; however, many are much thinner, ranging from 10 to 30 ft thick. Frequently, the correlation of these thinner coals in cross section leads to either a termination or combination of multiple thin coalbeds into one thicker coalbed. The raised bog scenario of the Flores model suggests that the thick coalbeds terminate abruptly as a want. As demonstrated in cross section U-U', the present data reveals that the thicker coalbeds often split into several thinner coalbeds that pinch-out or recombine as another thick coalbed.

The 70-mile correlation of a coalbed in cross section U-U' is common in the three north-south cross sections. The lowermost, thick coalbed located at the southernmost well of cross-section T-T' (Figure 39) is another example of thicker coalbeds splitting and thinning. This coalbed extends northward approximately 37 mi before splitting into two

thinner coalbeds. The two thinner coals extend at least another 12 mi before pinching out. This example contradicts the raised bog model due to a lack of an abrupt terminus of the thick coalbed. The lateral extent of the main coalbed and resulting splits extend over 49 mi north from the southernmost well.

Finally, the low ash and sulfur content of the Tongue River Member coals suggest to Flores (1993) that the depositional setting for peat accumulation must be a raised bog. In the Sarawak, Malaysia modern analogy, the bogs are rain-fed and topographically disconnected from the ground and surface water. According to Flores (1993), the lack of interaction with surface and groundwater greatly reduces the sulfur and ash contents of the peat and resulting coal. The McClurg (1988) model suggests that the dense vegetation of such a low-lying, swamp environment may act as a filter for the peatlands.

McClurg's (1988) model also points to a low-lying swamp as being the depositional environment responsible for the formation of the coalbeds. He compares the Tongue River depositional environment to the Okefenokee Swamp of southern Georgia and northern Florida. The swamp is essentially a shallow lake with trees and other water vegetation. The swamp is fed by several streams at the margins and drained by the Suwanee River, which originates in the middle of the swamp (Figure 10). The swamp may reach 6 to 7 ft in depth and still allow for rooted vegetation and peat accumulation. If the depth exceeds 7 ft, the rooted vegetation drowns, peat accumulation halts, and lacustrine deposition begins. This process explains the presence of lacustrine sediments, such as laterally extensive shale beds, in the Tongue River Member deposits. It also explains how a thick coalbed may laterally split into two or more coalbeds. The thick coalbed represents the core swamp area in the region. If a part of this environment is

drowned, peat accumulation is replaced by fine sediments, while the core swamp area continues to accumulate peat. Such a scenario may be due to differential subsidence, rainfall pattern fluctuations, or a combination of the two. Deposition is likely to be greater than McClurg's projected average subsidence rate of 6 in/1000 yrs (McClurg, 1988). Once the depth of the drowned part of the swamp is filled to accommodate rooted vegetation, peat accumulation is resumed. The resulting stratigraphic section will display one thicker coalbed in the core swamp area and two thinner coalbeds separated by shale in the once drowned part of the area.

The core swamp location may also migrate through time, as found in the Goolsby and Finley (2000) coal analysis project. That being said, the Goolsby and Finley study considers the migrating coal system to be the effect of differential uplift in the surrounding margins of the basin. For example, uplift in the Black Hills region would increase sediment input, forcing the swamp environment and ensuing peat accumulation to migrate to the west. A similar event along the Big Horn margin would cause migration of the coal-forming environment to the east; however, the present sandstone data do not express migration as a factor of sediment input. Rather, the location of the north-south trending sandstone swell appears persistent throughout the study area.

The McClurg (1988) model also explains the low percentage of ash and sulfur content in the Tongue River Member coalbeds. The vegetation in a swamp can effectively filter the sediments well enough that a murky, sediment-rich river may exist within a few feet of the clear, stagnant water of the surrounding swamp. McClurg states that this is the case even during times of flood (McClurg, 1988). He notes that the red, murky waters of the Atchafalaya River in southern Louisiana exist within a few yards of

the clear backswamp waters without any levees or other dry land intervening. The filtering effects of the vegetation will, therefore, limit the sulfur and ash concentrations within the swamp.

The major problem with the McClurg (1988) model in comparison to the Powder River Basin arises when considering the fluvial aspects of the environment. The Okefenokee Swamp analogy contains a river system; however, the river originates within the swamp and does not transport or deposit much sediment. During Tongue River time, the Powder River Basin contained a much higher amount of sediment due to the erosion of the surrounding Black Hills, Laramie Mountains and Big Horn Mountains. Ayers (1986) and Flores (1993) both note that the clastic sediments present in the Basin during Tongue River deposition to have a common fine sand-size limit. The majority of the sediments in a fluvial environment would be transported as suspended load. According to Flores (1993), the current study area is far enough removed from the surrounding uplifts to be considered within the transfer zone of the drainage system. Under such conditions, sediment input equals sediment output along stable channels and floodplains.

The current data suggest that the depositional environment of the Tongue River Member of the Fort Union Formation within the study area was predominantly a low-lying swamp with fluvial drainage to the north. The meandering fluvial system in the current study area represents the transfer zone of the basin drainage system, in which sediment input is equivalent to sediment output. The lack of coarse sediments in the system prevents the fluvial system from migration through avulsion. The vegetation of the surrounding swamplands acts to filter sediment and results in the low ash and sulfur contents found in the Tongue River Member coalbeds.

The data support the Flores (1993) model for raised bogs in parts of the study area, but it is not limited to the raised bog scenario for thick coal formation. Thick coalbeds end abruptly, replaced by sandstone bodies, before resuming over short lateral intervals. However, several coalbed correlations suggest that the thick coalbeds may instead split and thin as they span far beyond the lateral limit of 32 mi² before pinching out.

Gas-producing Sandstones

The presence of the north-west trending fluvial system in the study area implies the potential for gas-charged sandstones. Fields like the Oedekoven gas field are present in the area; it is located within the limits of the fluvial system. The present overall dip of the study area is between one and two degrees west towards the basin axis; therefore, the Oedekoven gas field lies on the updip meander of the fluvial system (Figure 47).

The updip parts of the fluvial system form stratigraphic traps for migrating gas. Due to the fluvial nature of the system, the sandstones grade laterally to the east and west into siltstones and shales. Local faulting due to differential compaction of the coals may act as conduits for the gas to migrate into the fluvial sandstone bodies. As a result, other updip meanders within the fluvial system may be charged with gas.

Similar stratigraphic conditions to that of the Oedekoven gas field do exist in the study area. These target locations are shown in Figures 50 and 51. Due to the stratigraphic thickness within the study interval, the areas chosen for potential gas-bearing sandstone bodies exceed those of the Oedekoven field. Further study coupled

with greater well control is needed to more accurately locate fields of potential gas-bearing sandstone bodies within these areas.

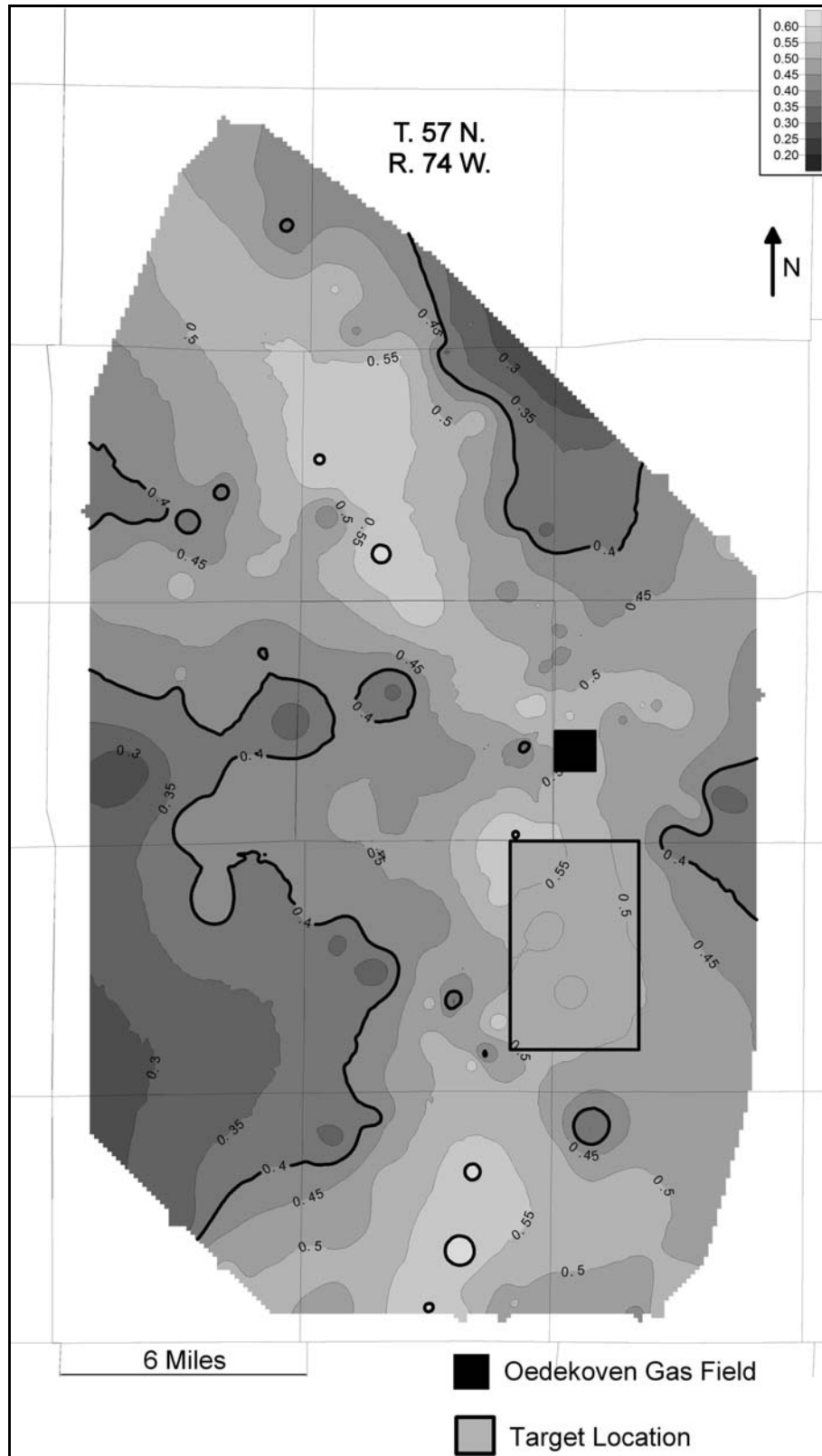


Figure 50: Target location in the north part of the study area. The location chosen lies on the updip meander of the fluvial system according to the northern abbreviated interval data.

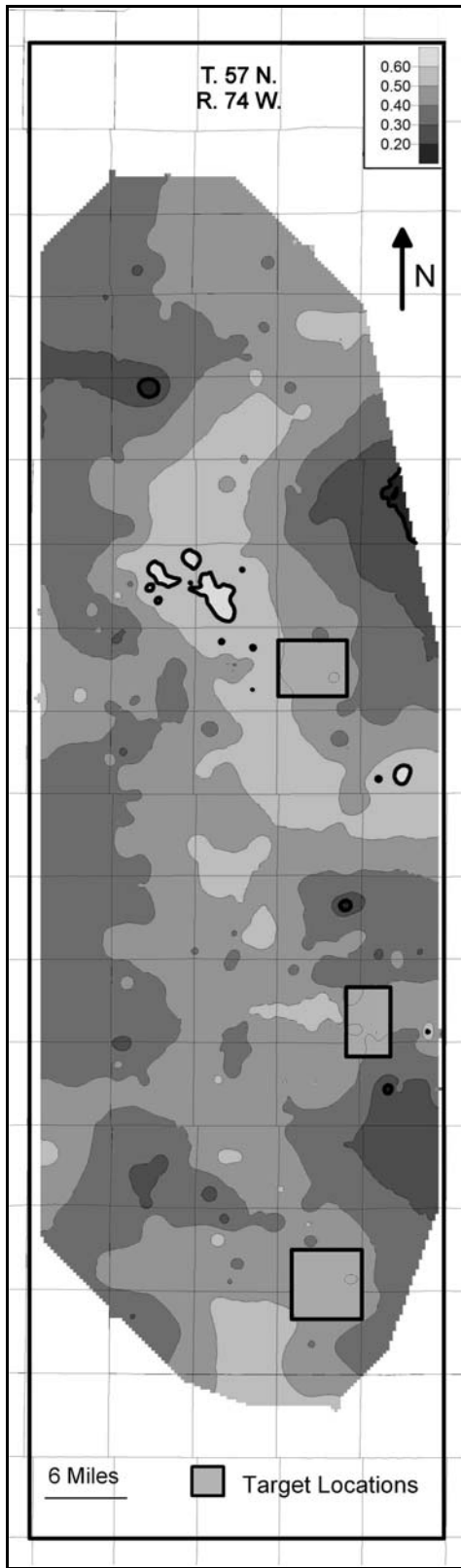


Figure 51: Target locations in the study area. The locations chosen lie on the updip meanders of the fluvial system according to the study interval data.

CHAPTER 6

CONCLUSION

The Powder River Basin formed during the early Paleocene and was well established by Tongue River time. The data presented in this thesis support the Flores (1993) fluvially dominated model and the McClurg (1986) swamp model for Tongue River sediment deposition. Fluvially dominated sandstones were deposited with the likely presence of raised peat bogs in the southern parts of the study area. The paleogeographic relief was low, and an extensive swamp developed with a fluvial system draining the basin to the north. The swamp underwent reduction and expansion, causing paludal deposition to migrate and the resulting coalbeds to split and thin as they expanded outwards from the depositional center of the basin.

The study area is located within the transfer zone of the basin's drainage system. The meandering fluvial system deposited sands, silts, and clays along the floodplain as the basin drained to the north. The resulting sandstone bodies form a fluvial sandstone swell in a north-south trend according to the isopach maps of the study interval. The current dip of the Tongue River Member is one to two degrees to the west; therefore, the Oedekoven gas field is located on one of the updip meanders of the fluvial system. Other updip meanders of the system present in the study area have the potential to contain gas-charged sandstone bodies. Greater well control and further study of the sandstone bodies in these target areas may identify additional reservoirs for gas-bearing sandstones.

APPENDIX

Well Data

Table 1. Study area well data. Well information is sorted by API number in ascending order. Data includes well location by section, township, and range, the total study interval thickness, total sandstone thickness and percentage, and the limited study interval thickness, sandstone thickness and sandstone percentage. All thickness values are in feet.

API #	TWP	RGE	SEC	TOTAL INTERVAL			LIMITED NORTHERN INTERVAL		
				THICKNESS	SS	% SS	THICKNESS	SS	% SS
505024	42N	74W	12	459	239	0.52			
505029	44N	74W	22	510	213	0.42			
505032	44N	73W	5	619	217	0.35			
505037	46N	73W	32	708	313	0.44			
505054	47N	74W	29	597	270	0.45			
505078	47N	74W	17	979	474	0.48			
505137	48N	74W	33	880	472	0.54			
505140	48N	75W	27	1016	447	0.44			
505149	48N	75W	27	1040	472	0.44			
505151	48N	74W	19	918	493	0.54			
505213	48N	75W	8	1015	477	0.47			
505251	48N	75W	5	1044	375	0.36			
505322	49N	75W	28	882	380	0.43			
505345	49N	75W	23	966	410	0.42			
505383	49N	74W	14	827	450	0.54			
505534	49N	75W	5	1002	387	0.39			
505558	50N	76W	35	1162	534	0.46			
505561	50N	75W	35	990	333	0.34			
505563	50N	76W	27	1224	660	0.54			
506412	50N	73W	8	740	350	0.47			
520106	50N	73W	18	721	350	0.49			
520211	53N	74W	11	987	584		950	579	0.61
520267	53N	74W	20		409		867	412	0.48
520270	53N	74W	26				938	452	0.48
520284	52N	74W	34	839	457	0.55			
520286	51N	73W	19	809	383	0.47			
520322	52N	75W	29	1286	400	0.31			
520324	49N	74W	9	815	373	0.46			
520383	53N	75W	26	1028			917	462	0.5
520385	57N	74W	30				647	326	0.5
520433	53N	74W	12				878	466	0.53
520436	57N	75W	24				725	281	0.39
520501	52N	74W	22	1018	482	0.47			

Table 1: continued.

API #	TWP	RGE	SEC	TOTAL INTERVAL			LIMITED NORTHERN INTERVAL		
				THICKNESS	SS	% SS	THICKNESS	SS	% SS
520527	55N	74W	4				590	354	0.6
520547	55N	74W	2				609	305	0.5
520564	52N	73W	10				638	267	0.42
520584	53N	74W	16				851	444	0.52
520763	51N	73W	20	715	292	0.43			
520795	56N	74W	26	822			706	351	0.5
520807	52N	73W	16	718	245	0.34			
520833	49N	73W	26	811	467	0.58			
520845	53N	74W	34	1008	580	0.58	862	519	0.6
520858	50N	73W	4	793	287	0.36			
520859	51N	73W	28	775	341	0.44			
520977	53N	74W	14	945	534	0.57	838	484	0.58
521090	51N	73W	22	680	162	0.45			
521123	55N	74W	13				533	315	0.59
521131	54N	74W	1				626	373	0.6
521154	48N	73W	26	825	352	0.43			
521182	51N	73W	22	570	253	0.44			
521209	49N	73W	21	781	453	0.58			
521343	54N	73W	18				874	438	0.55
521347	55N	74W	13				642	314	0.49
521402	52N	74W	9	902	424	0.47			
521423	55N	74W	12				630	290	0.46
521497	57N	75W	13				687	301	0.44
521505	55N	74W	25				805	394	0.5
521522	55N	74W	12				637	277	0.43
521539	57N	75W	14				708	326	0.46
521619	52N	74W	13	904	445	0.49			
521632	50N	73W	9	748	319	0.43			
521676	52N	73W	18	820	315	0.38			
521752	55N	75W	13				817	258	0.32
521805	49N	73W	1	683	294	0.43			
521901	50N	73W	10	738	300	0.41			
521909	56N	73W	26				677	351	0.51
521980	54N	75W	4	1029	344	0.33	943	330	0.35
522008	55N	74W	1				642	324	0.5
522047	53N	75W	25	1063	503	0.47	937	466	0.5
522070	56N	75W	4				711	258	0.36
522218	52N	73W	27	750	266	0.36			
522232	52N	73W	15	768	204	0.27			
522248	50N	74W	29	951	508	0.53			
522253	56N	75W	19	883	334	0.38	794	309	0.39
522256	55N	73W	21				622	284	0.46
522262	55N	73W	7				630	279	0.44
522367	50N	73W	36	583	235	0.4			
522444	51N	74W	15	907	478	0.53			
522494	50N	73W	15	664	308	0.46			
522583	52N	73W	17	760	317	0.42			
522637	50N	72W	32	625	229	0.37			

Table 1: continued.

API #	TWP	RGE	SEC	TOTAL INTERVAL			LIMITED NORTHERN INTERVAL		
				THICKNESS	SS	% SS	THICKNESS	SS	% SS
522676	53N	74W	4	1078	488	0.45	1010	472	0.47
522734	57N	75W	3				664	316	0.48
522744	57N	75W	27				622	333	0.54
522803	54N	73W	6				669	358	0.54
522815	49N	75W	32	1074	485	0.45			
522820	56N	73W	21				569	251	0.44
522831	50N	72W	33	584	182	0.31			
522869	45N	73W	17	730	325	0.45			
522882	50N	74W	6	933	481	0.52			
522884	53N	73W	28				792	333	0.42
522898	50N	73W	12	685	262	0.38			
522912	50N	72W	31	601	204	0.34			
522932	50N	73W	32	734	362	0.49			
522937	50N	73W	34	730	297	0.41			
522946	45N	73W	19	605	240	0.4			
522961	48N	72W	18	809	352	0.44			
522969	56N	75W	15				861	439	0.5
522986	45N	73W	30	621	237	0.38			
523024	55N	74W	13	754			614	355	0.58
523026	56N	74W	35				631	258	0.41
523036	54N	73W	17	778	418	0.54	654	325	0.5
523056	49N	74W	30	1023	554	0.54			
523057	49N	74W	28	819	326	0.4			
523063	44N	74W	1	562	235	0.42			
523094	49N	74W	22	898	512	0.57			
523097	50N	73W	31	848	433	0.51			
523130	50N	73W	26	714	332	0.46			
523131	46N	72W	31	570	180	0.32			
523133	43N	74W	22	411	148	0.36			
523151	55N	73W	27				687	333	0.48
523184	52N	73W	14				548	211	0.39
523188	50N	73W	35	710	246	0.35			
523203	51N	75W	9	1094	701	0.64			
523230	56N	75W	32				838	408	0.48
523270	47N	75W	17	836	291	0.35			
523294	55N	75W	34	1005	466	0.44	888	399	0.44
523322	56N	75W	21	929	382	0.39	873	362	0.39
523338	54N	74W	20	1002			930	293	0.32
523347	52N	73W	21	873	206	0.24			
523356	55N	73W	6				690	324	0.47
523358	54N	75W	11	1008	361	0.36	897	324	0.36
523372	54N	75W	6	1028	383	0.37			
523392	50N	73W	33	740	359	0.49			
523405	56N	75W	28				845	412	0.49
523409	56N	75W	35				877	448	0.51
523431	47N	75W	29	753	321	0.43			
523457	47N	74W	8	932	474	0.51			
523461	47N	75W	35	678	296	0.44			

Table 1: continued.

API #	TWP	RGE	SEC	TOTAL INTERVAL			LIMITED NORTHERN INTERVAL		
				THICKNESS	SS	% SS	THICKNESS	SS	% SS
523465	54N	74W	33	1019			956	469	0.49
523467	50N	73W	35	724	292	0.4			
523477	53N	75W	31	914	358	0.39			
523479	49N	73W	14	736	265	0.36			
523496	56N	75W	27				855	322	0.38
523543	46N	74W	16	573	249	0.43			
523546	56N	75W	35				790	383	0.49
523548	54N	75W	10	951	407	0.43	884	381	0.43
523571	49N	74W	31	966	402	0.42			
523588	53N	74W	7				887	303	0.34
523599	51N	73W	14	677	210	0.31			
523604	52N	75W	11	611	320	0.52			
523606	53N	75W	4	1074	196	0.14			
523611	50N	73W	33	690	322	0.47			
523658	50N	75W	20	1052	509	0.48			
523660	47N	73W	28	695	271	0.39			
523675	56N	75W	27				798	336	0.42
523676	55N	75W	10				839	393	0.46
523680	55N	75W	15	953	398	0.42	797	306	0.39
523688	52N	73W	32	858	315	0.37			
523690	51N	73W	23	672	226	0.34			
523705	53N	74W	22	1089			878	566	0.64
523707	53N	73W	17	884	455	0.51	779	406	0.52
523735	56N	74W	24				615	233	0.38
523793	47N	74W	31	716	283	0.39			
523820	53N	73W	17				886	456	0.51
523828	51N	73W	35	716	340	0.47			
523865	42N	73W	24	622	206	0.33			
523937	53N	74W	35				919	413	0.45
523941	44N	74W	15	505	203	0.4			
523943	52N	75W	17	1070	501	0.47			
523951	56N	75W	23	925	372	0.4	848	320	0.38
523953	53N	74W	5	960	400		894	363	0.39
523957	46N	74W	27	543	210	0.39			
523979	53N	75W	21	1053	369	0.35	990	303	0.31
523991	54N	75W	21	1100	366	0.33			
524041	54N	74W	32				878	361	0.41
524042	52N	73W	7	892	360	0.4			
524076	53N	73W	6	927	354	0.38	863	304	0.35
524089	48N	73W	18	822	413	0.5			
524096	50N	74W	16	902	329	0.36			
524097	46N	75W	5	709	285	0.4			
524100	53N	74W	25				885	427	0.48
524106	53N	74W	36				958	484	0.5
524127	53N	74W	34	1005	564	0.56	841	474	0.56
524149	55N	73W	29	884	402	0.45	696	328	0.47
524160	44N	74W	29	382	98	0.26			
524167	43N	73W	21	622	310	0.5			

Table 1: continued.

API #	TWP	RGE	SEC	TOTAL INTERVAL			LIMITED NORTHERN INTERVAL		
				THICKNESS	SS	% SS	THICKNESS	SS	% SS
524172	54N	74W	22	982	353	0.36	883	300	0.34
524204	46N	75W	22	666	238	0.36			
524213	45N	74W	17	544	288	0.53			
524269	42N	75W	8	658	196	0.3			
524290	46N	75W	24	653	272	0.42			
524293	49N	75W	18	1174	352	0.26			
524294	49N	75W	19	867	280	0.43			
524296	55N	73W	33				595	212	0.36
524355	56N	74W	25				619	211	0.34
524356	56N	74W	10				648	225	0.35
524358	45N	74W	35	583	249	0.43			
524397	44N	74W	11	574	252	0.44			
524406	56N	74W	20	754			571	324	0.57
524413	47N	74W	17	948	403	0.43			
524490	46N	75W	31	571	174	0.31			
524497	45N	75W	20	619	223	0.45			
524536	44N	75W	5	633	227	0.36			
524539	45N	75W	29	832	343	0.41			
524570	43N	74W	22	444	205	0.46			
524601	43N	74W	12	513	182	0.35			
524655	43N	75W	33	561	251	0.45			
524762	43N	74W	4	384	104	0.27			
524772	44N	75W	13	366	153	0.42			
524799	46N	75W	28	430	393	0.34			
524806	43N	75W	30	588	259	0.44			
524813	50N	75W	14	943	294	0.31			
524835	43N	74W	22	455	194	0.43			
524877	45N	75W	7	599	254	0.42			
524915	42N	73W	14	628	278	0.44			
524973	54N	73W	3				625	297	0.48
524981	43N	74W	17	504	283	0.56			
525046	45N	75W	6	605	132	0.22			
525075	53N	75W	5				993	274	0.28
525101	45N	74W	16	557	193	0.35			
525110	44N	75W	8	757	274	0.36			
525146	42N	73W	18	482	258	0.54			
525149	50N	74W	30	989	462	0.47			
525180	49N	74W	20	868	521	0.6			
525377	43N	75W	24	580	276	0.48			
525385	57N	75W	24				670	298	0.44
525564	51N	74W	31	888	489	0.55			
525612	46N	73W	27	672	258	0.38			
525633	46N	73W	28	763	390	0.51			
525734	50N	73W	23	703	389	0.54			
525762	48N	73W	13	794	402	0.51			
525818	48N	75W	29	1064	479	0.45			
525858	46N	74W	10	573	261	0.46			
525878	50N	74W	11	1056	648	0.61			

Table 1: continued.

API #	TWP	RGE	SEC	TOTAL INTERVAL			LIMITED NORTHERN INTERVAL		
				THICKNESS	SS	% SS	THICKNESS	SS	% SS
525920	45N	74W	30	530	216	0.41			
525929	56N	73W	20				583	213	0.37
525930	42N	75W	7	756	235	0.31			
525945	54N	74W	27	945	433	0.46	882	425	0.48
525989	54N	73W	27				599	281	0.47
526063	47N	75W	8	952	326	0.34			
526147	54N	73W	19				691	397	0.57
526157	53N	74W	31	959	508	0.52	842	390	0.46
526196	48N	75W	17	1084	517	0.48			
526235	57N	74W	34				600	208	0.35
526278	52N	74W	22	1046	538	0.51			
526282	52N	74W	17	937	552	0.59			
526311	48N	73W	35	830	365	0.44			
526325	48N	75W	21	1029	428	0.42			
526345	56N	74W	3				565	199	0.35
526376	47N	74W	26	752	450	0.6			
526394	48N	75W	8	1053	334	0.32			
526476	51N	74W	32	926	544	0.59			
526533	47N	74W	5	968	544	0.56			
526565	51N	74W	21	802	486	0.61			
526614	47N	73W	14	769	103	0.13			
526617	54N	74W	22	964			894	463	0.52
526665	51N	75W	26	1206	688	0.57			
526681	46N	75W	31	643	231	0.36			
526726	51N	75W	26	1058	609	0.58			
526732	50N	75W	2	1125	514	0.46			
526752	48N	75W	18	1082	434	0.4			
526759	50N	75W	19	1085	505	0.47			
526760	50N	75W	5	1019	365	0.36			
526767	48N	75W	32	893	288	0.32			
526773	50N	76W	1	945	333	0.35			
526776	47N	74W	21	916	427	0.47			
526785	50N	75W	4	897	396	0.44			
526787	51N	75W	29	990	423	0.43			
526800	55N	73W	17	784	400	0.51	666	350	0.53
526803	56N	74W	3				570	213	0.37
526902	51N	75W	1	794	485	0.61			
526903	51N	75W	30	1010	365	0.36			
526933	48N	73W	12	922	437	0.47			
526948	50N	75W	3	1107	458	0.41			
526955	50N	75W	6	1084	302	0.26			
526970	50N	75W	6	838	238	0.28			
526973	51N	75W	27	1177	645	0.55			
526981	55N	75W	12				791	314	0.4
527000	55N	74W	1	821			688	330	0.48
527008	52N	74W	21	1084	629	0.58			
527021	50N	74W	27	938	529	0.56			
527026	50N	74W	28	927	488	0.53			

Table 1: continued.

API #	TWP	RGE	SEC	TOTAL INTERVAL			LIMITED NORTHERN INTERVAL		
				THICKNESS	SS	% SS	THICKNESS	SS	% SS
527045	50N	76W	15	1071	428	0.41			
527047	51N	75W	29	1005	504	0.5			
527048	51N	75W	30	1195	377	0.32			
527066	54N	74W	18	945	361	0.38	849	290	0.34
527068	50N	75W	18	1073	455	0.42			
527070	50N	75W	33	924	418	0.45			
527110	51N	74W	22	849	452	0.53			
527156	49N	72W	27	701	362	0.52			
527158	49N	74W	24	901	538	0.6			
527163	42N	73W	34	636	289	0.45			
527185	51N	75W	21	1095	608	0.55			
527200	53N	73W	3				544	263	0.48
527218	51N	75W	28	1146	511	0.45			
527225	51N	75W	25	856	506	0.59			
527231	52N	75W	16	960	491	0.49			
527233	49N	74W	16	931	468	0.5			
527243	50N	76W	28	1160	544	0.47			
527248	51N	75W	19	1070	575	0.54			
527288	55N	74W	11	723	362	0.5	625	325	0.52
527325	51N	75W	20	1106	556	0.5			
527339	51N	74W	29	890	579	0.65			
527380	46N	74W	19	629	254	0.4			
527392	50N	75W	32	1042	400	0.38			
527398	47N	75W	5	855	320	0.37			
527425	45N	75W	18	637	226	0.35			
527432	56N	74W	19	812	356	0.44	651	268	0.41
527459	53N	74W	30	1000	507	0.49	869	460	0.52
527460	51N	75W	27	1151	724	0.63			
527488	44N	73W	30	612	324	0.52			
527493	49N	73W	36	780	374	0.48			
527502	51N	75W	25	992	585	0.59			
527503	51N	75W	23	1008	580	0.58			
527507	49N	72W	3	486	215	0.44			
527528	51N	75W	7	1278	724	0.57			
527539	51N	75W	30	1089	551	0.51			
527546	48N	73W	8	975	498	0.51			
527603	51N	75W	21	1022	657	0.64			
527615	41N	73W	14	689	367	0.53			
527630	50N	74W	6	954	565	0.59			
527648	47N	75W	5	852	346	0.41			
527693	51N	75W	6	1408	571	0.41			
527714	46N	73W	23	857	451	0.53			
527796	51N	76W	28	1260	455	0.36			
527806	50N	73W	19	594	276	0.46			
527826	48N	73W	15	1024	541	0.53			
527855	56N	75W	34				824	438	0.53
527904	50N	74W	26	887	537	0.61			
527907	51N	73W	20	704	315	0.45			

Table 1: continued.

API #	TWP	RGE	SEC	TOTAL INTERVAL			LIMITED NORTHERN INTERVAL		
				THICKNESS	SS	% SS	THICKNESS	SS	% SS
528048	44N	75W	14	417	147	0.35			
528056	49N	73W	13	735	295	0.4			
528072	50N	76W	4	1221	470	0.38			
528076	51N	75W	22	1126	646	0.57			
528107	52N	75W	26	1075	594	0.55			
528158	50N	74W	23	950	533	0.56			
528163	52N	75W	8	1039	521	0.49			
528207	52N	75W	27	1198	619	0.52			
528215	49N	75W	29	1089	455	0.42			
528225	48N	74W	5	968	453	0.47			
528262	51N	74W	3	847	400	0.47			
528264	51N	74W	10	933	567	0.61			
528269	49N	74W	8	915	318	0.35			
528308	44N	75W	15	547	146	0.27			
528358	50N	74W	20	985	505	0.51			
528381	51N	75W	16	971	529	0.54			
528406	43N	75W	34	579	232	0.4			
528425	50N	74W	25	702	418	0.6			
528447	50N	74W	12	948	516	0.54			
528465	57N	74W	34	727			602	220	0.37
528479	51N	73W	19	777	380	0.49			
528482	51N	75W	17	1185	429	0.36			
528516	52N	75W	22	762	420	0.55			
528547	50N	74W	36	805	420	0.52			
528557	55N	75W	28	1059	287	0.27	950	250	0.26
528566	46N	75W	8	720	294	0.41			
528730	55N	75W	28	1030	354	0.34	915	300	0.33
528735	55N	73W	31				617	334	0.54
528745	51N	75W	16	992	577	0.58			
528804	56N	74W	22				636	330	0.52
528880	49N	72W	30	836	346	0.41			
528888	57N	74W	34				617	262	0.42
528890	50N	74W	15	913	395	0.43			
528897	57N	74W	34				615	190	0.31
528933	48N	73W	15	1001	488	0.49			
528943	55N	73W	6	820			619	275	0.44
529006	57N	74W	34				605	190	0.31
529075	54N	73W	4				619	290	0.47
529125	53N	74W	34	980	471	0.48			
529140	53N	74W	26	1006	581	0.54	857	461	0.51
529155	55N	73W	31				603	316	0.52
529175	56N	74W	3				580	195	0.34
529176	56N	74W	3				609	214	0.35
529265	56N	75W	7				852	345	0.41
529293	48N	74W	26	744	389	0.52			
529321	55N	73W	31	890	395	0.44	670	374	0.55
529336	53N	74W	23	1009			846	468	0.55
529371	52N	75W	28	1247	593	0.47			

Table 1: continued.

API #	TWP	RGE	SEC	TOTAL INTERVAL			LIMITED NORTHERN INTERVAL		
				THICKNESS	SS	% SS	THICKNESS	SS	% SS
529414	47N	73W	4	853	325	0.38			
529428	47N	73W	2	807	271	0.34			
529429	55N	73W	31				584	298	0.51
529435	47N	73W	24	807	266	0.33			
529479	54N	74W	2				778	459	0.59
529548	55N	73W	30				716	384	0.54
529556	54N	74W	2				750	433	0.58
529584	56N	74W	8				634	375	0.59
529668	55N	74W	12	802	324	0.4	642	260	0.53
529669	55N	74W	24	695			616	319	0.52
529731	56N	74W	29				613	377	0.61
529774	55N	74W	24	681			661	339	0.51
529788	55N	74W	22	962	392	0.41	820	343	0.42
529805	46N	73W	15	776	418	0.54			
529836	55N	73W	27				548	181	0.33
529889	55N	74W	12	784	354	0.45	617	240	0.53
529891	45N	74W	29	535	225	0.42			
529961	49N	72W	27	724	496	0.68			
529997	52N	75W	29	1256	570	0.45			
530014	54N	74W	22	999			888	424	0.48
530017	56N	74W	11				522	273	0.52
530107	56N	74W	25				635	294	0.46
530111	55N	73W	18	830			693	386	0.56
530126	56N	74W	25				615	231	0.38
530187	42N	73W	21	712	324	0.39			
530237	49N	72W	29	834	508	0.61			
530269	48N	73W	13	841	475	0.56			
530356	45N	75W	19	649	292	0.45			
530567	47N	75W	30	748	309	0.41			
530613	42N	75W	15	616	205	0.33			
530635	47N	73W	25	846	406	0.48			
530658	55N	73W	12				629	257	0.41
530673	48N	73W	1	847	380	0.45			
530685	47N	75W	33	661	273	0.41			
530892	56N	75W	21	949	379	0.39	877	349	0.39
530906	46N	74W	27	560	218	0.39			
530918	46N	74W	22	660	325	0.49			
531281	43N	73W	9	641	325	0.52			
531389	45N	72W	22	467	124	0.27			
531453	45N	72W	24	507	207	0.41			
531537	43N	73W	16	612	219	0.36			
531622	45N	75W	32	733	276	0.37			
531695	46N	74W	34	548	214	0.39			
531798	44N	73W	33	593	221	0.37			
531857	43N	73W	18	505	230	0.46			
531913	45N	74W	3	576	219	0.38			
532355	42N	73W	24	621	223	0.36			
532475	44N	73W	9	510	188	0.37			

Table 1: continued.

API #	TWP	RGE	SEC	TOTAL INTERVAL			LIMITED NORTHERN INTERVAL		
				THICKNESS	SS	% SS	THICKNESS	SS	% SS
532480	45N	74W	13	543	260	0.48			
532815	45N	73W	31	608	253	0.42			
532817	44N	73W	5	507	192	0.38			
533060	47N	72W	33	410	181	0.44			
533091	47N	72W	31	510	188	0.37			
533118	45N	73W	18	609	309	0.51			
533310	45N	73W	16	570	287	0.5			
533396	46N	75W	29	465	173	0.37			
534146	44N	76W	16	841	414	0.49			
534201	55N	73W	14				522	240	0.45
534204	55N	73W	14				504	208	0.41
534307	55N	75W	19	1114	348	0.31			
534439	52N	75W	6	1042	484	0.46			
534440	52N	75W	6	1031	509	0.49			
534442	52N	75W	7	956	453	0.47			
534620	55N	73W	16				594	315	0.53
534667	46N	73W	5	678	261	0.38			
534824	54N	74W	14	886	339	0.38			
534825	54N	74W	14	977	421	0.43	905	413	0.46
534862	54N	74W	11				949	541	0.56
534906	50N	75W	36	1017	410	0.4			
535120	47N	72W	34	493	148	0.3			
535137	54N	74W	33	1035			987	442	0.45
535141	50N	75W	36	1065	422	0.4			
535202	45N	75W	23	426	191	0.45			
535225	47N	72W	32	495	131	0.26			
535292	47N	73W	27	687	316	0.46			
535305	45N	75W	14	449	200	0.45			
535343	56N	75W	19	997	356	0.36	882		
535361	47N	73W	34	656	240	0.37			
535505	47N	73W	26	589	247	0.42			
535520	46N	73W	10	640	220	0.34			
535525	47N	73W	34	646	296	0.46			
535620	47N	73W	27	567	172	0.3			
535928	50N	74W	16	993	444	0.45			
536290	45N	72W	21	511	169	0.33			
536294	45N	72W	21	414	62	0.15			
536296	45N	72W	23	501	113	0.23			
536771	52N	75W	6	1031	384	0.37			
537137	46N	73W	10	623	223	0.36			
537228	56N	75W	29				787	345	0.44
537282	57N	74W	31				651	334	0.51
537286	57N	74W	32				615	266	0.44
537287	57N	74W	32				519	253	0.49
537290	56N	74W	4				633	369	0.58
537291	56N	74W	4				553	285	0.52
537293	56N	74W	4				631	358	0.57
537294	56N	74W	4				634	348	0.55

Table 1: continued.

API #	TWP	RGE	SEC	TOTAL INTERVAL			LIMITED NORTHERN INTERVAL		
				THICKNESS	SS	% SS	THICKNESS	SS	% SS
537296	56N	74W	4				626	340	0.54
537304	57N	74W	30				620	345	0.56
537519	51N	75W	11	884	498	0.56			
537528	55N	74W	16				932	314	0.34
537770	50N	74W	15	975	539	0.55			
538009	43N	74W	28	420	171	0.41			
538734	56N	74W	18				648	391	0.6
538735	56N	74W	18				674	402	0.6
538746	56N	75W	23				915	462	0.5
538751	56N	75W	24				943	475	0.5
538752	56N	75W	24				886	456	0.51
538955	54N	74W	27	1017			970	527	0.54
538984	46N	74W	23	609	316	0.52			
539009	46N	74W	24	684	357	0.52			
539140	47N	74W	27	680	394	0.58			
539247	46N	72W	36	483	190	0.39			
539290	47N	74W	21	638	273	0.43			
539297	47N	74W	33	665	230	0.35			
539330	47N	74W	28	528	213	0.4			
539333	47N	74W	28	704	354	0.5			
539336	47N	74W	28	612	223	0.36			
539460	46N	73W	19	692	350	0.51			
539464	46N	73W	21	597	308	0.52			
539466	46N	73W	21	666	359	0.54			
539509	55N	73W	16	777	399	0.51	647	317	0.49
539513	55N	73W	16				657	365	0.56
539685	44N	74W	36	540	217	0.41			
539698	45N	75W	16	534	207	0.39			
539802	47N	75W	20	701	307	0.44			
539841	44N	74W	26	590	246	0.42			
540613	46N	74W	4	630	242	0.38			
540786	55N	75W	18	862	311	0.36			
540929	44N	73W	1	568	163	0.29			
541046	57N	74W	33				666	327	0.49
541086	43N	74W	25	422	188	0.45			
541457	46N	72W	34	515	186	0.36			
541461	46N	72W	34	388	150	0.39			
541605	43N	73W	35	586	228	0.39			
541622	44N	73W	15	475	158	0.33			
541729	45N	74W	14	552	249	0.45			
542212	42N	73W	11	556	266	0.48			
542229	43N	73W	29	363	168	0.46			
542236	43N	73W	26	615	287	0.47			
542341	44N	74W	14	324	152	0.47			
542343	44N	74W	14	369	184	0.5			
542460	52N	75W	25	898	510	0.57			
542981	50N	74W	8	978	554	0.57			
542990	50N	74W	8	967	593	0.61			

Table 1: continued.

API #	TWP	RGE	SEC	TOTAL INTERVAL			LIMITED NORTHERN INTERVAL		
				THICKNESS	SS	% SS	THICKNESS	SS	% SS
543034	54N	76W	1	933	269	0.29			
543068	44N	76W	16	767	386	0.5			
543089	43N	73W	17	520	240	0.46			
543152	52N	73W	36				612	252	0.41
543178	46N	73W	35	618	312	0.5			
543271	46N	73W	36	532	286	0.54			
543273	46N	73W	36	527	265	0.5			
543331	55N	73W	17	755	319	0.43	635	281	0.44
543355	45N	73W	15	627	314	0.5			
543377	55N	74W	24	750			628	316	0.5
543401	55N	73W	18	814	395	0.49	645	321	0.5
543403	55N	74W	24	732	245	0.37	598	192	0.36
543473	50N	74W	16	938	496	0.53			
543859	42N	74W	4	412	186	0.45			
544042	52N	73W	4				720	240	0.33
544383	44N	74W	16	389	213	0.54			
544628	45N	73W	14	550	249	0.45			
544808	46N	72W	35	511	314	0.62			
544894	46N	73W	13	437	150	0.34			
545068	46N	73W	27	729	392	0.54			
545069	46N	73W	26	548	295	0.54			
545309	42N	75W	13	471	200	0.43			
545325	42N	75W	14	551	209	0.38			
545416	44N	76W	24	648	229	0.35			
545418	44N	75W	30	606	205	0.34			
545474	53N	73W	33				747	320	0.43
545478	53N	73W	33				733	395	0.54
545685	47N	73W	30	637	314	0.49			
545760	54N	76W	3	1031	394	0.38			
545773	54N	76W	4	1047	412	0.39			
545790	46N	75W	23	700	294	0.42			
546289	55N	74W	13				617	344	0.56
546391	44N	74W	13	275	126	0.46			
546394	43N	73W	27	651	312	0.48			
546400	54N	74W	35	891	494	0.55	850	481	0.56
546401	54N	74W	35				890	508	0.57
546405	54N	74W	35	934	383	0.41	856	335	0.39
546418	54N	74W	13				841	384	0.46
546430	54N	74W	26				905	520	0.57
546432	54N	74W	27	1037	381	0.37	959	355	0.37
546559	44N	73W	15	531	202	0.38			
546580	42N	74W	4	415	242	0.58			
547067	47N	74W	29	631	289	0.46			
547295	44N	74W	15	364	198	0.54			
547297	46N	72W	32	536	279	0.52			
547496	55N	75W	25	1035	457	0.44	897	395	0.44
547786	45N	73W	13	518	209	0.4			
547791	44N	73W	11	536	160	0.3			

Table 1: continued.

API #	TWP	RGE	SEC	TOTAL INTERVAL			LIMITED NORTHERN INTERVAL		
				THICKNESS	SS	% SS	THICKNESS	SS	% SS
548130	50N	75W	15	1083	476	0.44			
548335	45N	75W	22	467	223	0.48			
548456	55N	75W	7				735	214	0.29
548554	55N	74W	32	1004	458	0.46	914	448	0.49
548558	55N	74W	30	1009	462	0.46	935	405	0.43
548963	43N	74W	33	394	153	0.39			
548997	55N	74W	33	1005	449	0.45	865	380	0.44
549003	42N	74W	1	415	211	0.51			
549007	42N	74W	2	393	199	0.51			
549011	42N	74W	3	404	207	0.51			
549064	44N	75W	29	688	234	0.34			
549065	44N	75W	29	678	150	0.22			
549134	54N	74W	17	1062	471	0.44	994	452	0.44
549140	54N	74W	7	1031	409	0.4	926	396	0.43
549217	44N	75W	33	577	164	0.28			
549220	43N	75W	3	484	217	0.45			
549429	50N	74W	21	924	364	0.39			
549451	50N	75W	2	1053	516	0.49			
549642	43N	75W	26	529	264	0.5			
549754	54N	74W	10	862	365	0.42	844	351	0.42
549940	46N	73W	20	700	353	0.5			
549992	52N	75W	21	1169	561	0.48			
549996	48N	74W	16	955	385	0.4			
549997	55N	74W	36				689	417	0.61
550760	46N	72W	32	468	171	0.36			
552391	49N	76W	23	744	229	0.31			
552984	50N	76W	36	1253	637	0.5			
552988	50N	76W	36	1159	413	0.36			
553451	51N	76W	25	987	348	0.35			
553459	51N	76W	27	1212	381	0.31			
553524	51N	76W	26	1147	497	0.45			
554785	49N	76W	22	916	342	0.37			
1906107	50N	76W	31	1081	595	0.55			
1906125	51N	76W	30	1332	673	0.51			
1920231	50N	76W	32	1086	484	0.46			
1920782	50N	76W	5	1255	599	0.48			

REFERENCES

- Ayers, W. B., Jr., 1986, Lacustrine and fluvial-deltaic depositional systems, Fort Union Formation (Paleocene), Powder River Basin, Wyoming and Montana: American Association of Petroleum Geologists Bulletin, v. 70, p. 1651-1673.
- Ayers, W. B., Jr., 2002, Coalbed gas systems, resources, and production and a review of contrasting cases from the San Juan and Powder River Basins: American Association of Petroleum Geologists Bulletin, v. 86, p. 1853-1890.
- Curry, W. H., III, 1971, Laramide structural history of the Powder River Basin, Wyoming: Wyoming Geological Association 28th Annual Field Conference Guidebook, p. 49-60.
- Flores, R. M., 1993, Coal-bed and related depositional environments in methane gas-producing sequences: American Association of Petroleum Geologists Studies in Geology 38, p. 13-38.
- Goolsby, J. E., and Finley, A. K., 2000, Correlation of Fort Union coals in the Powder River Basin, Wyoming: a proposed new concept: Wyoming Geological Association 51st Field Conference Guidebook, p. 51-74.
- Lisenbee, A. L., 1988, Tectonic history of the Black Hills uplift: Wyoming Geological Association 39th Annual Field Conference Guidebook, p. 45-52.
- McClurg, J. E., 1988, Peat forming wetlands and the thick Powder River Basin coals: Wyoming Geological Association 39th Annual Field Conference Guidebook, p. 229-236.
- Oldham, D. W., 1997, Exploration for shallow compaction-induced gas accumulations in sandstones of the Fort Union Formation, Powder River Basin, Wyoming: The Mountain Geologist, v. 34, p. 25-38.
- Seeland, D., 1988, Laramide paleogeographic evolution of the eastern Powder River Basin, Wyoming and Montana: Wyoming Geological Association 39th Annual Field Conference Guidebook, p. 29-34.
- U. S. Geological Survey, Central Region Energy Resources Team, 2007, <<http://pubs.usgs.gov/of/2001/ofr-01-126/figures.html>> Accessed March, 2007.

Weichman, Geological history of the Powder River Basin: American Association of Petroleum Geologists Bulletin, v. 48, p. 1881.

Wyoming Geological Association Technical Studies Committee, 1965, Geologic history of the Powder River Basin: American Association of Petroleum Geologists Bulletin, v. 49, p. 1893-1907.

Wyoming Oil and Gas Conservation Commission, 2007, <<http://wogcc.state.wy.us/>> Accessed June, 2003 through February, 2007.